People's Democratic Republic of Algeria

Ministry of Higher Education and Scientific Research

Dr MOULAY Tahar University of Saida

Faculty of Technology

Department of Electronics

A Dissertation Submitted to the Department of Electronics In Partial Fulfillment of the Requirement for Master's Degree in Telecommunications

Specialty: Telecommunication systems

THEME

Fundamental Analysis for Li-FI System

By:

Mr. MOULAI Sidi Mohammed

Examined by Dr. BERBER R

Before the jury:

Examiner 1: Dr. Chami N

Examiner 2: Dr. Bouarfa A

Academic Year: 2019/2021

Contents:

I-Section One

II-Section Two25

III-Section Three

Acknowledgement

Firstable I would like to thank Allah the almighty and merciful, who gave me strength and patience to do this work. I would like to thank my supervisor Mr. BERBER.R for his help and advises and his support . my greetings also go to all the professors who helped me through my academic journey. I would like to thank my colleagues and friends & everyone who gave me and encouraged me. Last but not least it is our pleasure to thank all the members of my families for their support, love, and their prayers.

Figures list:

FigureIII.7. Eyediagram of the received signal for the bit rate of 2 Gbps at (a) 2 meter link distance (b) 4 meter link distance.

FigureIII.8 .construction of li-fi system with an external modulation

FigureIII.9. Q factor of the received signal for the NRZ-OOK and RZ-OOK modulation with respect to the different link range.

FigureIII.10. NRZ electrical drive signal at transmitter & the Received NRZ electrical signal after the low pass Filter

FigureIII.11 RZ electrical drive signal at transmitter & the Received RZ electrical signal after the low pass Filter

FigureIII.12. Q factor of the received signal for the different external white light power in dBm and for the different Bit rate at link range of 3 meter.

FigureIII.13 Experimental setup for the OFDM modulated VLC system using white LED

FigureIII.14 output of our OFDM modulated VLC system for the bit rate of 10 Gbps and the link range of 1 m

FigureIII.15 .Received signal constellation diagram for the bit rate of 10 Gbps and link range of 2.5 m

FigureIII.16 Bit error rate of the received signal for various bit rates and link ranges

FigureIII.17. Bit error rate of the received signal for large number of subcarriers and for diferent link ranges at higher bit rates

FigureIII.18. Received signal constellation diagram for 512 OFDM subcarrier and bit rate of 20 Gbps at the link range of 1.5 m

FigureIII.19. Received signal constellation diagram for 1024 OFDM subcarrier and bit rate of 20 Gbps at the link range of 1.5 m

List Of Abbreviations

LED :light emitting diode

POE: power over ethernet

WOC: wireless optical communication

Li-Fi: light fidility

VLC: visibile light communicaiton

WLAN : wireless local area network

RF : radio frequency

UV : ultraviolet

IR : infrared

PIN : positive intrinsic negative

FDMA : frequency division multiple access

MUX : multiplexer

RZ generator : (Return to Zero)

NRZ: generator : (Non Return to Zero)

BER : Bit Error Rate

SNR : signal noise ratio

MIMO: multiple input multiple output

LOS: line of sight

OFDM: orthogonal frequency division multiplexing

TX: transmitter

RX: receiver

IoT: internet of things

FOV: field of view

QAM: quadrature amplitude modulation

Tables list

I-Section One

Abstract:

White LED offers advantageous properties such as high brightness, reliability, lower power consumption and long lifetime. White LEDs are expected to serve in the next generation of lamps. In the proposed system, these devices are not used only for illuminating rooms but also for an optical wireless communication system.

The solid-state lighting is revolutionizing the indoor illumination. Current incandescent and fluorescent lamps are being replaced by the LEDs at a rapid pace. Apart from extremely high energy efficiency, the LEDs have other advantages such as longer lifespan, lower heat generation and improved color rendering without using harmful chemicals. One additional benefit of LEDs is that they are capable of switching to different light intensity at a very fast rate. This functionality has given rise to a novel communication technology (known as Visible Light Communication - VLC) where LED luminaires can be used for high speed data transfer. This paper provides this technology overview in general and some applications based on VLC system in order to gain so much more speed & a larger bandwidth that can fit the 5G and its uses .

Imagine a world when light becomes data Li-Fi is a simple, but powerful. We all know how a light pomp works when an electronic current is applied to an LED light bulb, a constant stream of light is emitted from the bulb, which we see as illumination. Since LED bulbs are electronic devices, the current and therefore the light can be modulated at extremely high speeds, this can be detected by a photo-detector, and converted back to electrical current therefore carrying data. This is the nervous system of an internet revolution.

Li-Fi doesn't replace your internet service provider, you also need them to get your internet to your home and office via wires, however, once you have that high speed connection, you can deploy your fast secure Li-Fi network using power over Ethernet (POE) or power line communication. Li-Fi offers a greater density than many other radio frequency solutions. For example if you have an average Wi-Fi in your office that provides 150Mbps per second, and 15 people are connected to it, that means you might be able to access 4Mbps, however, with Li-Fi network of lights applied that offers 42 Mbps per light even if you have only 8 lights in your room, those same 15 people could share more than 300 Mbps, that's dense and fast wireless communication.

Li-fi is also bi-directional full duplex and high speed , data is transmitted and received at the same time resulting a really fast reliable user experience especially when doing things like skype calls, video streaming and virtual reality , and also Li-Fi is fully networked that means all the lights in your Li-Fi network can speak to each other and handover as you move around the space each light even has its own IP address which means you can offer location tracking and geo-fencing within your network.

1-Introduction:

Current wireless networks that connect us to the internet are very slow when multiple devices are connected. As the number of devices that access the internet increases, the fixed bandwidth available makes it more and more difficult to enjoy high data rates and connect to a secure network. Therefore, there's many options in wireless communications one of them is the Visible Light Communication (VLC) which is an optical communication technology that use visible light rays, these rays locate between 400 THz (780 nm) and 800 THz (375 nm), as optical carrier for data transmission by illumination. It uses fast pulses of light, which cannot be detected by the human eye, to transmit data. It includes any use of the visible light portion of the electromagnetic spectrum to transmit information.

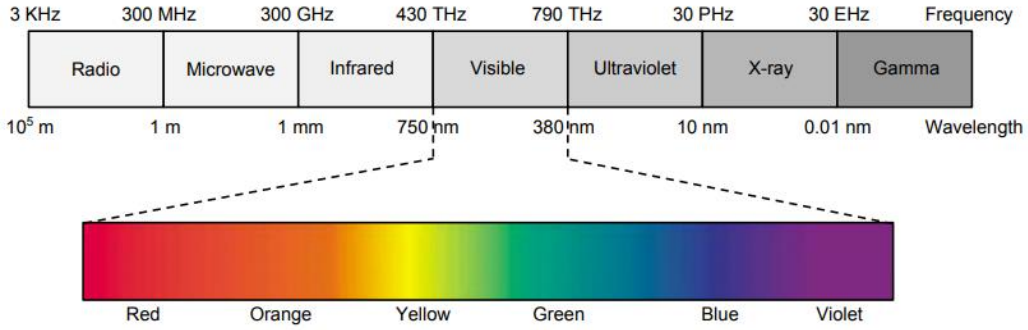

Fig.1 Human eye can perceive the electromagnetic signals between the frequency range of 430 THz and 790 THz which is referred as the visible light spectrum. [2]

Optical communication is any form of telecommunication that uses light as a transmission channel , whether its is visible or invisible, wired or wireless.

Wireless optical communication has evolved to a high-capacity complementary technology to radio frequency (RF) communication. Wireless optical communication is considered as the next frontier for high-speed broadband connection due to its unique features that are highly required for the 5G and above,it has an extremely high bandwidth, ease of deployment, free bandwidth allocation, low power (1/2 of radio-frequency (RF) systems), less mass (1/2 of RF systems), small size (1/10 the diameter of RF antenna), and an improved channel security. It has emerged a good commercial alternative to existing radio-frequency communication as it supports larger data rates and provides high gain due to its narrow beam divergence. It is capable of transmitting data up to 10 Gbps and voice and video communication through the atmosphere/free space. WOC have two broad categories, namely, indoor and outdoor wireless optical communications.

indoor wireless optical communication links provide a flexible interconnection within a building where setting up a physical wired connection is cumbersome. It consists of lasers or light-emitting diodes as transmitter and photodetectors as the receiver. These

devices along with their drive circuits are much cheaper as compared to radio-frequency equipment or existing copper cables. Further, indoor WOC is inherently secure technology since the optical signals do not penetrate walls unlike electromagnetic waves which can cause interference and thus provides a high degree of security against eavesdropping. These optical waves are either in the visible light spectrum or in the IR spectrum which is able to provide very large (THz) bandwidth. Since these devices consume very little power, they are also suitable for mobile terminal systems. Besides many advantages, indoor optical wireless system is influenced by various impairments that impact the performance of the communication system. Some of the factors that lead to these impairments are (i) limiting speed of optoelectronic devices; (ii) large path loss; (iii) noisy indoor environment due to incandescent, fluorescent lighting or sunlight that contributes to noise in the detector; (iv) multipath dispersion; and (v) interference due to artificial noise sources. The range of the system is restricted as the average transmitted power is limited due to eye safety regulations [14].

In this paper we're going to talk about the VLC (Visible Light communication) which is basically the indoor OWC or what it's called Li-Fi (Wireless Fidelity) and discuss its features and applications and the advantages and disadvantages ; and if it's capable of replacing the Wi-Fi and if it can satisfact the needs of high rates communication channels like in 5G .

2-Advantages of OWC:

In the last two decades, unprecedented spread of wireless communication systems has been witnessed. While at the beginning these systems were only able to provide voice service and some rudimentary data services, they have now matured to high-speed packet data networks which allow Internet browsing at the same speed as is achieved with fixed line connections [36]. However, there is still the need to increase data throughput and, consequently, data rates [37]. With the increasing popularity of smartphones, the wireless data traffic of mobile devices is growing exponentially. There have been many independent warnings of a looming "RF spectrum crisis" [38] as mobile data demands continue to increase, while the network spectral efficiency saturates despite newly introduced standards and great technological advancements in the field. By 2015, it is expected that total wireless data traffic will reach 6 exabytes per month, potentially creating a 97% gap between the traffic demand per device and the available data rate per device in the mobile networks [39]. In addition, it is estimated that by 2017 more than 11 exabytes of data traffic will have to be transferred through mobile networks every month [40]. Recently, the Wireless Gigabit Alliance has proposed the utilization of the mm-waves in the license-free 60 GHz band, where the availability of 7 GHz bandwidth enables 7 Gbps short-range wireless links [41]. The 60 GHz band has also been considered as a part of the IEEE 802.11ad framework for very high throughput data links in wireless local area networks (WLANs) using MIMO techniques [42]. However, due to the high path loss of the radio waves in this spectrum range, 60 GHz links are highly directional, and, therefore, require sophisticated digital beamforming and tracking algorithms for application in mobile wireless networks. Since the

RF spectrum is limited and expensive, new and complementary wireless transmission techniques are currently being explored that can relieve the spectrum utilization. One such promising emerging alternative approach is OWC, which offers many advantages over RF transmission. Most recently, VLC has been identified as a potential solution for mitigating the looming RF spectrum crisis. VLC is particularly enticing as lighting is a commodity that has been integrated into virtually every inhabited environment, and sophisticated infrastructures already exist. The use of the visible light spectrum for high-speed data communication is enabled by the emergence of the LED, which at the same time is at the heart of the next wave of energy-efficient illumination. In that sense, the concept of combining the functions of illumination and communication offers the potential for tremendous cost savings and carbon footprint reductions. First, the deployment of VLC access points (AP) becomes straightforward as the existing lighting infrastructure can be reused. Off-the-shelf technologies, such as power line communication (PLC) and power-over-Ethernet (PoE), are viable backhaul solutions for retrofit installations and new installations, respectively. Second, because lighting is on most of the time in indoor environments even during day time, the energy used for communication is significantly reduced as a result of the piggybacking of data on illumination. However, even if illumination is not required, energy-efficient IM/DD techniques exist that allow data communication, even if the lights are visually off [43]. These are already compelling benefits, but the case does not end there. In OWC, the signal can occupy license-free wavelengths in the visible light spectrum from 380 nm to 750 nm, and/or the NIR spectrum from 750 nm to 2.5 μm. The total available bandwidth resource amounts to approximately 670 THz, which is a factor of 10, 000 larger than the RF spectrum including the 60 GHz band. In addition to being a complementary noninterfering solution alongside the RF technology, OWC has the advantage of licensefree operation over a huge spectrum resource. In addition, very high data rates can be realized by the use of low-cost front-ends with commercially available LEDs and PDs [20]. Furthermore, it is free of any health concerns as long as eye safety regulations are fulfilled [44]. This constraint is much less severe when using incoherent LEDs rather than laser diodes. With the advent of highly efficient high-power incoherent LEDs and highly sensitive PDs, OWC has become a viable candidate for medium-range indoor data transmission that can contribute to the cause of solving the spectrum deficit.

3-Application areas:

OWC is generally realized in a line-of-sight (LOS) or a non-line-of-sight (NLOS) communication setup [20, 21]. LOS links can be generally employed in static communication scenarios such as indoor sensor networks, where a fixed position and alignment between the transmitter and receiver are maintained. In mobile environments such as commercial offices, mechanical or electronic beam steering [4] can be used to maintain an LOS connection. Such techniques, however, increase the cost of the optical frontends. Therefore, in a mobile OWC network, where LOS links are likely to be blocked, transmission robustness can be facilitated through NLOS communication. Single-carrier pulse modulation techniques such as pulse width modulation (PWM), pulse interval modulation (PIM), pulse position modulation (PPM), and pulse amplitude modulation (PAM) experience inter-symbol interference (ISI) in

the dispersive NLOS channel, and they therefore exhibit limited data rates unless computationally expensive equalizers are used [4, 20, 45]. Because of its inherent robustness to multipath fading, OFDM with multi-level quadrature amplitude modulation (M-QAM) is envisaged to enable NLOS communication, and therefore high-capacity wireless networking [8, 46, 47]. In addition, due to the fact that light does not propagate through opaque objects and walls, optical wireless signals can be confined within a room. This feature inherently eliminates concerns over the intercepting and eavesdropping of the transmission, resulting in secure indoor data links and networks. The same feature can be exploited to eliminate interference between neighboring cells. Furthermore, OWC is free of any health concerns as long as eye safety regulations are fulfilled [44]. Since optical radiation does not interfere with other electromagnetic waves or with the operation of sensitive electronic equipment, OWC enables safe data transmission in areas where RF communication and electromagnetic radiation are prohibited or refrained to avoid interference with critical systems. These include aviation, homeland security, hospitals, and healthcare, as well as petrochemical and nuclear power plants. Last but not least, radio waves are strongly attenuated in water, disallowing underwater RF transmission. However, since light propagates through water, OWC can be employed for underwater communication.

4-Challenges for OWC:

The following challenges are relevant for the implementation of an OWC system in practical single-link and multi-user communication scenarios. First, optical transmitter front-ends based on off-the-shelf LEDs exhibit a strong non-linear transfer of the information-carrying signal. Therefore, the optimum conditioning of the time-domain signal within the limited dynamic range of the transmitter front-end is essential in order to minimize the resulting non-linear signal distortion and to maximize the system throughput. In order to formulate this optimization problem, the mathematical details of the optical-to-electrical (O/E) signal conversion of the unipolar optical signals are required. Since the energy efficiency of the system is measured by the amount of electrical power required for a given quality of service (QoS), a relationship with the output optical power needs to be established. Through pre-distortion of the signal with the inverse of the non-linear transfer function, the dynamic range of the transmitter can be linearized between levels of minimum and maximum radiated optical power. While single-carrier signals can fit within the linearized dynamic range of the transmitter without distortion, in an OFDM system the non-linear distortion for a given signal biasing setup needs to be analyzed. Therefore, the achievable information rates of the OFDM system for a practical linear dynamic range of the transmitter under average electrical power and average optical power constraints are to be established. Currently, OWC systems with IM/DD cannot fully utilize the entire available optical spectrum, because of the small electrical modulation bandwidth compared to the optical center wavelength of the optical front-ends. Therefore, system designers often resort to increasing the signal bandwidth beyond the 3-dB electrical bandwidth of the optical elements for the sake of increasing the system throughput. However, such an approach requires channel equalization techniques such as linear and non-linear equalization for single-carrier signals, and bit and power loading for multi-carrier signals. This requires

channel knowledge at the receiver and the transmitter. As a result, the spectral efficiency and electrical SNR requirement of single-carrier and multi-carrier modulation schemes need to be compared in a flat fading channel and a dispersive channel under an average electrical power constraint and minimum, average, and maximum optical power constraints. Moreover, this comprehensive comparison needs to take into account the equalization penalties and the total invested electrical signal power, i.e. alternating current (AC) power and DC power. Finally, the system model and the optimum front-end biasing setup are often tailored only to a single-link OWC scenario. Capacity enhancing techniques, where multiple LEDs are employed at the transmitter and multiple PDs are employed at the receiver, are still an open issue. The mechanisms that increase the probability of detection of the individual signals and the associated diversity techniques need to be investigated further in the context of MIMO systems. In addition, studies of the OWC systems are to be expanded with the simulation and optimization of multiple access scenarios in a network of mobile users. Because of the fact that the center wavelength is significantly larger than the modulation bandwidth of the optical front-ends, wavelength reuse in cellular OWC systems can be performed without a perceivable reduction of capacity as opposed to RF cellular systems. Therefore, a larger insight is to be gained into the maximization of the capacity of cellular OWC networks with a transition towards autonomous self-organizing interference-aware networks.

5- Some Issues With Radio Waves (Wi-Fi):

First of all the Radio waves are limited ,expensive, and they consume massive amount of energy most of this energy is not used for transmission only, but for cooling down the base stations. RF only have a certain range [0:4x10^10] Hz , with the advent of the new generation technologies like 2.5G, 3G, 4G and so on we are running out of spectrum. Secondly RF are not advisable to use mobiles at places like petrochemical plants, petrol pumps and in aero planes, and in some cases radio waves might be another cause of concern. Plus radio waves can be intercepted If someone has knowledge and bad intentions then he may misuse it. Plus Wi-Fi can only reach the speed of 300 Mbps,400 in some cases [2]. Actually, there are numbers of technologies that provide realistic and applicable solutions to these issues. One of them is the Li-Fi. It is a new sort of wireless communication which is based on VLC.its transmission of data uses visible light illumination which are very high frequency.

6- Definition of Li-Fi:

Indoor wireless optical communication links provide a flexible interconnection within a building where setting up a physical wired connection is cumbersome. It consists of lasers or light-emitting diodes as transmitter and photodetectors as the receiver. These devices along with their drive circuits are much cheaper as compared to radio-frequency equipment or existing copper cables. Further, indoor WOC is inherently secure technology since the optical signals do not penetrate walls unlike electromagnetic waves which can cause interference and thus provides a high degree of security against eavesdropping. These optical waves are either in the visible light spectrum or in the IR spectrum which is able to provide very large (THz) bandwidth. Since these devices consume very little power, they are also suitable for mobile terminal systems. Besides many advantages, indoor optical wireless system is influenced by various impairments that impact the performance of the communication system. Some of the factors that lead to these impairments are (i) limiting speed of optoelectronic devices; (ii) large path loss; (iii) noisy indoor environment due to incandescent, fluorescent lighting or sunlight that contributes to noise in the detector;(iv) multipath dispersion; and (v) interference due to artificial noise sources. The range of the system is restricted as the average transmitted power is limited due to eye safety regulations [4].

LiFi is a mobile wireless technology that uses light rather than radio frequencies to transmit data. The technology is supported by a global ecosystem of companies driving the adoption of LiFi, the next generation of wireless that is ready for seamless integration into the 5G core. [2] Radio frequency communication requires radio circuits, antennas and complex receivers, whereas LiFi is much simpler and uses direct modulation methods similar to those used in low-cost infrared communications devices such as remote control units. LED light bulbs have high intensities and therefore can achieve very large data rates. Figure 2 show a basic way of how Li-Fi works.

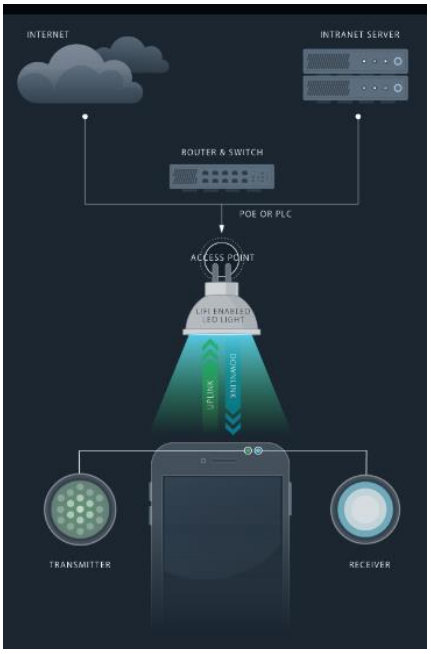

Fig 2. How Li-Fi works [2]

Li-Fi is a new technology for short range wireless communication system; which is suitable for data transmission via LEDs by illumination. It uses the visible light, a part of the electromagnetic spectrum that is still not greatly utilized, instead of RF part. It is possible to encode data in the light by varying the rate at which the LEDs flicker on and off to give different strings of 1s and 0s, it's very simply, if the LED is on, you transmit a digital 1, if its off you transmit a 0, they can be switched on and off very quickly, which gives nice opportunities for transmitting data. The LED intensity is modulated so rapidly that the human eye cannot notice, so the output appears constant; also more sophisticated techniques could dramatically increase Li-Fi data rates such as using array of LEDs, where each LED transmits a different data stream, to provide parallel data transmission. Other ideas are using mixtures of red, green and blue LEDs to alter the light frequency encoding different data channels. [3].

The way Li-Fi works is simple but powerful. When a constant current is applied to an LED light bulb, a constant stream of photons are emitted from the bulb which is seen as illumination. LED bulbs are semiconductor devices, and therefore the illumination can be modulated at extremely high speeds which can be detected by the photo-detector (light sensor) The photo detector registers a binary one when the LED is on; and a binary zero if the LED is off. Using this technique allows for high-speed information can be transmitted from an LED light bulb. [3].

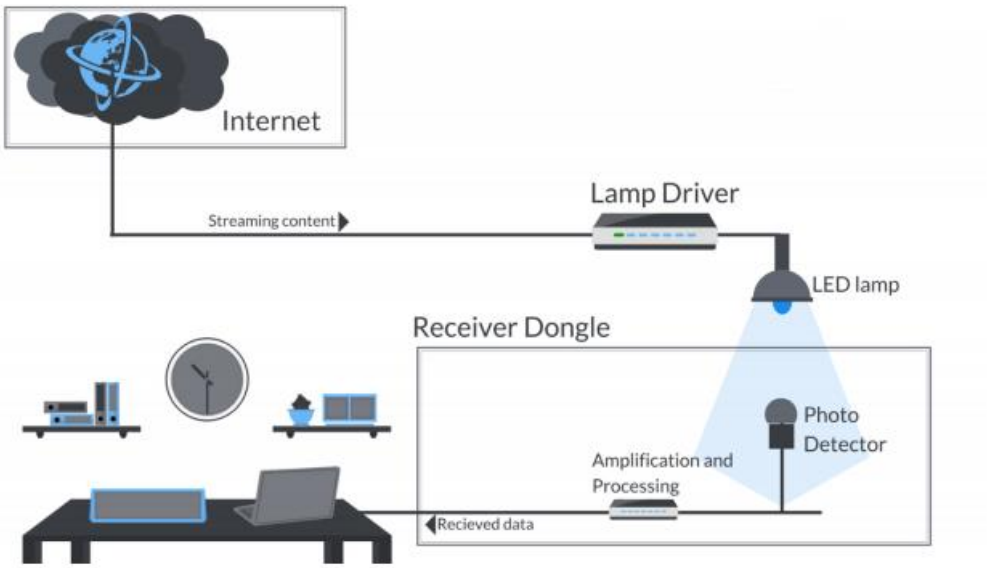

Fig 3. Block diagram of Li-Fi system [3]

7-LIFI VERSUS VLC:

VLC uses LEDs to transmit data wirelessly by using intensity modulation (IM). At the receiver the signal is detected by a photodiode (PD) and by using the principle of direct detection (DD). VLC has been conceived as a point-to-point data communication technique – essentially as a cable replacement. This has led to early VLC standardisation activities as part of IEEE 802.15.7 [6]. This standard, however, is currently being revised to include Li-Fi. Li-Fi in contrast describes a complete wireless networking system. This includes bidirectional multiuser communication, i.e. point-to-multipoint and multipoint-to-point communication. Li-Fi also involves multiple access points forming a wireless network of very small optical attocells with seamless handover. This means that Li-Fi enables full user mobility, and therefore forms a new layer within the existing heterogeneous wireless networks. The fact that LEDs are natural beamformers enables local containment of Li-Fi signals, and because of the blockage of the signals by opaque walls, CCI can effectively be managed and physical layer security can be enhanced. Fig. 4 illustrates the principal techniques that are needed to create optical attocell Li-Fi networks. At the core are novel devices such as gallium nitride (GaN) micro-LEDs and single photon avalanche diodes (SPADs). These are embedded in optical front-ends and subsystems which include adaptive optics and also the analogue circuitry to drive the LEDs and shape the signals obtained from the PDs at the receivers. In order to correctly model link margins, establish the coherence bandwidth of the channel and correctly model CCI, precise channel models are required which take the spectral composition of the signal into account [7]. Link level algorithms are required to optimally shape the signals to maximise the data throughput. In this context, due to the positivity of the power signals in IM, a new theoretical framework is needed to establish the channel capacity since the traditional Shannon framework is not strictly applicable [8]. In order to enable multiuser access, new medium access control (MAC) protocols are required that take the specific features of the Li-Fi physical layer into account. Similarly, interference mitigation techniques are needed to ensure fairness and high overall system throughput. Lastly, the optical attocell network should be integrated into software defined networks governed by the separation of the control and data planes as well as network virtualisation [9]. This requires the development of novel Li-Fi agents. There has been significant research activity around the inner two layers which form VLC, but little research in remaining areas including channel modelling where recently, however, significant activity has been seen.

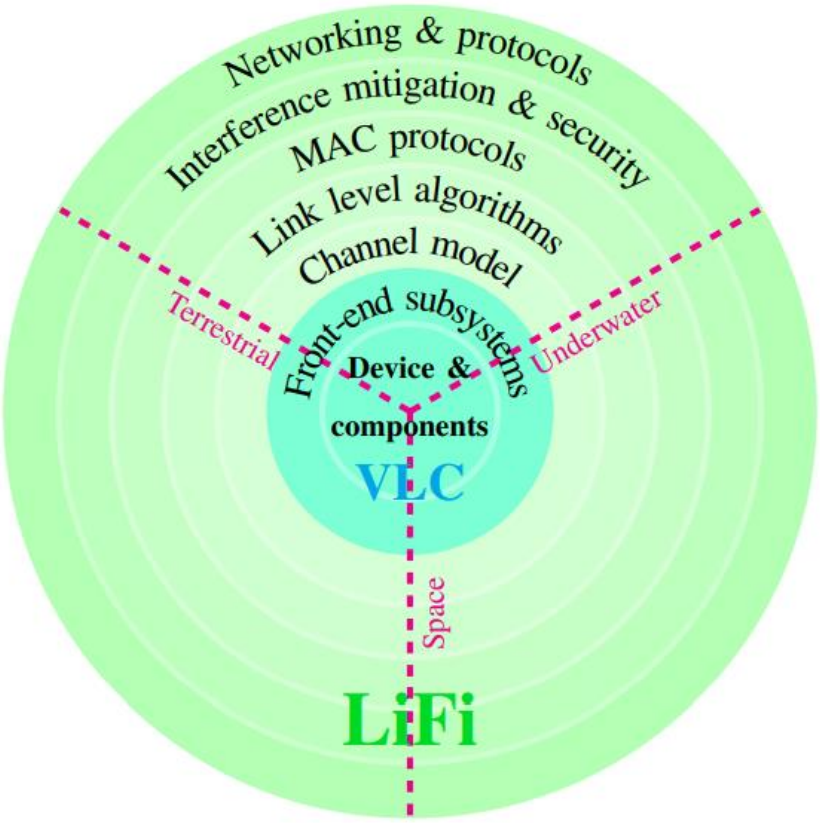

Fig 4. The principal building blocks of Li-Fi and its application areas [3]

8-Li-Fi System Overview:

8.1 -System setup:

The geometry of a wireless communication scenario is defined by the position and radiation/detection characteristics of the transmitters and receivers in an indoor or outdoor environment, with certain reflection properties of the objects in the setup. Based on the propagation path of the light radiated by the transmitter and detected by the receiver, there are two general link arrangements, i.e. LOS and NLOS communications [32]. In addition, a cellular network can be deployed in order to maximize the coverage and capacity over the area of the OWC setup [34, 35, 36]. the building blocks of the transmitter and receiver front-ends are introduced, and the general communication setup arrangements are discussed. A generalized OWC link is illustrated in Fig. 5. The transmitter consists of a digital signal processor (DSP) with a digital-to-analog converter (DAC), which cater for the modulation of the digital information bits and their transformation into an analog current signal. The current drives the optical emitter, i.e. an LED or an array of LEDs. Here, the information-carrying current signal is transformed into optical intensity. The optical signal can be passed

through an optical system in order to further shape the transmitted beam. Here, an optical amplifier lens, a collimator, or a diffusor can be employed to concentrate or broaden the beam. The optical signal is then transmitted over the optical wireless channel. A portion of the optical energy is absorbed by the objects in the environment, and the rest is reflected back in a diffuse or specular fashion [34]. LOS and NLOS signal components arrive at the receiver. An optical filter can be applied to select a portion of interest in the optical spectrum. In addition, the optical filter greatly reduces the interference from ambient light. Thereafter, the optical signal is passed through a system of optical elements, e.g. collimator lenses, to amplify the signal and to align the impinging light for optimum detection [36, 37]. At the photodetector, i.e. a PD or an array of PDs, the optical signal is converted back to electrical current. The current signal is electronically pre-amplified by means of a transimpedance amplifier (TIA). A DSP with an analog-to-digital converter (ADC) is employed for transformation of the analog current signal into a digital signal and demodulation of the information bits.

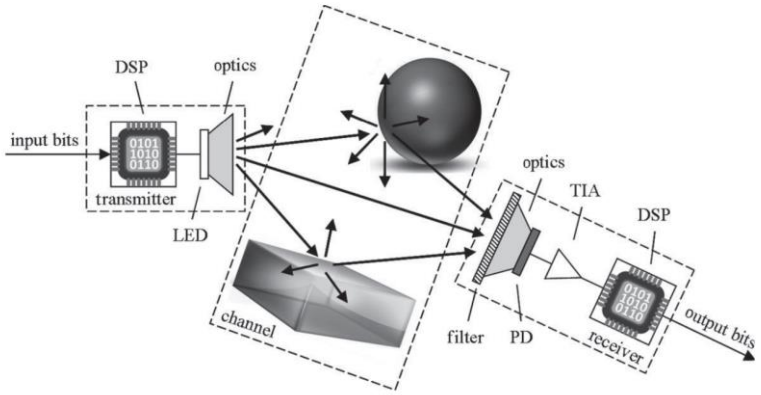

Fig 5.Transmission link in OWC. The general building blocks of the transmitter and receiver [36]

8.2-LI-FI Components:

A key to the commercial adoption of Li-Fi in applications such as the Internet-of-Things (IoT), 5G and beyond, light as a service (LaaS) in lighting, car-to-car communication, security and defence, underwater communication and wireless interconnects in data centres, is the availability of low cost and low power miniaturised transceiver technology. It is therefore essential to develop Li-Fi ASICs. In this section, to the authors' best knowledge, a first transmitter ASIC and receiver ASIC based on complementary metal oxide semiconductor (CMOS) technology are presented. Both chips have recently been developed as part of the UK Engineering and Physical Sciences Research Council (EPSRC) ultra-parallel visible light communication (UPVLC) project.

- **VLC Transmitter:** The transmitter in a visible light communication system is an LED luminaire. An LED luminaire is a complete lighting unit which consists of an LED lamp, ballast, housing and other components. The LED lamp (also referred as an LED bulb in simpler terms) can include one or more LEDs. The lamp also includes a driver circuit which controls the current flowing through the LEDs to control its brightness. When an LED luminaire is used for communication, the driver circuit is modified in order to modulate the data through the use of emitted light. For example, in a simple On-Off Keying modulation, the data bit "0" and "1" can be transmitted by choosing two separate levels of light intensity. A crucial design requirement for VLC system is that illumination, which is the primary purpose of the LED luminaries, should not be affected because of the communication use. Hence, performance of the VLC system is also affected depending on how the LED luminaires are designed. White light is by far the most commonly used form of illumination in both indoor as well as outdoor applications. This is because colors of objects (also known as color rendering) as seen under the white light closely resemble the colors of the same objects under the natural light. In solid-state lighting.

Fig 6. Li-Fi LED lamp

- **VLC Receiver:** the photodetector is a semiconductor device that converts the received light into current. The current commercial photodetectors can easily sample the received visible light at rates of tens of MHz. This is made of semi-conductor material and containing a PIN junction. The current is propagated in the photodiode when photons are absorbed and a very less amount of current is also propagated when there is no existing light. Accompanied by the increase of the surface area, photodiodes have lingering 3 response times. Photodiode technology has been victorious and widely used due to its normal and low-cost rugged structure. Photodiodes have two apart operation modes, firstly rarely photovoltaic mode and secondly photoconductive mode. In photovoltaic mode, credence in light is non-linear and the dynamic range achieved is justly small and highest speed is also not acquire in photovoltaic mode. In photoconductive mode, the credence on the light is very linear and opposite voltage has no significant impact on light, but has a weak impact on dark current (current achieved without light). The Photodiodes is comprehensively

used in the electronics industry, especially in detectors and wide bandwidth optical telecommunications systems.

Fig 7. PIN photodiode

8.3 Types of Link Configurations:

The classification of an indoor optical link depends upon two major factors: (i) transmitter beam angle, i.e., degree of directionality, and (ii) the detector' s field-of-view (FOV), i.e., whether the view of the receiver is wide or narrow. Based on this, there are mainly four types of link configuration, i.e., directed line-of-sight (LOS), non-directed LOS, diffused, and multi-beam quasi diffused links.

1. **Directed LOS Link:** In this type of link, the beam angle of transmitter as well as FOV of receiver are very narrow. The transmitter and receiver are directed toward each other. This configuration is good for point-to-point link establishment for indoor optical communication. The advantages and disadvantages of directed LOS link are as follows:

Advantages:

- Improved power efficiency as path loss is minimum
- Reduced multipath distortion
- Larger rejection of ambient background light
- Improved link budget

Disadvantages:

- Links are highly susceptible to blocking (or shadowing), and therefore, they cannot provide mobility in a typical indoor environment.
- Reduced flexibility as it does not support point-to-multipoint broadcast links.

● Tight alignment between transmitter and receiver is required making it less convenient for certain applications.

Figure 8 shows the pictorial representation of the link. This configuration has been used for many years at low data rate for electronic appliances using remote control applications like television or audio equipment. It provides point-to-point connectivity between portable electronic devices such as laptops, mobile equipment, PDAs, etc. Depending upon the degree of directionality, there is another version of LOS link called hybrid LOS. In this case, transmitter and receiver are facing each other, but the divergence angle of transmitter is much larger than FOV of receiver. This configuration provides larger coverage area than directed LOS, but at the cost of reduced power efficiency, and it also suffers from blocking problems.

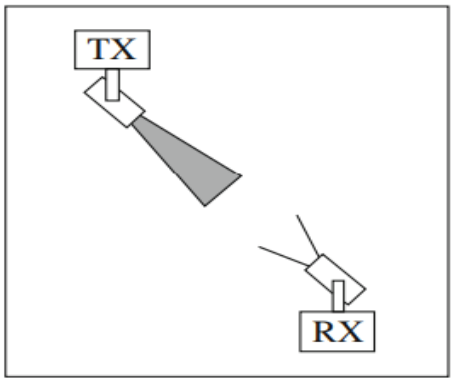

Fig 8. Directed LOS link. [5]

2. **Non-directed LOS Link:** In this type of link, the beam angle of transmitter and detector FOV is wide enough to ensure the coverage throughout the indoor environment. Such links do not require tight pointing and alignment as compared to directed LOS. However, in this case, the received irradiance is reduced for a given link distance and transmitted power. This link is suited for point-to-multipoint broadcast applications since it provides the desired high degree of mobility. In case of larger room dimensions, the entire room can be divided into multiple optical cells, and each cell is controlled by a separate transmitter with controlled beam divergence. The advantages and disadvantages of this link configuration are as follows:

   Advantages:
   - Allows high user mobility
   - Increased robustness against shadowing
   - Alleviate the need of pointing
   - Well suited for point-to-multipoint broadcast applications

   Disadvantages:
   - The received signal suffers from multipath distortion as the beam gets reflected from walls or other objects in the room due to wider beam divergence
   - Less power efficient

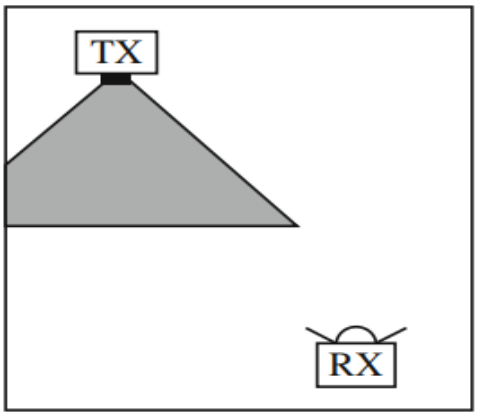

Fig 9. Multi-beam non-directed LOS link [5]

3. **Diffused Link:** In this type of link, the transmitter is facing the ceiling/roof, and it emits a wide beam of data energy toward the ceiling. The signal after it undergoes multiple reflections from walls or room objects is collected by a receiver placed on the ground with wider FOV. Its advantages and disadvantages are as follows:

   Advantages:
   - There is no requirement of alignment between transmitter and receiver as the optical signal is uniformly spread within the room by making use of reflective properties of walls and ceilings.
   - This link is most robust and flexible as it is less prone to blocking and shadowing.

   Disadvantages:
   - Severe multipath distortion
   - High optical path loss typically 50–70 dB for a link range of 5 m

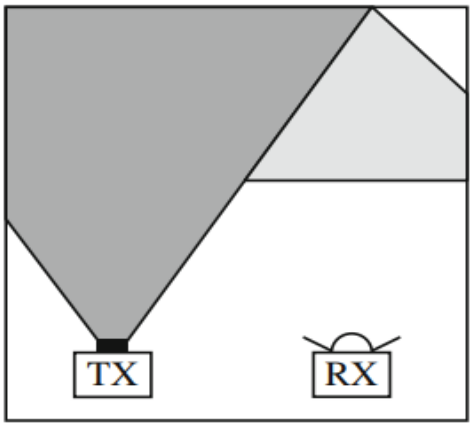

Fig 10. Diffused link [5]

4. **Multi-Beam Quasi Diffused Link**: In this type of link, a single wide beam diffuse transmitter is replaced by multi-beam transmitter, also known as quasi diffused transmitter. The multiple narrow beams are pointed outward in different directions. These optical signals are collected by angle diversity receiver [16, 5] placed on the ground. Angle diversity of the receiver can be achieved in two ways: First is to employ multiple non-imaging receiving elements oriented in different directions, and each

element is having its own lensing arrangement/concentrators. The purpose of the lensing arrangement or the concentrators is to improve the collection efficiency by transforming the light rays incident over a large area into a set of rays that emerge from a smaller area. This allows the usage of smaller photodetectors with lesser cost and improved sensitivity. However, this approach is not a good choice as it will make the receiver configuration very bulky. Second is by using the improved version of angle diversity, also called "fly-eye receiver" [5]. It consists of imaging optical concentrator with a segmented photodetector array placed at its focal plane. In both the cases, the photocurrent generated by the individual receiver is amplified and processed using various combining techniques. Various advantages and disadvantages of this link are [5]:

Advantages:

- Provides high optical gain over wide FOV
- Reduced effect of ambient light source
- Reduced multipath distortion and co-channel interference
- Immunity against blockage near receiver
- Reduced path loss

Disadvantages:

- Complex to implement
- Costly

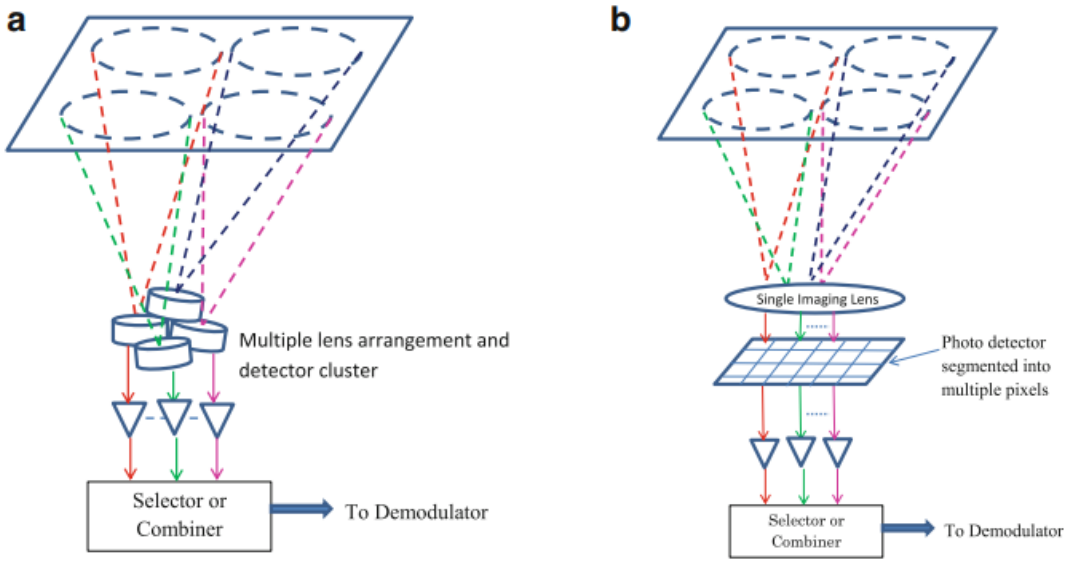

Fig 11. Multi-beam quasi diffused links. (a) Receiver with multiple lens arrangement. (b) Receiver with single lens arrangement [5]

8.4-Multipath Propagation with Reflected Paths:

Typically there are more than one LED in a luminaire. The receiving photodetector can simultaneously receive (intensity modulated) signals from multiple LEDs. The received optical power of the receiver can be calculated by summing the received power of each LOS link within receiver's fieldof-view (FOV) can be expressed as

$$P_R(total) = \sum_{i=0}^{N} P_R(i) \qquad \text{(I.1)}$$

where N is the total number of LEDs and PR(i) is the received optical power from LOS link of (i) th LED.

Since the majority of the indoor surfaces are more or less reflective of visible light, it is necessary to understand the impact of reflected paths on the performance of communication. Spectral reflectance (ρ(λ)) represents reflectivity of a surface (such as wall, ceiling etc.) as a function of wavelength. It was noted in [10] that reflectivity of Infrared signal is higher compared to the visible band. The spectral reflectance of commonly used building materials like plaster wall, ceiling etc. was measured in [10] using a spectrophotometer. Fig. 12 shows the results of measured reflectivity. It can be observed that plastic wall has the least reflectivity while the plaster wall has the highest reflectivity. Because of the reflections, the receiver receives signal from many different paths. Such multipath propagation can be characterized using Power Delay Profile. The PDP gives the distribution of received power as a function of propagation delay. A non-LOS signal can be bounced from many surfaces before it reaches the receiver photodetector as shown in Fig. 13.

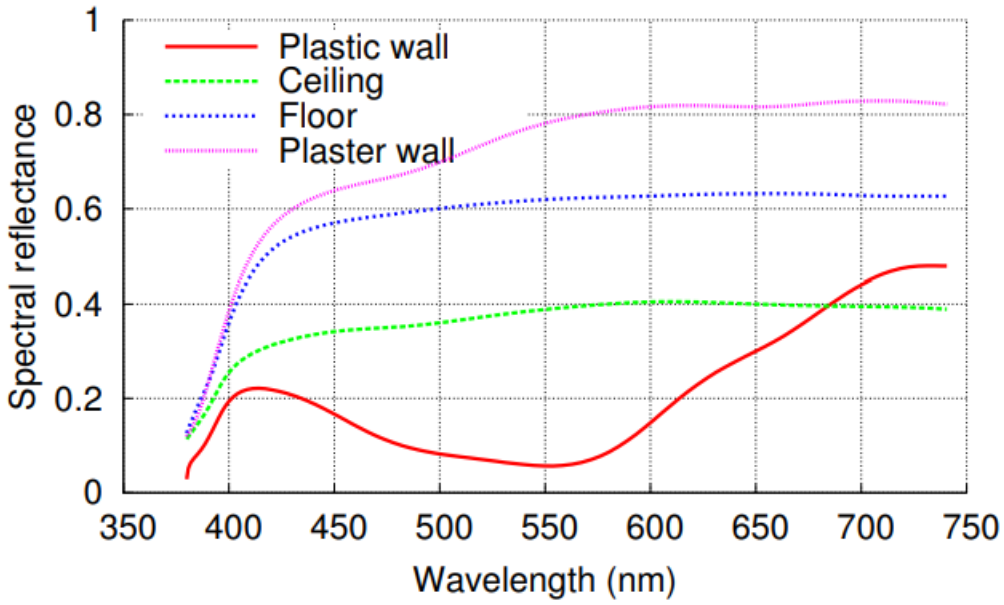

Fig. 12: Different indoor surfaces exhibit different levels of spectral reflectance depending on the wavelength; reproduced from [10].

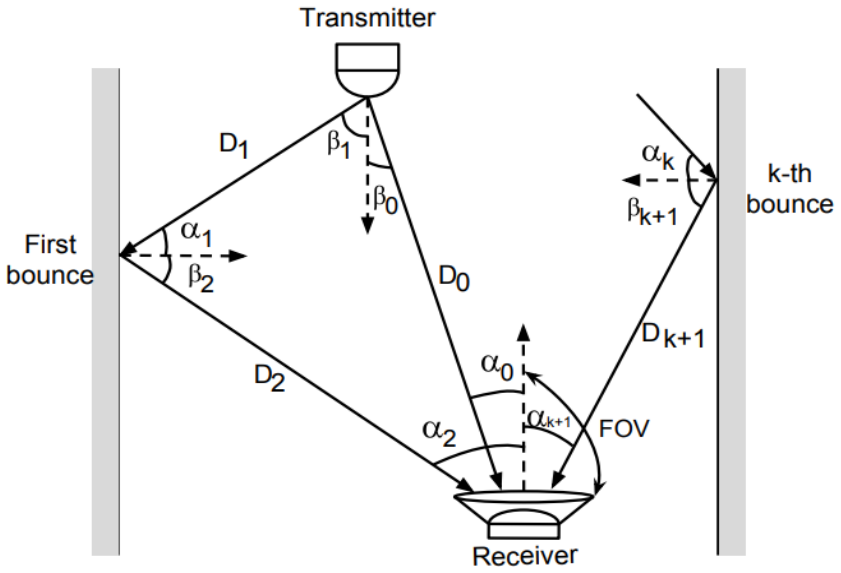

Fig 13. A non-LOS signal can bounce off the surfaces many times before reaching the receiver; β and α denote the angle of irradiation and incident respectively; reproduced from [10].

8.5-Receiver Noise and SNR:

There are three major sources of noise in indoor visible light optical link ambient light noise due to solar radiation from windows, doors etc. and noise due to other illumination sources such as incandescent and fluorescent lamps, shot noise induced in the photodetector by the signal and the ambient light and electrical pre-amplifier noise (also known as thermal noise) of the photodetector. The ambient noise of solar radiation and artificial illumination sources such as lamps results in ambient noise floor which is a DC interference. The effect of such noise can be mitigated by using a electrical high pass filter at the receiver. Most of the previous studies assume that this ambient noise floor remains stationary over space and time, however, no systematic evaluation is present in the literature. For example, the indoor solar radiation changes at different places depending on windows and doors. The radiation also changes depending on the time of the day (and year) and orientation of the windows/doors. Radiation from other illumination sources will also remain an unavoidable source of noise until we completely transition to LED technology. It is required that exhaustive indoor measurements are carried out to accurately account for such noise. Once the noise due to solar radiation and artificial illumination sources is filtered, the SNR at the receiver can be calculated based on the shot noise and the thermal noise of the photodetector circuitry as

$$SNR = \frac{{P_{R_E}}^2}{(\sigma_{shot})^2 + (\sigma_{thermal})^2} \qquad \text{(I.2)}$$

where σshot and σthermal are the standard deviation of shot noise and thermal noise respectively. The shot noise is due to inherent statistical fluctuation in the amount of photons collected by the photodetector. It is known that the photon counting follows a poisson distribution which means that if the mean of number of photons collected by the photodetector in a unit time is x, then the standard deviation of number of photons collected is ✓ x. This also results in poisson distributed variation in photoelectrons generated by the photodetector.

The noise existing in VLC systems can be classified into two categories: noise from the light including the quantum noise (or photon fluctuation noise) from the optical signal itself and the background radiation noise from ambient light, and noise from the receiver devices such as dark current noise, thermal noise, and 1/f noise. Many types of noise can be regarded as shot noise in the wireless optical link, such as dark current noise, quantum noise, and background radiation noise. Specifically, dark current noise is due to random generation of electrons and holes within the depletion region without photon-induced excitation, which is signal-independent. Quantum noise is produced by the random arrival rate of photons from the optical source, which is signal-dependent. On the other hand, background radiation noise is caused by the reception of the photons from ambient light, which is signal-independent and can be modeled as being additive, white, and Gaussian due to its high intensity. For many application scenarios, the received signal-to-noise ratio (SNR) is limited by the background radiation noise, which is much stronger than the quantum noise from the optical source as well as other noise sources. Next, various noise types in VLC systems are detailed as below.

A. **Quantum noise**: Quantum noise or photon fluctuation noise is caused by the discrete nature of the photons from the optical source. When the optical power from the light source is kept unchanged, the number of arrival photons is statistically constant during a long period. However, in a short time interval, the number of photons follows a Poisson distribution.

$$P(n=k)=\frac{\lambda^k}{k!}e^{-\lambda},\quad k=1,2,\cdots \tag{I.3}$$

where λ is the average number of arrival photons per interval and n is the number of arrival photons in a given time interval. Since intensity modulation is usually employed in VLC systems, the quantum noise always appears to be shot noise, which has a one-sided power spectral density in unit of A^2/Hz as

$$\sigma^2=2qi_{\text{pc}} \tag{I.4}$$

where q is the electronic charge, ipc denotes the photocurrent and we have ipc = RPLED, where R is the photodiode responsivity and PLED is the light source power.

B. **Background radiation noise**: Background radiation noise or ambient light noise is caused by the reception of the photons from the environment. Ambient light sources include the sun, the sky, incandescent lamps, and fluorescent lamps. Background radiation noise is signal independent and can be modeled as being additive, white, and Gaussian due to its high intensity. In the NLOS link case where a wide FOV receiver is employed, the received SNR is limited by the background radiation noise that is much stronger than the quantum noise from the optical source as well as other noise sources even with the adoption of the optical filters.
When the spectral radiance L_e ($W\cdot m^{-2}\cdot sr^{-1}\cdot Hz^{-1}$) is assumed to be independent of the wavelength, the received background noise power can be expressed as [18]

$$P_{\text{bg}}=L_e\Omega_s AT_0 g(\psi)B_{\text{opt}}\frac{\cos(\psi)}{\cos(\theta)} \tag{I.5}$$

where Ωs is part of the FOV subtended by the background source at the receiver, T_0 is the transmittance of the atmosphere, and B_{opt} is the bandwidth of the optical filter, the background noise power strongly depends on the FOV and the optical bandwidth of the receiver, and its variance is given by

$$\sigma_{\text{bg}}^2=2qB_{\text{pd}}RP_{\text{bg}} \tag{I.6}$$

where B_{pd} is the electrical bandwidth of the photodiode

C. **Thermal noise:** Thermal noise or Jonson-Nyquist noise is caused by the random fluctuation of the charge carriers (usually electrons) in any conducting medium at a temperature higher than the absolute zero temperature. The power spectral density of thermal noise remains constant ("white") in a wide frequency range up to the near-infrared frequency. Considering the independent agitation of massive charge carriers, the thermal noise obeys Gaussian distribution according to the central limit theorem. The variance of the thermal noise in the noisy resistor in $A^2 \cdot Hz^{-1}$ is given by

$$\sigma^2_{\text{thermal}} = \frac{4KT}{R_F} \quad \textbf{(I.7)}$$

where R_F is the resistance. Thermal noise in the noisy resistor can be modeled as a voltage source ($V_{eq} = \sqrt{4KTR_F}$) in series or a current source ($I_{eq} = \sigma$ thermal) in parallel with a noiseless resistor with a resistance R_F. In both cases, the sources generate the Gaussian white noise.

D. **1/f noise:** 1/f noise is an intermediate between white noise and Brownian noise caused by Brownian motion, whose power spectral density is given by

$$S_{1/f}(f) = \frac{c}{f^{\alpha}} \quad \textbf{(I.8)}$$

where c is a constant and α denotes the exponent satisfying $0 < \alpha < 2$ (usually close to 1). 1/f noise is not white and becomes strong at low frequencies.

E. **Dark current noise:** Dark current is an electric current, which exists in the photodiode even when there is no incident light. The dark current in the p-n junction based devices consists of the surface and bulk currents which are caused by the random generation of the electron-hole pairs thermally or tunneling between the conduction band and the valence band. Thus, it is related to the loaded bias voltage and photodiode temperature. The dark current can be divided into two categories: the surface dark current and the bulk current. The surface current contains the surface generation-combination current and the surface leakage shunt current, while the bulk current is made of the bulk diffusion current, the bulk generation-combination current and the bulk tunneling current. Since the dark current causes random fluctuations of the average photocurrent, it usually exhibits as shot noise with a variance of

$$\sigma^2_{\text{d}} = 2qB_{\text{pd}}i_{\text{d}} \quad \textbf{(I.9)}$$

where i_d is the dark current.

8.6 -Multiple access:

A seamless all-optical networking solution can only be realized with a suitable multiple access scheme that allows multiple users to share the communication resources without any mutual cross-talk. Multiple access schemes used in RF communications can be adapted for OWC as long as the necessary modifications related to the IM/DD nature of the modulation signals are performed. OFDM comes with a natural extension for multiple access – OFDMA. Single-carrier modulation schemes such as PPM and PAM require an additional multiple access technique such as frequency division multiple access (FDMA), time division multiple access (TDMA), or code division multiple access (CDMA). OFDMA has been compared with TDMA and CDMA in terms of the electrical power requirement in a flat fading channel with additive white Gaussian noise (AWGN) and a positive infinite linear dynamic range of the transmitter [27]. FDMA has not been considered due to its close similarity to OFDMA, and the fact that OWC does not use superheterodyning. In addition, due to the limited modulation bandwidth of the front-end elements, FDMA would not present an efficient use of the LED modulation bandwidth. CDMA demonstrates the highest electrical power requirement, since the use of unipolar signals creates significant ISI. TDMA is shown to marginally outperform OFDMA in this setup. The increased power requirement of OFDMA comes from the higher DC-bias level needed to condition the OFDM signal within the positive dynamic range of the LED. However, in a practical VLC scenario, where the functions of communication and illumination are combined, the difference in power consumption between OFDMA and TDMA would diminish as the excess DC-bias power would be used for illumination purposes. Furthermore, TDMA and CDMA systems experience low-frequency distortion noise due to DC wander in electrical components or flickering of background illumination sources, as well as severe ISI in the practical dispersive and frequency selective channel. Therefore, the design complexity of TDMA and CDMA systems increases as suitable techniques to deal with these issues need to be implemented. In OWC, there exists an additional alternative dimension for achieving multiple access. This is the color of the LED, and the corresponding technique is wavelength division multiple access (WDMA). This scheme can reduce the complexity of signal processing at the expense of increased hardware complexity. This is because each AP would require multiple LEDs and PDs with narrow-band emission and detection spectra. Alternatively, narrow-band optical filters can be employed. However, the variation of the center wavelength generally results in variation of the modulation bandwidth, the optical emission efficiency of the LED, and the responsivity of the PD. This corresponds to a variation of the signal-to-noise ratio (SNR) and capacity in the different multiple access channels, which complicates the fair distribution of communication resources to multiple users.

8.7 –Uplink:

Until now, research has primarily focused on maximizing the transmission speeds over a single unidirectional link [30,31]. However, for a complete Li-Fi communication system, full duplex communication is required, i.e. an uplink connection from the mobile terminals to the optical AP has to be provided. Existing duplex techniques used in RF such as time division duplexing (TDD) and frequency division duplexing (FDD) can be considered, where the downlink and the uplink are separated by different time slots or different frequency bands, respectively. However, FDD is more difficult to realize due to the limited bandwidth of the front-end devices, and because superheterodyning is not used in IM/DD systems. TDD provides a viable option, but imposes precise timing and synchronization constraints similar to the ones needed for data decoding. However, TDD assumes that both the uplink and the downlink transmissions are performed over the same physical wavelength. This can often be impractical as visible light emitted by the user terminal may not be desirable [28]. Therefore, the most suitable duplex technique in Li-Fi is wavelength division duplexing (WDD), where the two communication channels are established over different electromagnetic wavelengths. Using IR transmission is one viable option for establishing an uplink communication channel [28]. A first commercially available full duplex Li-Fi modem using IR light for the uplink channel has recently been announced by pureLi-Fi [29]. There is also the option to use RF communication for the uplink [28]. In this configuration, Li-Fi can be used to off-load a large portion of data traffic from the RF network, thereby providing significant RF spectrum relief. This is particularly relevant since there is a traffic imbalance in favor of the downlink in current wireless communication systems.

8.8-The Attocell:

In the past, wireless cellular communication has significantly benefited from reducing the inter-site distance of cellular base stations. By reducing the cell size, network spectral efficiency has been increased by two orders of magnitude in the last 25 years. More recently, different cell layers composed of microcells, picocells, and femtocells have been introduced. These networks are referred to as heterogeneous networks [38, 39]. Femtocells are short-range, low transmission power, low-cost, plug-and-play base stations that are targeted at indoor deployment in order to enhance coverage. They use either cable Internet or broadband digital subscriber line (DSL) to backhaul to the core network of the operator. The deployment of femtocells increases the frequency reuse, and hence throughput per unit area within the system, since they usually share the same bandwidth with the macrocellular network. However, the uncoordinated and random deployment of small cells also causes additional inter- and intra-cell interference which imposes a limit on how dense these small base stations can be deployed before interference starts offsetting all frequency reuse gains. The small cell concept, however, can easily be extended to VLC in order to overcome the high interference generated by the close reuse of radio frequency spectrum in heterogeneous networks. The optical AP is referred to as an attocell [40]. Since it operates in the optical spectrum, the optical attocell does not interfere with the macrocellular network. The optical

attocell not only improves indoor coverage, but since it does not generate any additional interference, it is able to enhance the capacity of the RF wireless networks. Li-Fi attocells allow for extremely dense bandwidth reuse due to the inherent properties of light waves. The coverage of each single attocell is very limited, and walls prevent the system from experiencing co-channel interference (CCI) between rooms. This precipitates the need to deploy multiple APs to cover a given space. However, due to the requirement for illumination indoors, the infrastructure already exists, and this type of cell deployment results in the aforementioned very high, practically interference-free bandwidth reuse. Also a byproduct of this is a reduction in bandwidth dilution over the area of each AP, which leads to an increase in the capacity available per user. The user data rate in attocell networks can be improved by up to three orders of magnitude [41]. Moreover, Li-Fi attocells can be deployed as part of a heterogeneous VLC-RF network. They do not cause any additional interference to RF macro- and picocells, and hence can be deployed within RF macro-, pico-, and even femtocell environments. This allows the system to vertically hand-off users between the RF and Li-Fi subnetworks, which enables both free user mobility and high data throughput. Such a network structure is capable of providing truly ubiquitous wireless network access.

II-Section Two

1-Multiuser Access in LIFI:

As a wireless broadband technology, Li-Fi can provide multiple users with simultaneous network access. In previous research [11], optical space division multiple access (SDMA) has been studied by using an angle diversity transmitter. When compared with the optical time division multiple access (TDMA) technique, it has been shown that optical SDMA can achieve more than tenfold increase in the system throughput within a Li-Fi network. However, such performance enhancement requires careful design of the angle diversity transmitter and time-consuming user-grouping algorithms based on exhaustive search. OFDM provides a straightforward method for multiuser access, i.e. orthogonal frequency division multiple access (OFDMA), where users are served and separated by a number of orthogonal subcarriers. However, unlike RF systems, no fast fading exists in Li-Fi systems and the indoor optical wireless channel shows the characteristic similar to the frequency response of a low-pass filter. Hence, subcarriers with lower frequencies generally provide users with high SNR statistics. Therefore, it is important in OFDMA to use appropriate user-scheduling techniques to ensure that fairness in the allocation of resources (subcarriers) is maintained. In order to enhance the throughput of cell edge users, non-orthogonal multiple access (NOMA) was proposed in [12] for RF communication systems. By utilizing the broadcasting nature of LEDs, it was shown in [13] that the performance of a Li-Fi network can be efficiently enhanced with the application of NOMA. Different from conventional orthogonal multiple access technologies, NOMA can serve an increased number of users via non-orthogonal resource allocation, and it is considered as a promising technology for 5G wireless communication [14]. There are various multiplexing schemes for NOMA, however, in this paper the focus is on a single variant, namely power-domain multiplexing. In this scheme, successive interference cancellation (SIC) is used at the receiver side to cancel the inter-user interference.

2-. Multiuser access in single Li-Fi attocell:

The basic principle of downlink NOMA is shown in Fig.II.2 where the LED broadcasts a super-positioned version of the messages intended for a group of users of interest. Based on power-domain multiplexing, the super-positioned signal is given as a summation of signals, with each multiplied by a weighing factor. Due the fact that the indoor LoS channel is deterministic and strongly related to the Euclidean distance of the transmission link, the channel qualities or the signal-interference-plus-noise ratios (SINRs) may fluctuate significantly among users. For this reason, the interfering signal is detected and canceled in a descending order of the SINR at each receiver (excluding the user with the worst channel quality). Furthermore, in the process of signal detection, the interfering signals whose power are smaller than the useful signal power are treated as noise. Consider the downlink Li-Fi transmission in a single attocell, in which the optical access point (AP) is located in the ceiling and K mobile users are uniformly scattered within a disc underneath. Without loss of generality, all of the users are first indexed based on their channel conditions, so that $h_1 \leq \cdots \leq h_k \leq \cdots \leq h_K$, where h_k represents the optical channel gain between the k-th user and the Li-Fi AP. In order to balance user data rate regardless of their geographical locations, the power partition parameters, denoted by a_k, are set so that users with poorer channel equalities are allocated more signal power ($a_1 \geq \cdots \geq a_k \geq \cdots \geq a_K$), at the same time satisfying the total power constraint. Assuming perfect knowledge of the channel state information (CSI) and SIC signal processing at the receiver side, the Shannon limit on spectral efficiency for each user, denoted by τ_k, can be found as:

$$\tau_k = \begin{cases} \log_2 \left(1 + \dfrac{(h_k a_k)^2}{\sum\limits_{i=k+1}^{K} (h_k a_i)^2 + \frac{1}{\rho}} \right), & k \neq K \\ \log_2 \left(1 + \rho (h_k a_k)^2 \right), & k = K \end{cases} \quad \text{(II.1)}$$

where ρ represents the transmitted SNR at the Li-Fi AP. As shown in Fig. 6, the performance of NOMA is simulated in a Li-Fi attocell setup with two users. The parameters listed in Table I are used. It can be seen from Fig. II.2 that, when compared with the conventional TDMA technique, NOMA can always increase the sum throughput of Li-Fi networks. Also, from the slope of the curves, it is indicated that NOMA can further enhance the performance of users at the cell edge, without significantly deteriorating the performance of other users with better channel qualities.

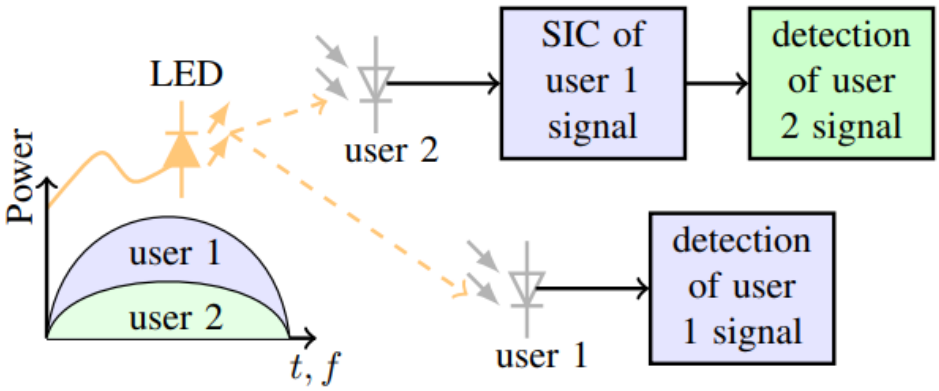

Fig II.1.Illustration of NOMA principle (two-user example). [15]

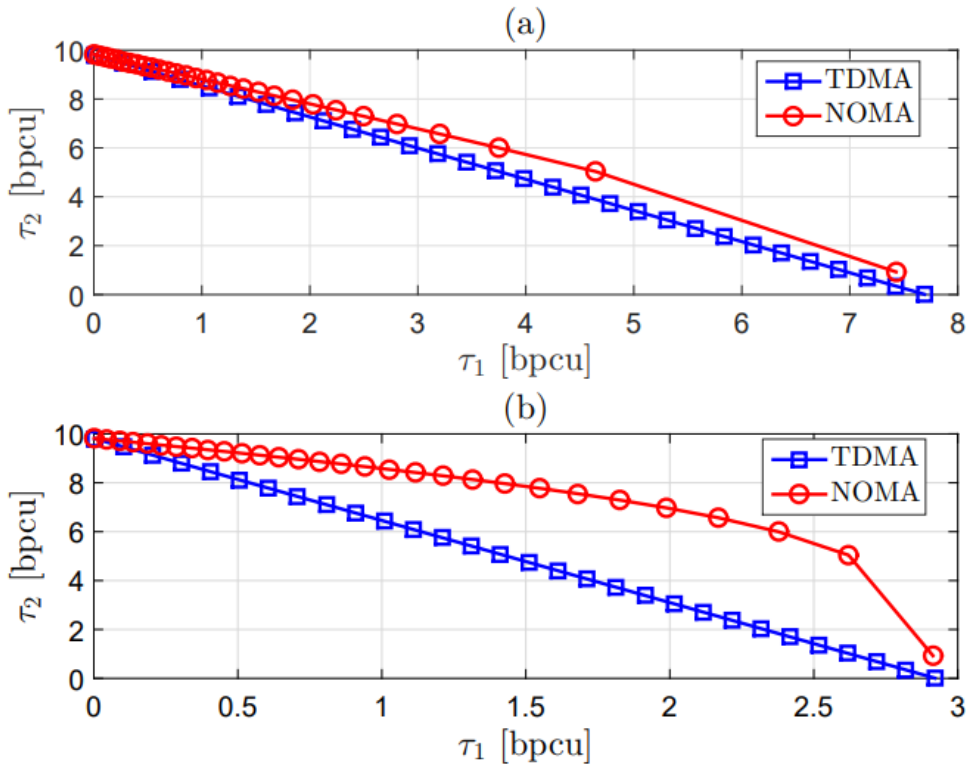

Fig. II.2 Shannon spectral efficiency comparison between NOMA and TDMA in a Li-Fi attocell setup (two-user example): (a) two users with similar channel conditions; (b) two users with distinctive channel conditions. [15]

3-Multiuser access in Li-Fi attocell network:

Due to the overlapping coverage area of adjacent Li-Fi APs, the cell edge users will experience increased interference from neighbouring attocells. As shown in Fig.II.3, cell edge user 1 in Li-Fi attocell 1 also receives the unwanted signal transmitted from the AP in LiFi attocell 2. Therefore, directly using NOMA in a Li-Fi network cannot efficiently mitigate interference transmitted from adjacent attocells. This inter-cell interference can be efficiently reduced or mitigated through intelligent frequency planning techniques, however, with the disadvantage of reducing the frequency utilisation efficiency. One promising and effective solution to enhance the performance of cell edge users in a Li-Fi network is the combination of NOMA and SDMA. Unlike [11], where SDMA is realised with the use of an angle diversity transmitter, in this paper SDMA is based on a coordinated multi-point (CoMP)-aided joint transmission technique. Specifically, users at different locations are served simultaneously with the use of transmit pre-coding (TPC). After the signal propagating through the optical channel to the receiver side, inter-user interference is mitigated aided by TPC and SDMA. Take Fig. II.3 as an example, since user 1 and user 3 can receive signals from both LED 1 and LED 2, their 'spatial signatures', i.e. optical channel gains, are exploited for designing the TPC vector. As a result, transmission links from both LEDs are added constructively to help enhance the performance of user 1 and user 3 at the cell edge. CoMP-aided SDMA requires the Li-Fi APs to have knowledge of both the message data and CSI of user 1 and user 3. Note that in such a Li-Fi network, only the cell edge users are coordinated for joint transmission. Therefore, the added signaling overhead and complexity in exchange for enhanced system performance are not significant. Different from Fig. II.1, where only user 2 needs to cancel the interfering signal for user 1, in Fig. II.3 user 2 needs to cancel the pre-coded version of the signals intended for both user 1 and user 3. As shown in Fig. 8, the performance of NOMA in combination with SDMA is simulated in a Li-Fi network with two neighbouring attocells. The setup for Li-Fi APs and users is similar as the one shown in Fig. 16, where the locations of user 1, 3 and 4 are fixed while user 2 is moved from the cell edge (Fig. II.4 (a)) to the cell center (Fig. II.4 (b)). The theoretical Shannon spectral efficiency is computed for both users in attocell 1. As shown in Fig. 17, if no intelligent interference management techniques are used, the performance of TDMA in a typical Li-Fi network is severely affected by inter-cell interference. On the other hand, the throughput of a Li-Fi network can be greatly increased by using NOMA and SDMA techniques.

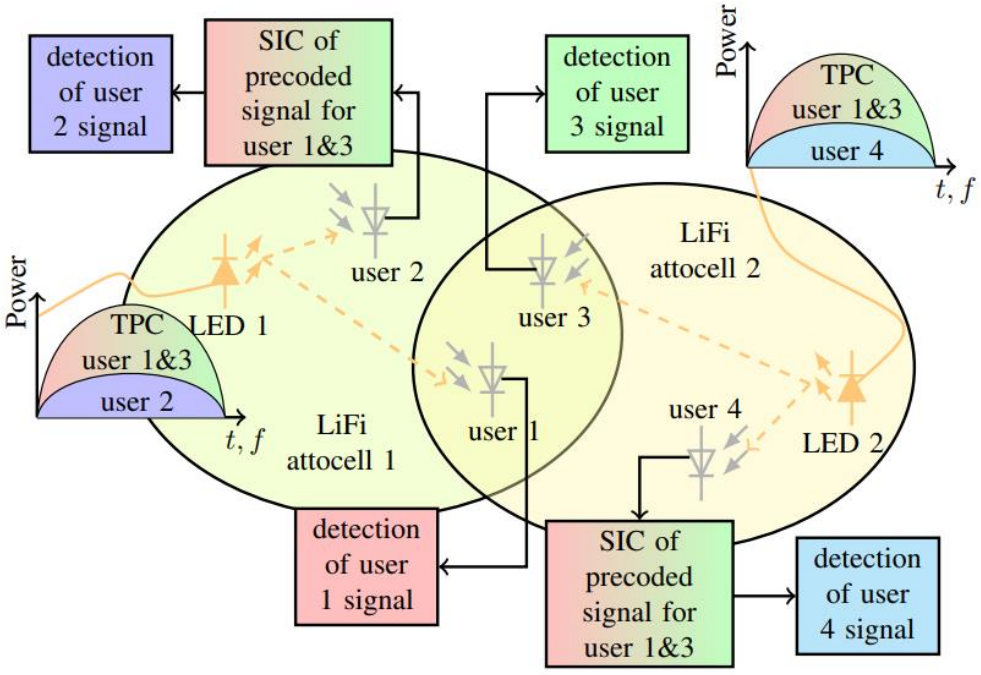

Fig. II.3. Illustration of combined use of NOMA and SDMA in a two-cell Li-Fi network. SIC is used to eliminate interference. [15]

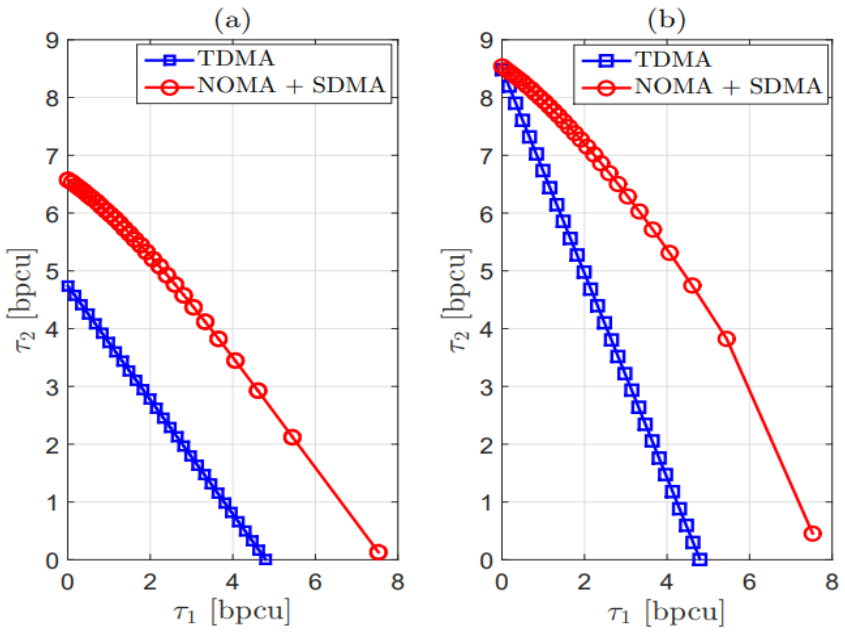

Fig. II.4. Shannon spectral efficiency comparison between hybrid NOMA/SDMA and TDMA in a Li-Fi network setup (two-attocell example): (a) user 1 and user 2 are both near the cell edge; (b) user 1 is near the cell edge while user 2 is near the cell center. [15]

4. Modulation schemes:

4.1-Introduction:

The data transmission in optical wireless communication (OWC) with incoherent light sources is realized through intensity modulation and direct detection (IM/DD). For this purpose, the transmitted signal needs to be real-valued and non-negative. In practice, this is achieved by single-carrier modulation techniques, such as multi-level pulse position modulation (M-PPM) and multi-level pulse amplitude modulation (M-PAM), and through multi-carrier modulation such as multi-level quadrature amplitude modulation (M-QAM) optical orthogonal frequency division multiplexing (O-OFDM). Conventionally, the average optical power is defined as the first moment of the transmitted signal, while the average electrical power is defined as the second moment of the transmitted signal. In practice, the dynamic range can be linearized through pre-distortion only between levels of minimum and maximum radiated optical power. In addition, eye safety regulations [15] and/or design requirements also impose an average optical power constraint. Because of these constraints, there is a fixed relation between average electrical power and the average optical power of the single-carrier and multi-carrier signals which varies with the change in the biasing setup, i.e. a combination of direct current (DC) bias and signal variance. The optical-to-electrical (O/E) conversion of the optical signals is investigated in this chapter. In this study, the electrical energy consumption of the OWC system is considered, and therefore the average electrical power carries the information [16]. Here, the received electrical signal-to-noise ratio (SNR) is presented as a function of the channel equalization penalty, the DC-bias penalty, and the nonlinear distortion parameters. The analytical framework is verified by means of a Monte Carlo bit-error ratio (BER) simulation [17, 18, 19].

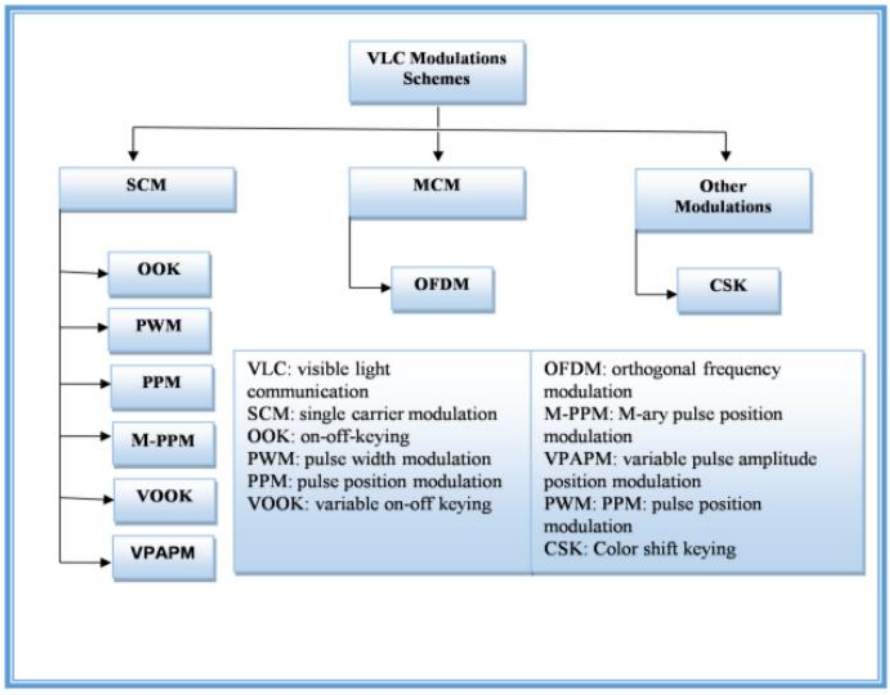

Fig II.5. Different Modulation schemes [16]

4.2-Modulation schemes

With comprehension of signal loss due to the distance range occurred is considered as path-loss, environmental noises, and signal to noise ratio (SNR). Various modulation schemes are used in VLC. The most prominent difference in VLC and RF technology is the VLC could not be encoded over phase and amplitude [3]. It implies that phase and amplitude encoding can't be employed in VLC. In VLC system encoding is done through the intensity of light waves. The demodulation relies upon the direct detection of the data receiver. VLC achieved higher data rates and convene the necessities of visible light to humans. The prerequisites about recognize light can be portrayed under below techniques.

4.2.1-Dimming:

It was proposed in [4] that various levels of lighting intensities are needed while performing different types of actions. The light intensity is measured in Lux and illuminance range of 30-100 Lux is sufficient for diminishing the darkness to perform the visual task in open spots. Conversely, a higher level of light intensity required for offices and residential applications in the range of 300 – 1000 Lux. The advancement in LED driver circuits day by day, it has turned out to be promising to dim an LED to a random level contingent upon the application needs to save energy source. It is necessary to understand the impact of random level of LED light intensity which is visible to human eye. It is shown in [20] that the nonlinear response has been observed between the measured and perceived light as shown in Fig. II.6. The human eye is able to acclimatize to the low level of illumination through expanding the pupil to permit more light to enter the eye. The calculated [20] perceived light from the measuring light as in Equation (1)

$$\text{Perceived light (\%)} = 100 \times \sqrt{\frac{\text{Measured light(\%)}}{100}} \qquad \text{(II.2)}$$

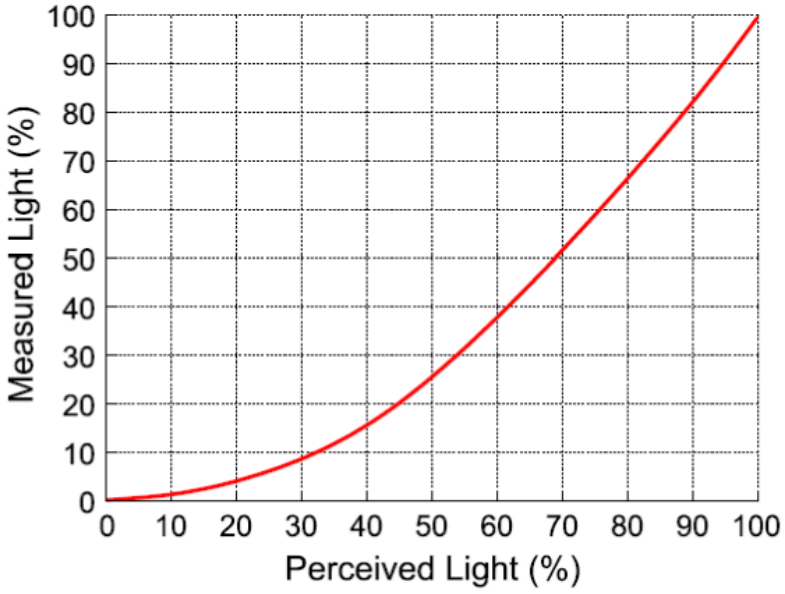

Fig. II.6 The human eye perceives the actual measured light differently due toenlargement/contraction of the pupil. [20]

It has been observed that the lamp is darkened 1% of its measured light but human eye perceived it with an increase of 9% and overall light intensity is 10%. The users have an authentication to select the arbitrary level depending on the application and required energy saving but dimming could not impact the communication. The modulation is deployed on the data which supports the dimming level for receiving complete information without affecting the data transmission.

4.2.2-Flicker mitigation:

The extra requirement for VLC modulation schemes are that it should not bring human eye perceive fluctuations in the intensity of light. It has been observed in [21] that fluctuations can cause genuine unfavorable physiological changes in humans. Therefore, it is important that fluctuations in the light intensity should occur faster than the human eye can perceive it. IEEE 802.15.7 standard [22] proposes that the flickering in the intensity of light should be faster than 200 Hz to escape any unsafe impacts. It was noted that the modulation schemes for VLC should alleviate the fluctuations while offering higher data rate for communication. The most prominent reason for flickering is the long run of 0s and 1s which can decrease the rate at which light intensity changes and cause the fluctuation. Long run of 0s and 1s can be alleviated by using the Run Length limited (RLL) codes. It guarantees that the output sequence has balanced reiterations of 0s and 1s. Manchester, 4B5B, and 8B10B are commonly used for RLL codes. In Manchester coding "0" is substituted with "down" transition ("10") and "1" is denoted "up" transition ("01"). The mapping of 4B6B is done through 4 bits symbol to 6-bit symbol that has to adapt the duplications. In the same way, the 8-bit symbol is mapped into 10 bits symbol in 8B10B. The number of extra data bits are included is required in Manchester coding make it a reasonable and suitable choice for low data rate services that require better control of the 0s and 1s balance. The poor performance

of 8B10B has been observed in the DC balancing and it removes the additional bits added for high data transmission. The discussion of modulation schemes is deliberated and used for VLC communication (1) OnOff Keying (2) Pulse Modulation (3) Orthogonal Frequency Division Modulation (OFDM) and (4) Color Shift Keying modulation. The mentioned above schemes will be discussed and also how they help in VLC communication to dimming factor.

4.2.3-On-Off Keying (OOK):

In OOK, the data bits 1 and 0 are represented by LED on-off respectively. In off state, the intensity of light decreased not completely turned off. The main feature of OOK is its simplicity and easy implementation. It is mostly adopted by the wireline communication. In early work, the majority of the researchers have used OOK modulation for VLC using White LED. It produces the blue emitter with a yellow phosphor. The significant limitation of white LED is its restricted transfer speed (few megahertz [23]) because of the slow response time of yellow phosphor. It is proposed by [24] to utilize NRZ (Non-Return-to-Zero) OOK with the white LED and VLC link was demonstrated with the data rate of 10 Mbps. The blue filter is used to remove the slow response rate of the yellow component resulting in a data rate of 40 Mbps [23]. Thus, [25] and [26] has proposed to consolidate the blue filtering with simple equalization at receiver to confine and achieve data rates of 100 Mbps and 125Mbps respectively. The performance can be enhanced through suitable photodiode selection. The authors in [42] demonstrated that the avalanche photodiode works well rather than the P-I-N photodiode at the receiver side. Through avalanche photodiode, the data rate was achieved up to 230 Mbps. The white light is produced by the combination of RGB frequencies. The main factor of the white LEDs is that they have not the slow response time. RGB white LEDs needs three separate driving circuits to escape the white light. In this paper [43] a distinctive approach is used and it has been observed that the RGB white LED was utilized but only the red LED is modulated by the data transmission while remaining to provide illumination. The authors have used P-I-N photodiode and achieved a data rate of 477 Mbps but could not provide the range of distance. The two methods were proposed in IEEE Standards in [22] as IEEE 802.15.7 which offers dimming support OOK is used as a modulation scheme.

1) **Redefine ON and OFF levels**: To accomplish the desired level of dimming, the different levels of light intensity are allocated to the ON and OFF levels. The benefit of this technique is that desired level of dimming can be acquired without adding an overhead bit. It retains the data rate which is same as NRZ-OOK modulation, similarly, the communication range reduces at low dimming levels. The noticeable drawback is utilizing lower intensities of light for ON/OFF makes the LEDs be worked at low power driving circuits which is, in turn, has shown to acquire changes in rendering (radiated shade of LED changes) [44].
2) **Compensation periods:** The solution of the problem is the additional compensation periods are added with the same ON and OFF level of modulation when the LED fully turned on is known as ON periods or off (OFF periods). The term duration of compensation periods is determined based on the desired level of dimming. In particular, if the required dimming level should be more than 50% the ON periods are added otherwise the OFF periods are added. In [45] authors have presented a

calculating method of dimming level based on the percentage time of active data transmission (γ) within the transmission interval T to obtain a dimming level of D as

$$\gamma = \begin{cases} (2-2D)\times 100 & : D > 0.5 \\ 2D\times 100 & : D \le 0.5 \end{cases} \quad \text{(II.3)}$$

When the desired dimming level is D with OOK, the maximum communication efficiency ED can be calculated [15] using information theoretic entropy as

$$E_D = -D\log_2 D - (1-D)\log_2 (1-D) \quad \text{(II.4)}$$

It implies that communication system efficiency is a triangular function of the dimming level with maximum proficiency at dimming level of 50%. The efficiency drops linearly when the dimming level decrease in between 0% to 100%. The data rate is reduced due to compensation periods used in dimming. The ON/OFF modulations have unchanged intensity property and also the range of communication is unchanged. To mitigate this problem of low data rate with compensation periods, in [46] suggested using inverse source coding to preserve high data rate while achieving the desired level of dimming.

4.2.4-Pulse Modulation Methods:

Pulse Modulation Methods: OOK offers different features such as simple and feasible implementation; the main restriction is its lower data rates particularly when maintaining various dimming levels. It is the motivation for design alternative modulation schemes based on pulse width and position which are expressed as follows: Pulse Width Modulation (PWM): A proficient method of accomplishing modulation and dimming through the use of PWM. In this scheme, the width of pulses is balanced based on the required dimming level while the pulses themselves take modulation signal in the form of a digital pulse. The data is transmitting when the brightness of the LED light is full. Based on dimming requirement data rate can be accommodated and adjusted. In [47] authors observed that the higher data rates can be achieved through any dimming level 0% to 100% with the modulation technique of PWM frequency. One of the most important advantages of PWM is that it achieves the dimming without changing light intensity; therefore it does not require any color shift like redefine on and off levels in the LED. PWM has a limited data rates up to 4.8kbps [47]. To cater this restriction, in [48] intended to consolidate PWM with Discrete multi-tone for jointing dimming control and communication. On transmitter-side communication based on DMT disjointed with dimming based on PWM. The Quadrature Amplitude Modulation (QAM) is bit-streamed and mapped to symbols as shown in Fig.II.7

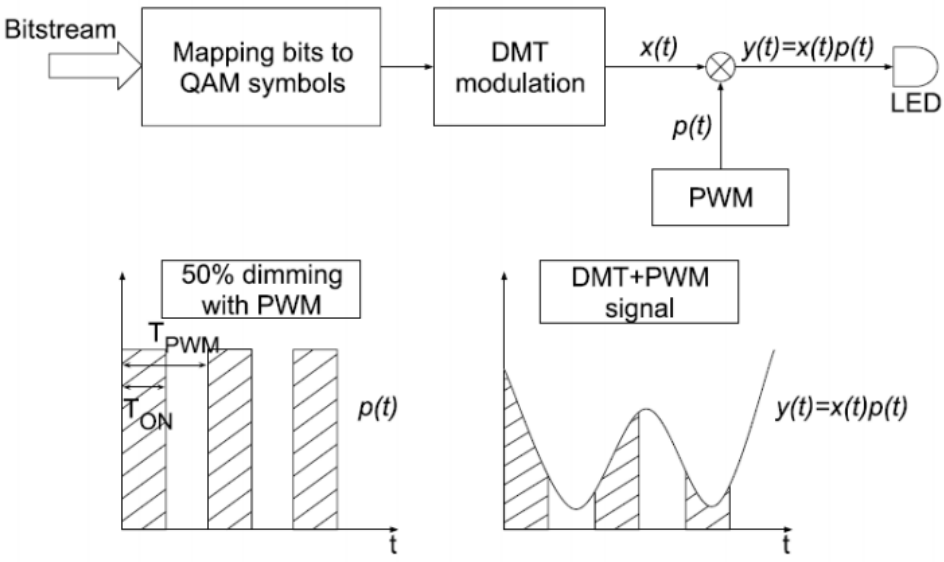

Fig. II.7 Transmitter block diagram of DMT transmitter with dimming control (top). An example of how 50% PWM-controlled dimming signal can be combined with a DMT signal [48]

Pulse Position Modulation (PPM): In visible light communication another modulation depends upon the pulse position. The symbol duration is segmented into t time slots of equal duration in PPM technique. In one time slot, the pulse is transmitted. The transmitted pulse is recognized through the position of the pulse due to its simplicity and numerous early designs [48], [49] of optical wireless communication adopt the PPM as a modulation. PPM is used for infrared communication in earlier work, in this work [50] has recommended the use of rate adaptive transmission schemes where redundancy coding is used to elegantly reduce data throughput in presence of poor channel condition. Researchers have proposed in [51] a rate variable penetrated convolution coded PPM applied in infrared communication systems and it adopts modulation order with the channel conditions through Convolution codes. For higher data rates both rate adaptive techniques were used. One is the repeated and another one is punctured convolution coded PPM [52]. Because of the restrictions of lower spectral efficiency and data rate of PPM (only one pulse per symbol duration), a different variation of pulse position based modulation has been suggested over time. The overlap PPM (OPPM) which enables the more symbols duration transmitted through one pulse [50] and the different symbols can be seen in Fig. II.8. [54] Demonstrated that OPPM not only acquired higher spectral efficiency but also a wide range of dimming levels can be achieved along with higher data rates. The other type of PPM was proposed by [55] which is known as Multi-pulse PPM (MPPM). OPPM, it enables numerous pulses to be transmitted amid the single symbol duration, however, the pulses within symbol duration do not need to be consistent as shown in Fig. 4. It has been observed and shown in [50] that MPPM can acquire a higher

spectral efficiency contrasted to OPPM. In [56] authors have suggested with introducing variation in PPM through a combination of OPPM and MPPM schemes is known as Overlapping MPPM (OMPPM). In this technique, more than one pulse position represents a single optical signal. It was observed that the OMPPM can improve the spectral efficiency of MPPM without the extension of data transfer capacity in noiseless photon tallying channel. Additional noisy channel performance analysis is demonstrated in [57]. In [58] OPPM with a low number of time slot and more number of pulses per symbol has better cut-off rate performance. In presence of background noise, the effectiveness in terms of direct detection addressed in Trellis-coded OMPPM [59]. [60], including other modulation schemes for VLC is differential PPM (DPPM) was proposed in [61] which is similar to PPM but the OFF symbol was removed and next symbol starts right after the pulse of the previous symbol. The DPPM requires low power than PPM for given bandwidth in the optical communication channel. Authors in [62] have proposed differential overlapping PPM (DOPPM) where differential cancellation of OFF symbols is used to OPPM and presents that it accomplish better spectral and cut-off performance than PPM, DPPM, and OPPM. This paper [61] has proposed EPPM (Expurgated PPM) where the symbol of MPPM are purged to maximize the inter-symbol distance. The number of pulses per symbol and length of symbols is changed to support dimming support through EPPM rather than PPM [62]. The flickering can be mitigated by EPPM as with the PPM modulation technique.

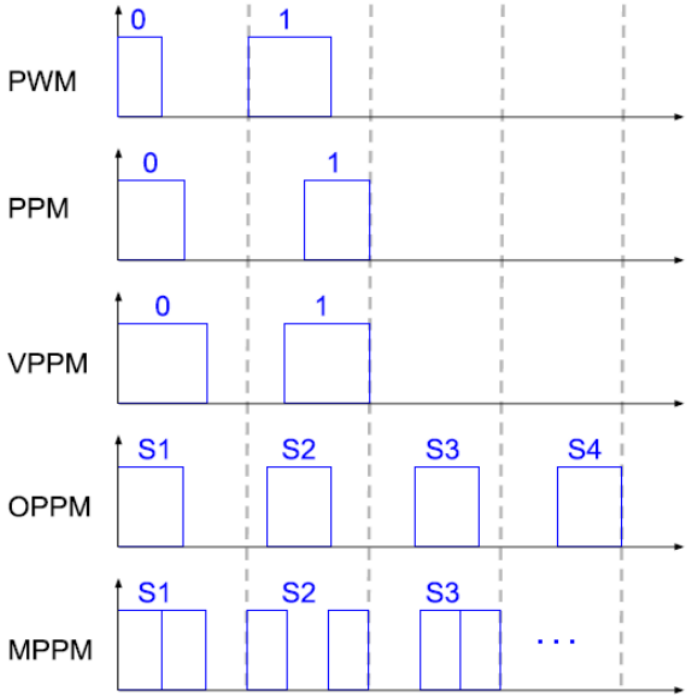

Fig.II.8 Schematic diagram showing the difference between Pulse Width Modulation (PWM), Pulse Position Modulation (PPM), Variable Pulse Position Modulation (VPPM), Overlapping Pulse Position Modulation (VPPM) and Multi-pulse Pulse Position Modulation (MPPM); Sn refers to the nth symbol. [54]

Multi level EPPM (MEPPM) broadens the EPPM design with support to multiple amplitude levels in order to increase the constellation size and spectral efficiency [63]. IEEE 802.15.7 [22] standard proposed a pulse modulation scheme call it a variable PPM (VPPM) which is

the consolidation of PPM and PWM. In this, different position of pulses is encoding with bits. The width depends on the requirement. VPPM holds that simplicity and heftiness of PPM while permitting distinctive dimming levels by change the pulse width.

4.2.5-Color Shift Keying (CSK) :

To overcome the lower data rate and limited dimming support issues of other modulation schemes, IEEE 802.15.7 standard [63] proposed CSK modulation which is specifically designed for visible light communication. CSK has attracted increasing amount of attention from research community in last couple of years [64]–[65]. As we discussed before, generating white light using blue LED and yellow phosphorus slows down the fast switching ability of LED and hinders high data rate communication. An alternative way to generating white light which is recently becoming more and more popular is to utilize three separate LEDs - Red, Green and Blue (RGB). This combined source with RGB LEDs is often referred as Tri-LED (TLED). CSK modulates the signal using the intensity of the three colors in the TLED source. CSK modulation relies on the color space chromaticity diagram as defined by CIE 1931 [66] Fig II.9.The chromaticity diagram maps all colors perceivable by human eye to two chromaticity parameters - x and y. The entire human visible wavelength is divided into seven bands as shown in Table II.1 and their centers are marked in Fig. II.9 Based on the diagram, the CSK modulation [63], [65] is performed as follows:

1) Determine RGB constellation triangle: The constellation triangle is decided based on the center wavelength of the three RGB LEDs used in the TLED source. TableII.1 shows the valid color band combinations as proposed by [65] that can be chosen as the constellation triangle depending on the central wavelength of the RGB LEDs. For the purpose of illustration, let us assume that we choose the CSK constellation triangle to be (110, 010, 000) as shown in Fig. 16a (example adapted from [65]).

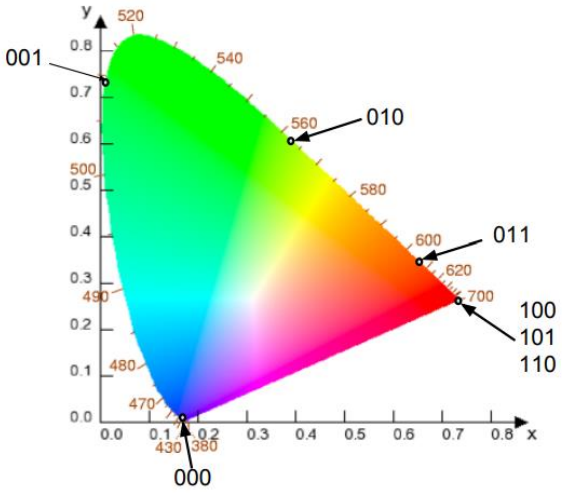

Fig. II.9. CIE 1931 Chromaticity Diagram; The seven color codes correspond to the centers of seven bands dividing the visible spectrum as shown in **Table II.1**; reproduced from [67].

Band (nm)	Code	Center (nm)	(x, y)
380-478	000	429	(0.169, 0.007)
478-540	001	509	(0.011, 0.733)
540-588	010	564	(0.402, 0.597)
588-633	011	611	(0.669, 0.331)
633-679	100	656	(0.729, 0.271)
679-726	101	703	(0.734, 0.265)
726-780	110	753	(0.734, 0.265)

TABLE II. 1: The seven bands used in CSK and their code, center and chromaticity coordinates.

	Band i	Band j	Band k
1	110	010	000
2	110	001	000
3	101	010	000
4	101	001	000
5	100	010	000
6	100	001	000
7	011	010	000
8	011	001	000
9	010	001	000

TABLE II.2: Valid color band combinations that can be chosen for building the constellation triangle for CSK. [65]

2) **Mapping data bits to chromaticity values:** Depending on 4CSK, 8CSK or 16CSK being used, the chromaticity values of symbols can be derived from the constellation triangle. For our example, Figs. 23b, 23c and 23d show how data bits can be represented using the symbols for 4CSK, 8CSK and 16CSK. Determining the position of the symbols in the constellation design requires solving an optimization problem where the distance between the symbols should be maximized to minimize the inter-symbol interference. Note that there is an additional constraint in the problem which ensures that the symbols should be equally distributed in the triangle so that the combined light emitted when transmitting different symbols is perceived by the human eye to be white light only. The optimization problem has been studied in [68]–[69] as we discuss next. Once the symbol coordinates are decided, each symbol is assigned a bit sequence (e.g. in 4CSK, the 4 symbols are assigned 00, 01, 10 and 11 respectively), which is then used to map the incoming bits to the symbols.

3) Determine the intensities of RGB LEDs:

The symbols are transmitted by varying the intensities of the RGB LEDs. The individual intensities of the three LEDs (P_i , P_j and P_k) for each symbol is calculated by solving the following equations (II.5):

$$x_s = P_i x_i + P_j x_j + P_k x_k$$
$$y_s = P_i y_i + P_j y_j + P_k y_k$$
$$P_i + P_j + P_K = 1 \quad \text{(II.5)}$$

where x_s and ys are the chromaticity values of the symbol (Fig. II.10), and (x_i , y_i), (x_j , y_j) and (x_k, y_k) are the chromaticity values of the central wavelength of the RGB LEDs being used (three points of the constellation triangle). The receiver uses the R, G and B intensities to decode the transmitted signal. Dimming support in CSK is simply amplitude dimming where the driving current of the LEDs is varied to change the brightness of resultant white light. Also, different from OOK and pulse modulations, flickering is not a problem with CSK since no amplitude variation is employed. Due to these advantages, researchers have recently attempted to improve the CSK scheme of IEEE 802.15.7 by designing its generalized forms with arbitrary constellation. Authors in [68] presented a CSK constellation design technique based on Billards equivalent disk packing algorithm. Similarly, [70] and [71] developed similar techniques with the use of different optimization algorithms such as interior point methods. All the constellation design techniques are designed to meet the color balance requirement where the TLED source is required to produce any desired color for illumination. The use of four LEDs (blue, cyan, yellow and red) was suggested in [69]. With four LEDs, it is possible to achieve a quadrilateral constellation shape that allows QAM-like constellation design. The presented system is shown to be more energy efficient as well as reliable (less inter-symbol noise) compared to the conventional CSK with 3 LEDs. The RGB tri-LED can also be used to implement Wavelength Division Multiplexing (WDM) - a multiplexing technique commonly used in fiber optics communication. Authors in [72] proposed modulating separate data streams on three colors which together multiplex to white light. With the use of DMT, an aggregate data rate of 803 Mbps was shown to be achievable using single RGB LED in [72]. Authors in [73] proposed the use of carrier-less amplitude and phase modulation on WDM VLC system with RGB LED to achieve a data rate of 3.22 Gbps.

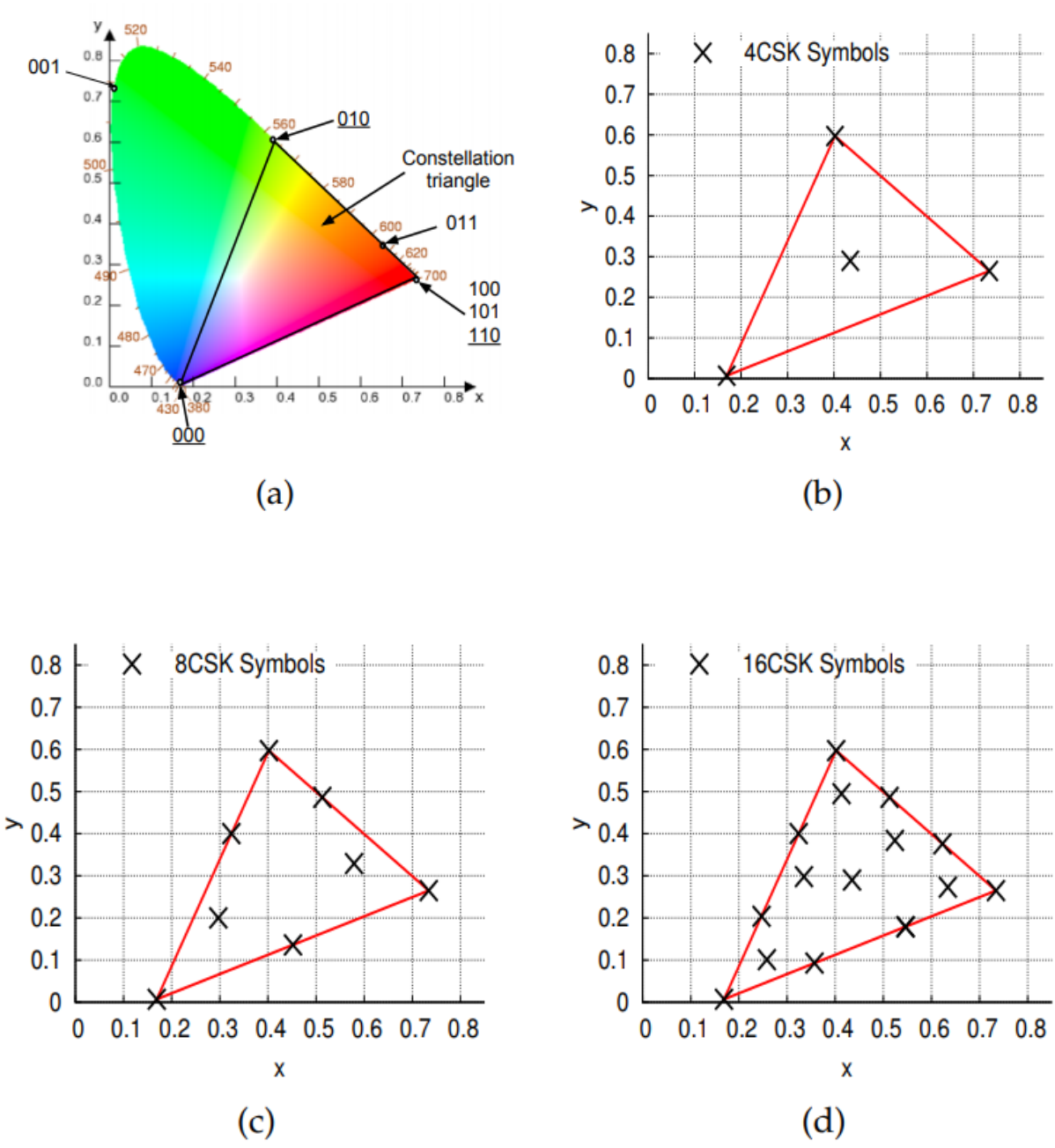

Fig. II.10: (a) RGB constellation triangle (110, 010, 000) (b-d) Symbols of 4-CSK, 8-CSK and 16-CSK. [67].

4.2.6- Orthogonal Frequency Division Multiplexing (OFDM):

Multicarrier modulation schemes can be more efficient than the baseband modulation schemes. The VLC has two main challenges: the limited bandwidth of the LEDs and the multipath propagation. The typical modulation bandwidth of LEDs is around couple tens of MHz. In order to achieve a higher data rate, complex modulation schemes such as phase shift keying (PSK), quadrature amplitude modulation (QAM), or OFDM modulations can be used. The most popular and applicable choice in VLC systems is OFDM, since it offers improved spectral efficiency than PSK, QAM and it has a strong robustness against the ISI airing from multipath propagation or limited system bandwidth [74–75]. The use of OFDM was noted first in [76] and its popularity increased significantly as the OFDM is robust against multipath propagation [74]. The multipath propagation causes linear distortion in the channel and it leads to ISI. In order to reduce the linear distortion of the dispersive channel, a cyclic prefix can be inserted to the OFDM symbols. Therefore, the symbol period of an OFDM symbol should be increased. This growth of the symbol period which is called guard interval needs to be higher than the impulse response of the channel [77,78]. The multipath propagation can also cause frequency selective fading in the RF system, and it leads to ISI as well [77]. However, by dividing the channel to N parallel parts, the bandwidth of each channel part is smaller than the coherence bandwidth of these parts. Thus, the linear distortion of the channel may be avoided; therefore, the OFDM system can reduce dispersion effect compared to the single carrier system [77]. The multicarrier systems like OFDM have an added advantage: unmodulated pilot tones can be used for characterizing the dispersive channel. The effect of the characterized dispersive channel can be equalized at the receiver [75]. The capacity of a multicarrier system can be increased by partly overlapped subcarriers. In this case, the subcarriers are orthogonal, hence, the nearby channels do not disturb each other. As OFDM does not need to apply guard bands, thus the capacity of the link is as large as the capacity of the single carrier system [77]. The comparison of the spectral efficiency of different modulation types is shown in Figure II.11.

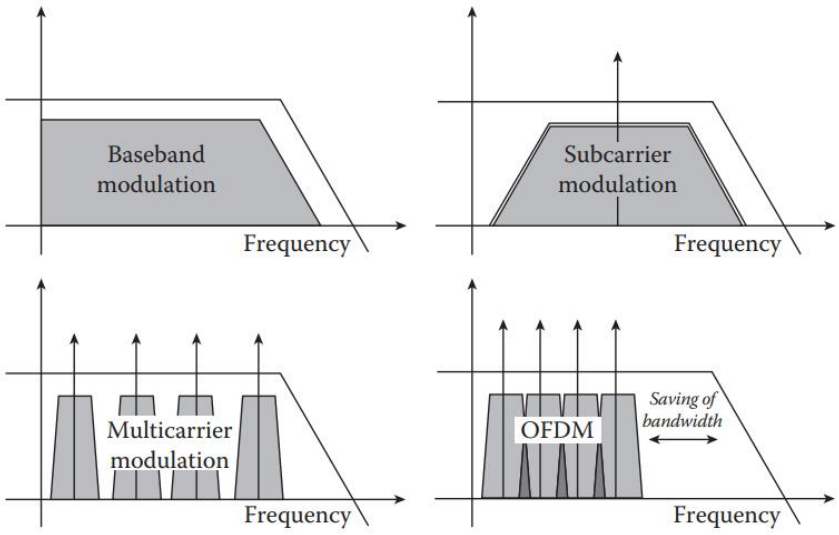

Fig. II.11 Spectral efficiency of different modulation types.

So, the OFDM is capable of combining the high channel capacity with the protection against multipath propagation, frequency selective fading. All of these reasons make the OFDM scheme a suitable modulation type of VLC system [79]. The traditional OFDM signal widely applied to RF system is complex and bipolar. Due to IM/DD, the signaling for VLC system must be a real and unipolar [80,81]. Therefore, the traditional OFDM signal is modified to make them real-valued and unipolar. There are a number of variations of the unipolar OFDM that are proposed for VLC system such as DC-biased optical OFDM (DCO-OFDM), asymmetrically clipped optical OFDM (ACO-OFDM), unipolar OFDM (U-OFDM), pulse-amplitude-modulated discrete multitone modulation (PAM-DMT), and Flip-OFDM.

A) **DC-biased optical OFDM:** DCO-OFDM is the easiest way to ensure the non-negativity of OFDM signals. DCO-OFDM adds a DC bias to the bipolar OFDM signal. The required DC bias to satisfy nonnegativity is equal to the maximum negative amplitude of the OFDM signal [36]. The time samples of the bipolar OFDM and DCO-OFDM are compared in Figure

In conventional RF OFDM schemes, the data are transmitted in parallel on multicarriers. The orthogonality of subcarriers ensures that the symbols in the same OFDM block do not interfere with each other. Because OFDM is capable of mitigating ISI effectively, it is an ideal modulation scheme for VLC for high-rate transmission. The optical OFDM scheme inherits the basic attributes from its RF counterparts but also exhibits several differences. Most of all, optical OFDM is directly modulated on the intensity of emitted light and constrained to be real-valued and nonnegative. Modification is embedded in optical OFDM to satisfy this constraint. In this subsection, a representative multicarrier scheme, referred to as DCO-OFDM [82], is introduced .Figure II.12 depicts the architecture of DCO-OFDM transceiver. Assuming that total N subcarriers are allocated in a single OFDM block, where N is typically a large even number. At the transmitter, the serial bit stream is first converted to a parallel sequence and then mapped to the N/2 − 1 complex-valued symbols according to the specific modulation constellation X such as quadrature amplitude modulation (QAM) [83]. The modulated OFDM block $X = [X_0\ X_1 \cdots X_{N-1}]$, where subscript number denotes the associated subcarrier index, is constructed as follows: $X0 = 0$ and X_1 to $X_{N/2-1}$ carry the N/2 − 1 information symbols, while $X_{N/2}$ to X_{N-1} satisfy the Hermitian symmetry as

$$X_k = X_{N-k}^*, k = N/2, \ldots, N-1, \quad \text{(II.6)}$$

mitter to generate real-valued timedomain signals. The OFDM symbol vector X is fed to the processor of inverse fast Fourier transform (IFFT) and converted to discrete time-domain samples

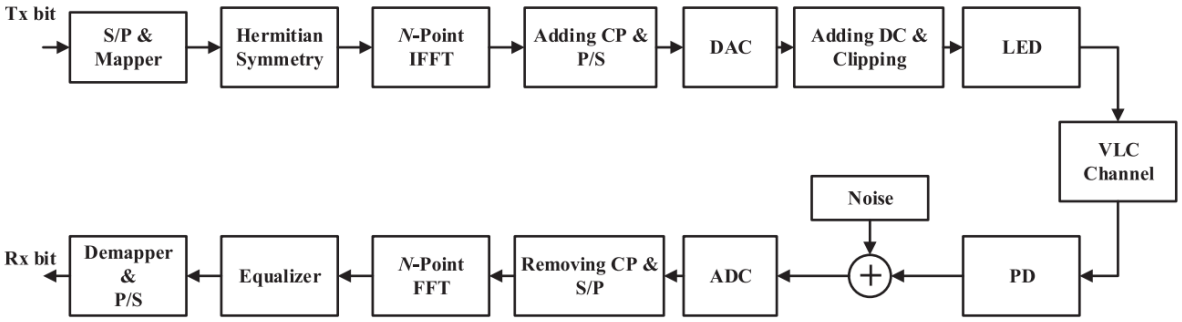

Fig.II.12 The block diagram of DCO-OFDM transceiver for visible light communications.

After IFFT, a CP of length L_{CP}, which is the copy of the last L_{CP} samples of each time-domain DCO-OFDM block, is appended in its front. CP provides guard interval without destroying the orthogonality of subcarriers. When L_{CP} exceeds the maximum delay of the dispersive channel, ISI is totally discarded .Then the discrete samples are converted into a serial sequence and fed to a digitalto-analog converter (DAC). The converted electrical signal x (t) is still bipolar and is not feasible for intensity modulation. A DC bias B_{DC} should be added to x (t). In DCO-OFDM, After biasing and clipping, the electrical DCO-OFDM signal x_{DCO} (t) is used to drive the LED and to be modulated on the intensity of illumination. According to the central limit theorem, x (t) approximates a Gaussian distribution with zero mean when N ≥ 64 [82] Therefore, the optical power of DCO-OFDM is BDC , BDC is set to :

$$B_{\mathrm{DC}} = \mu\sqrt{E\left\{x^2\left(t\right)\right\}}, \quad \text{(II.7)}$$

At the receiver, the photodiode (PD) component captures the optical signal from the VLC channel and transforms it into the electrical signal y (t). A lens can be placed in front of the PD to filter the background light. In the PD, the thermal noise and shot noise interfere with the received signal. These two types of noise can be both modeled as additive white Gaussian noise (AWGN) [84]. Thus, for the dispersive VLC channel with the impulse response h (t), the received signal y (t) is expressed as:

$$y\left(t\right) = h\left(t\right) \star x_{\mathrm{DCO}}\left(t\right) + w\left(t\right), \quad \text{(II.8)}$$

where the notation "*" denotes the convolution operation and w (t) is the AWGN with zero mean. After analog-to-digital converter (ADC), the received DCO-OFDM discrete sample block is acquired with the CP removed and then is reshaped as the parallel sequence $\{y_n, n = 0, 1, N - 1\}$.

To recover the transmitted data symbols, the N-point FFT component converts the time-domain samples into the frequency-domain symbols $\{ Y_k, k = 0, 1, ..., N - 1 \}$. For each subcarrier, the associated channel is flat. Hence, simple one-tap equalization method is imposed. The equalizer divides the received symbols $\{Y_k, k = 1, 2, ..., N/2 - 1\}$ on the used

subcarriers by the associated channel state information (CSI) H_k, which can be estimated according to the pilot embedded in DCO-OFDM signals.

The DCO-OFDM is a simple solution to get unipolar OFDM signal, but the main disadvantage is the lower power efficiency.

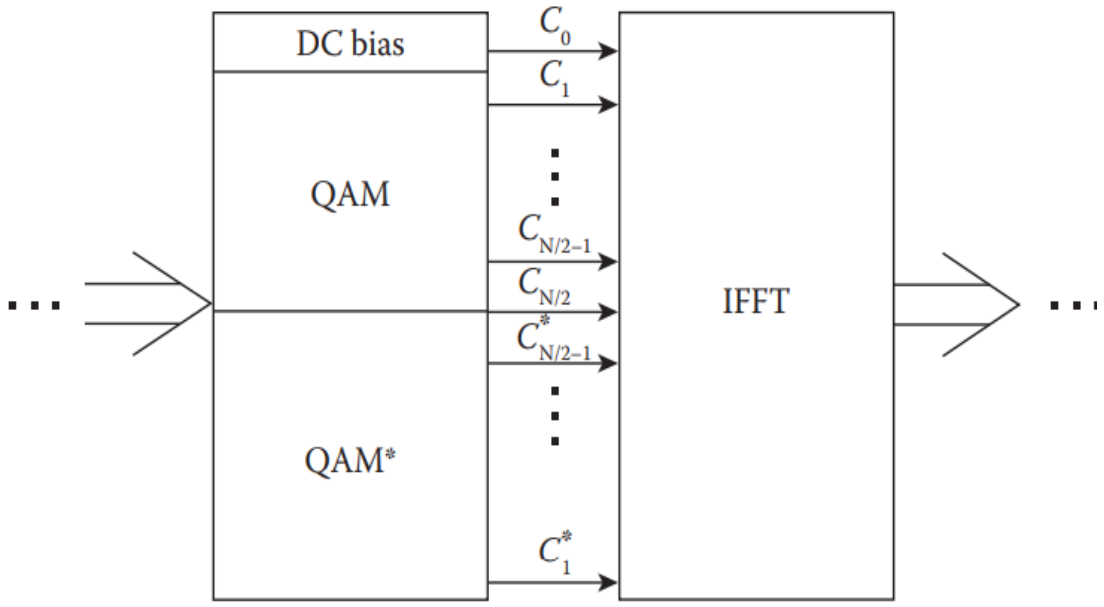

Fig.II.13 Block diagram of DCO-OFDM. [84]

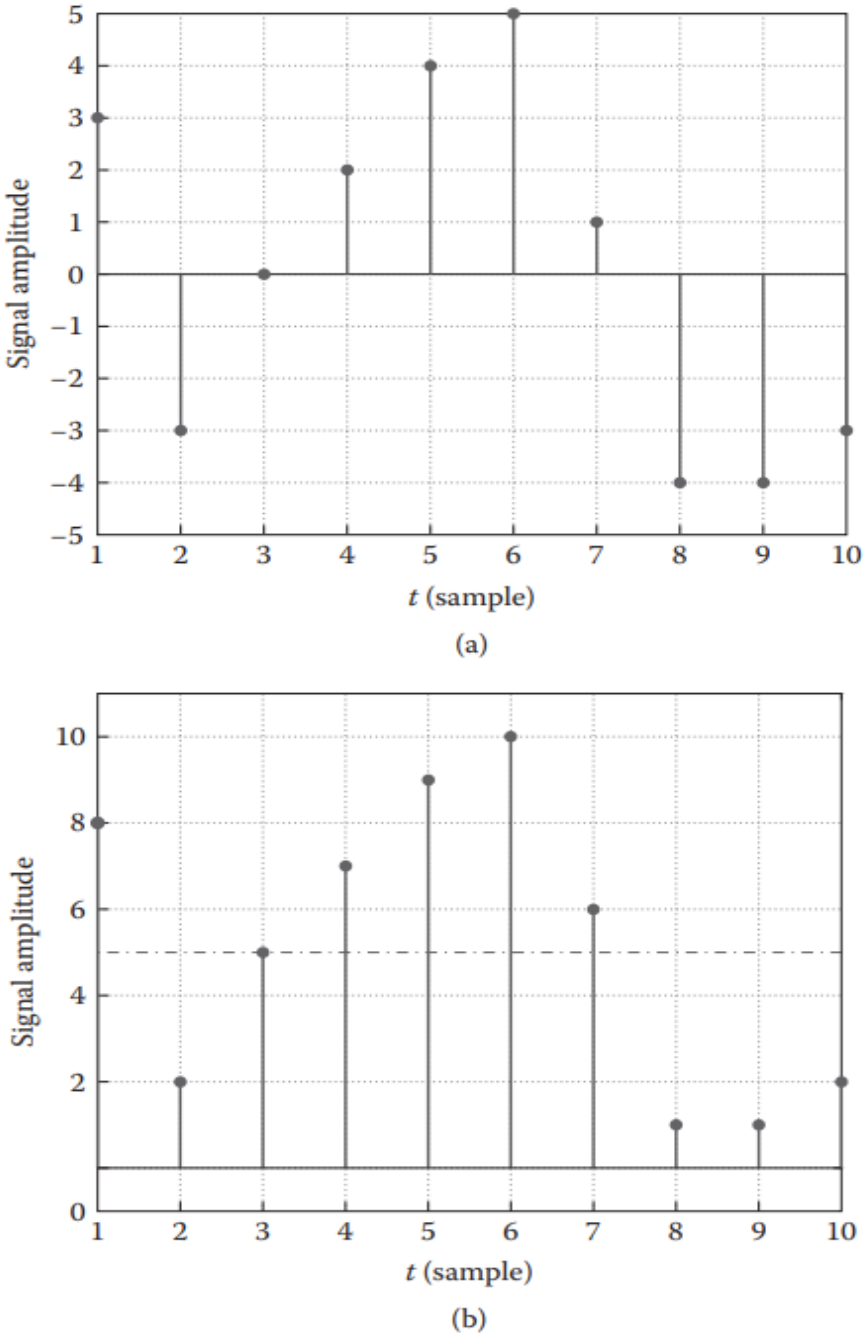

Fig.II.14 The samples of (a) bipolar OFDM and (b) DCO-OFDM. [84]

B) **Asymmetrically Clipped Optical OFDM (ACO-OFDM) :** The block diagram of ACO-OFDM is similar to its DCO-OFDM counterpart. The major difference is the allocation of data symbols. In the ACO-OFDM scheme, the data symbols are only placed on the odd subcarriers of the first N/2 subcarriers and hence, an ACO-OFDM block of N subcarriers can only accommodate N/4 information symbols. Considering the constraint of real-valued amplitude, the Hermitian symmetry constraint of (II.1) is also imposed on the (N/2)th to (N - 1)th subcarriers.
In order to improve the power efficiency of the unipolar OFDM modulation format, negative signal clipping at zero level is applied. The ACO-OFDM can be expressed mathematically as [81]:

$$s_{ACO-OFDM}(t) = \begin{cases} s_{OFDM}(t) & \text{if } s_{OFDM}(t) \geq 0 \\ 0 & \text{if } s_{OFDM}(t) < 0 \end{cases}. \quad \text{(II.9)}$$

The clipped signal is shown in Figure II.16 When the DC bias is set to zero, the hard clipping might be avoided by applying ACO-OFDM [86]. It is shown in [85,87] that the clipping noise can be avoided by encoding information symbols on only the odd subcarriers as shown in Figure II.15 [80]. Since only odd subcarrier is modulated, the ACO-OFDM has only the half the spectral efficiency of DCO-OFDM. However, there is no information loss when the signal is clipped, because of the antisymmetry of the modulated signal.

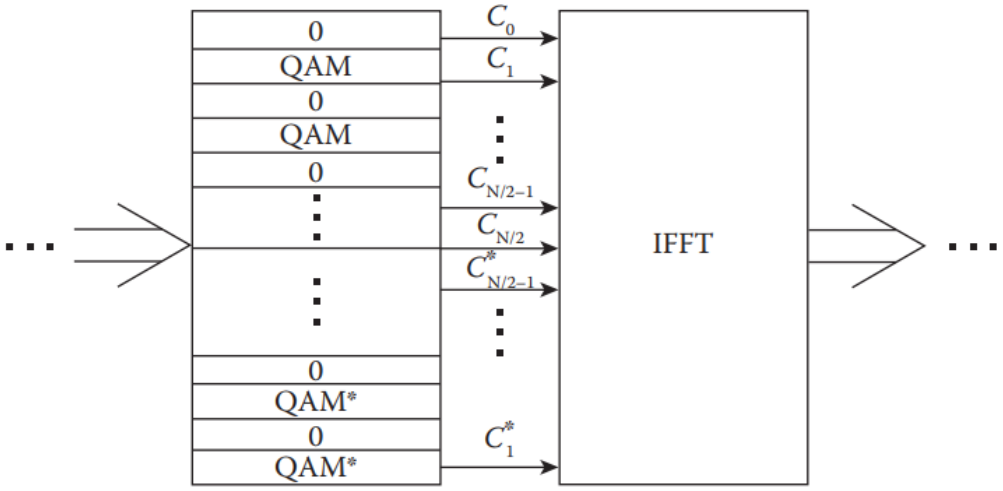

Fig II.15 .Modulation scheme of ACO-OFDM. [80]

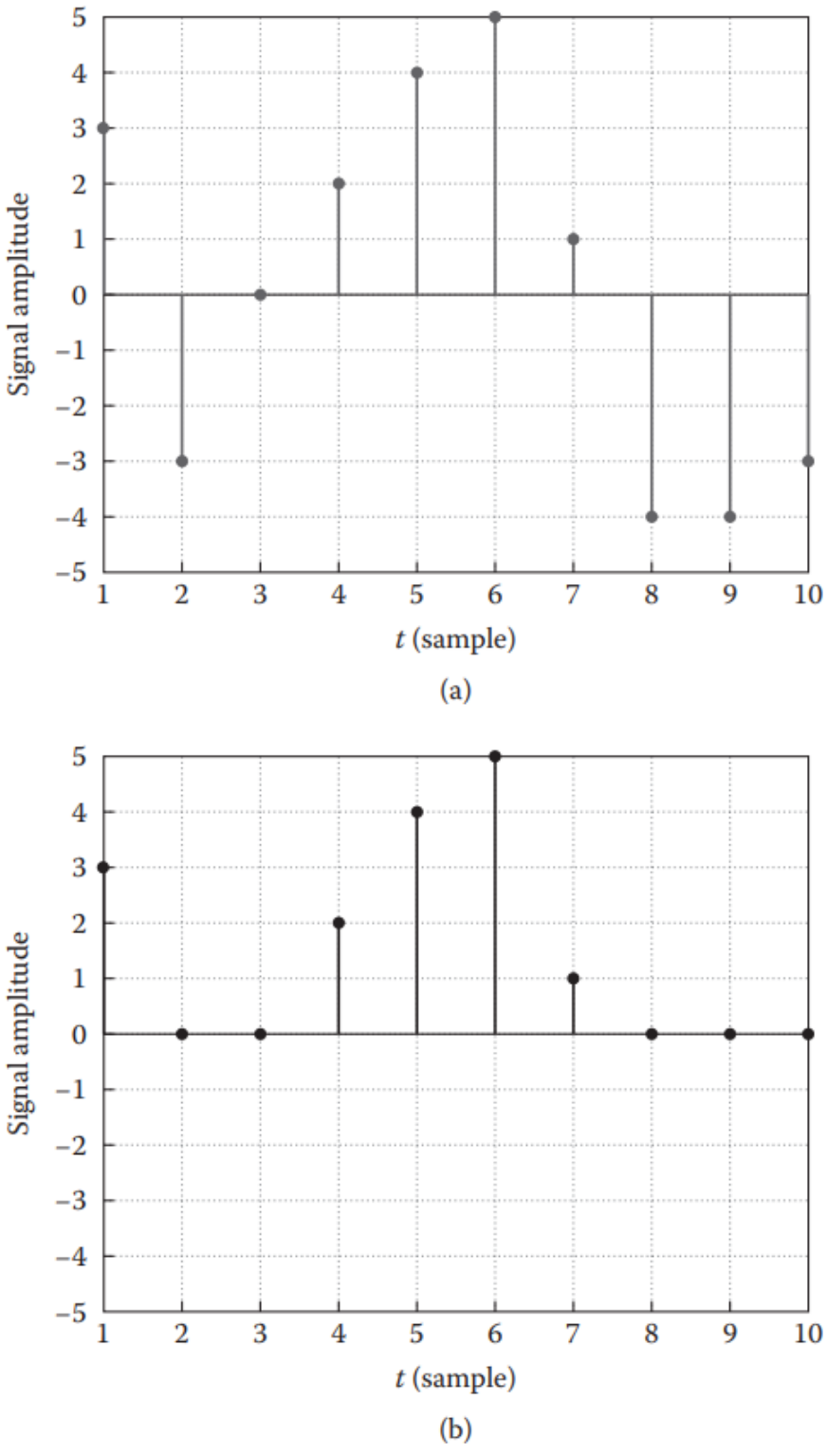

Fig.II.16 The samples of (a) bipolar OFDM and (b) clipped OFDM. [86]

C) Pulse-Amplitude-Modulated Discrete Multi-tone (PAM-DMT):

PAM-DMT is similar to ACO-OFDM, but the subcarriers are modulated by PAM. Furthermore, the mathematical expression of PAM-DMT is equal to the mathematical expression of ACO-OFDM (Equation II.9), as it applies asymmetrical clipping. The figure of the clipped signal is also the same for PAM-DMT (Figure II.18). According to [88], if the data are modulated using PAM only on the imaginary components of the subcarriers, clipping noise does not affect the system performance since noise is a real value signal, so it is orthogonal to the modulation [85]. The modulation scheme of PAM-DMT is shown in Figure II.17 [80]. In a PAM-DMT system, there is no DC bias. All of the subcarriers are modulated, but the modulation uses only the imaginary part of the subcarrier, thus the spectral efficiency is the same as ACO-OFDM [85]. Although it has a limited spectral efficiency, it is more power efficient than DCOOFDM, because it has also an antisymmetry (Hermitian symmetry). It is described in [79,89]

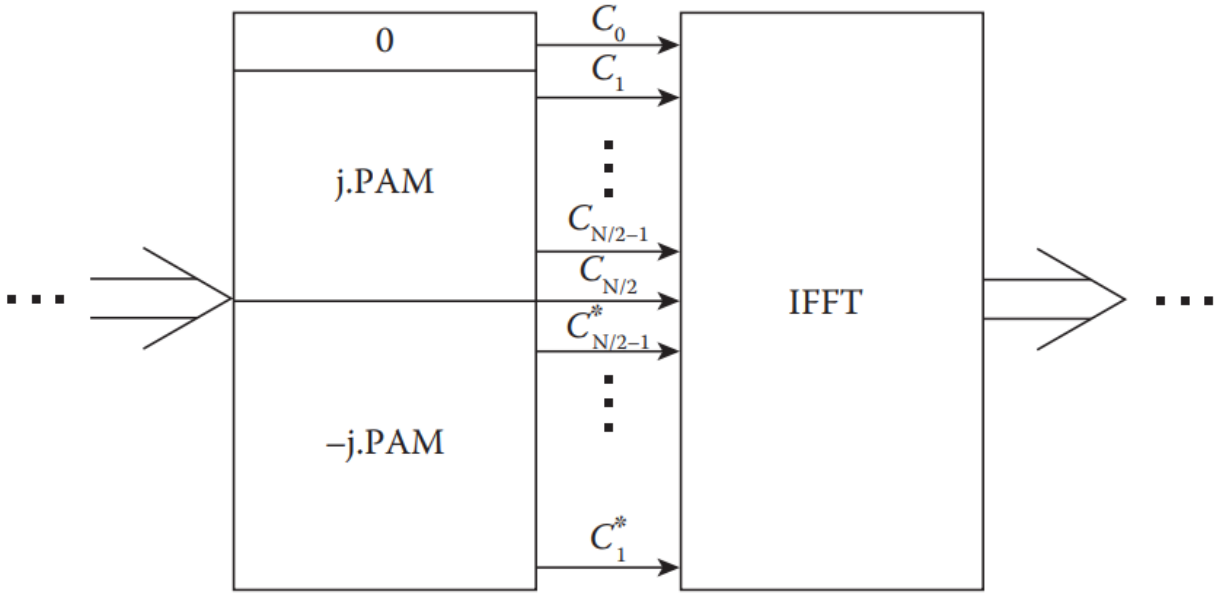

Fig II.17.Modulation scheme of PAM-DMT. [85]

Similar to ACO-OFDM, the clipping of the negative signals does not lead to the information loss, because the clipped signal components can be reconstructed by using this anti-symmetry [76]. The clipping noise is also orthogonal to the modulation, as the data have only imaginary part, but the clipping noise is a real value [86]. The next equation describes the clipped PAM-DMT according to [79] is given by:

$$\mathrm{Im}\{X_c(k)\} = \frac{D_k}{2}, \qquad \mathrm{Re}\{X_c(k)\} = \mathrm{Re}\{X_c^n(k)\}, \tag{II.10}$$

where D_k is chosen from PAM symbols. The original PAM-DMT is $X_{(k)} = j*D_k$ [76]. The imaginary part of the clipped signal is half of the original signal, the real part of the signal is only the clipping noise.

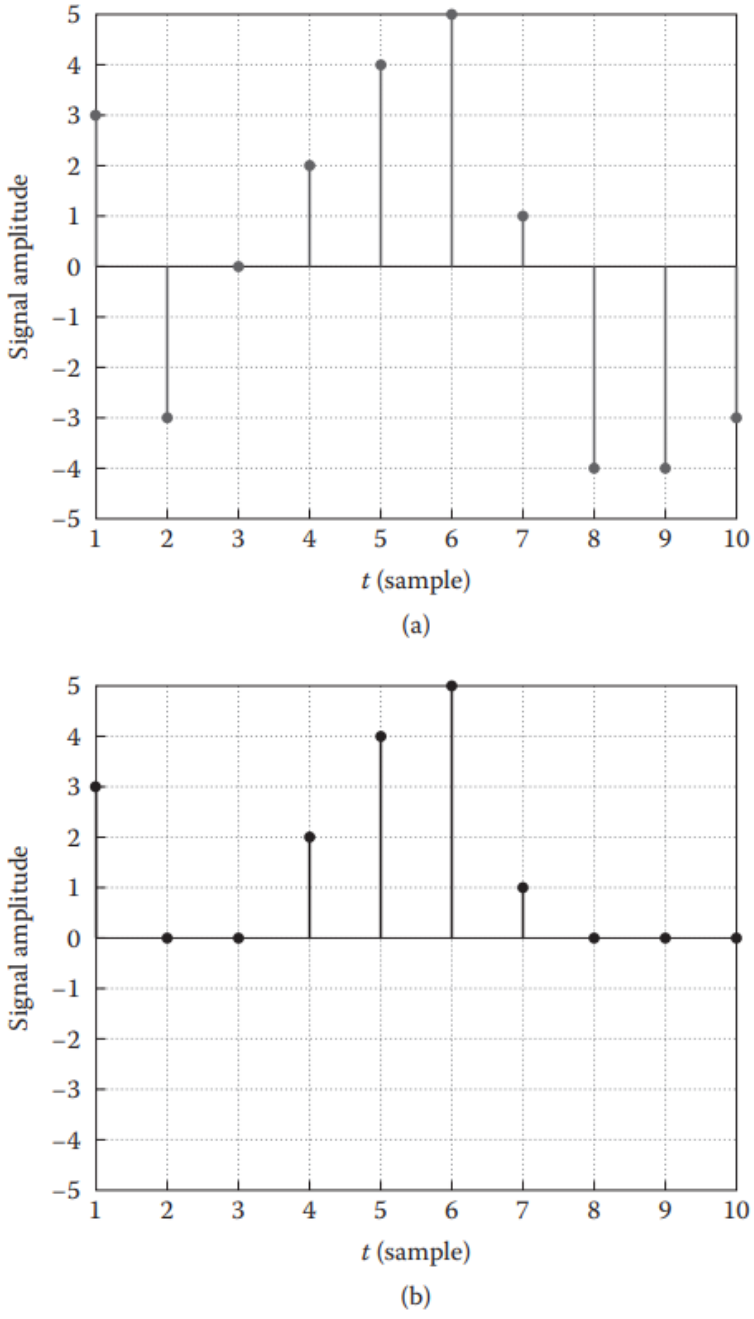

Fig II.18 The samples of (a) bipolar OFDM and (b) clipped OFDM. [76]

D) **Unipolar OFDM (U-OFDM)** : The U-OFDM was introduced in [88], and an almost the same concept named Flip-OFDM was suggested in [45]. In U-OFDM (or Flip-OFDM), the negative and the positive part of the real bipolar OFDM signal are extracted. Hence, the Hermitian symmetry is preserved. The polarity of the negative parts of the symbol is inverted before the transmission of both positive and negative parts in a consecutive OFDM symbol [88]. The bipolar OFDM symbol and the U-OFDM symbol are compared in Figure II.19 and also Figure II.20.

The mathematical formula of the U-OFDM symbol can be expressed as [45] :

$$s_H[i] = s_H^+[i] + s_H^-[i - \frac{N_{SC}}{2}], \quad \text{(II.11)}$$

At the demodulator side, the original OFDM can be recombined by subtracting the negative frame [89].

Figure II.19 exemplifies the encoding procedure in U-OFDM. The eight-point bipolar sequence is the original OFDM signal ,this sample sequence is extended into a 16-point sample signal. The first half of the U-OFDM signal, denoted by the blue circle, allocates the positive part of the original OFDM signal and sets the negative sample as zero. In the second half with the legend of red circle, the absolute values of the original negative samples are placed.

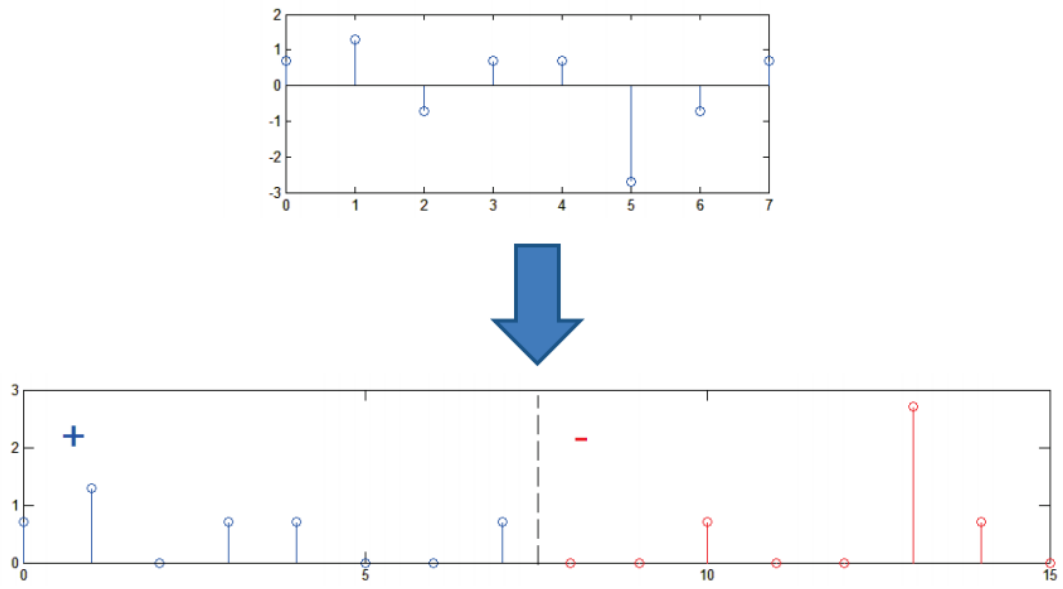

Fig II.19 Unipolar optical OFDM signal encoding. [89]

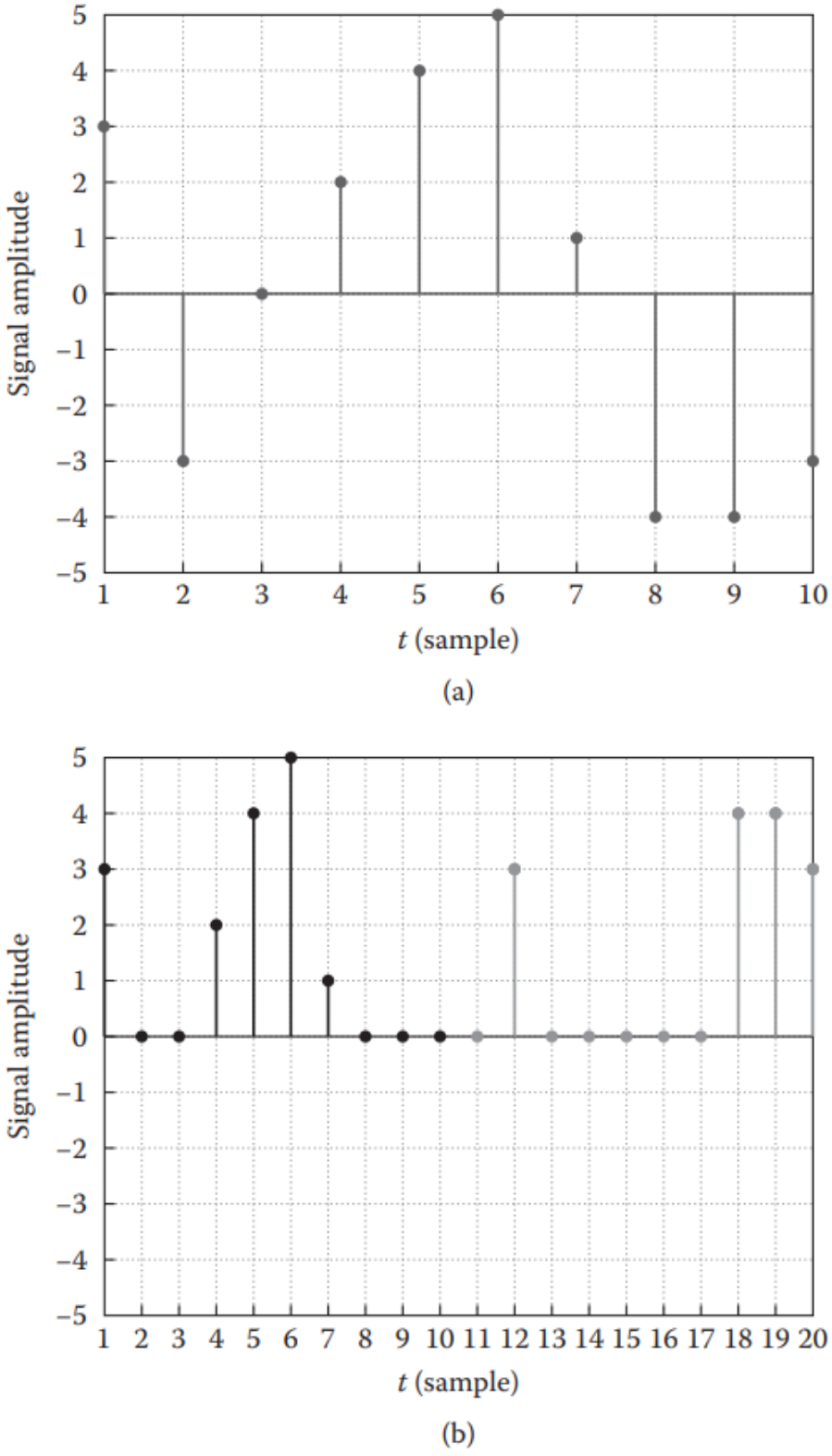

Fig II.20 The samples of (a) bipolar OFDM and (b) U-OFDM. [88]

5-Multiple Input Multiple Output (MIMO):

In order to provide sufficient illumination, most of the luminaires typically contain multiple LEDs. These multiple LEDs can be treated as multiple transmitters that can enable visible light MIMO communication. In RF communications, MIMO systems are commonly used (in IEEE 802.11n, Long-Term Evolution - LTE) to obtain higher data rates. Similarly, multiple LEDs can be used for higher spectral efficiency in VLC.MIMO systems in VLC are difficult to realize compared to RF communications. In RF MIMO systems, the throughput gains are largely attributed to spatial diversity (existence of multiple spatial paths that are diverse in nature). However, such diversity gains are limited in VLC MIMO because paths between the transmitter and receiver are very similar (less diverse) especially in indoor scenarios. This limits the available spatial diversity of VLC MIMO systems. The other challenge in VLC MIMO is the design of the receiver.

5.1-.MIMO Receiver:

There can be two types of receivers in VLC MIMO systems - photodiode and image sensor. The performance of the system depends on whether imaging (image sensor) or non-imaging (photodiode) receiver is used [90].

A) **Non-imaging receiver** in a MIMO system is a set of independent photodiodes each with its individual concentrator optics. The advantage of such a receiver is that a very high gain can be achieved due to narrow FOV of each photodiode. The disadvantage, however, is that such a receiver requires careful alignment with the transmitters because of the narrow FOV, and the capacity can reduce dramatically even with minor misalignment.

B) **Imaging Receiver:** Since an image sensor contains a projection lens and a large matrix of photodiodes, it has the potential to create a high data-rate MIMO link. The projection lens ensures a large FOV which nearly eliminates the alignment requirement. The disadvantage of such as a receiver is that individual photodiodes have limited gain and advance image processing is required to create an efficient MIMO channel. Also, the sampling rate of the image sensor is comparatively lower further reducing the achievable throughput. The channel models of both imaging and non-imaging receiver MIMO, and their relative benefits and limitations were presented in [90]. It was shown in [91] that an "ideal" MIMO receiver can be a hybrid of imaging and non-imaging sensors which can achieve high gains of LOS paths using narrow FOV like photodiodes and can be robust by leveraging non-LOS paths whenever needed like an image sensor. Authors in [92] proposed the design of a spherically-shaped receiver that is made of a large number of photodiodes. Each of the photodiode has a narrow FOV and points in different direction in the room. The photodiodes pointing to transmitter LED can receive the signal with high gain while other photodiodes pointing to other directions can establish non-LOS channels to increase spatial diversity. However, using such a receiver incurs cost for additional hardware. Instead, authors in [93] proposed a way to improve the lower sampling rate of the image sensor. A token-based pixel selection method was proposed where

instead of conventional row-scanning approach, only the pixels of interest are selectively scanned to improve the sampling rate.

MCS	Modulation	RLL code	Optical clock rate	FEC		Data rate (kbps)
				Outer code (RS)	Inner code (CC)	
0	OOK	Manchester	200 KHz	(15,7)	1/4	11.67
1				(15,11)	1/3	24.44
2				(15,11)	2/3	48.89
3				(15,11)	none	73.3
4				none	none	100
5	VPPM	4B6B	400 KHz	(15,2)	none	35.56
6				(15,4)	none	71.11
7				(15,7)	none	124.4
8				none	none	266.6

TABLE II.3: 802.15.7 PHY I operating mode specifications and achievable throughput. [90]

MCS	Modulation	RLL code	Optical clock rate	FEC	Data rate (Mbps)
16	VPPM	4B6B	3.75 MHz	RS(64,32)	1.25
17				RS(160,128)	2
18			7.5 MHz	RS(64,32)	2.5
19				RS(160,128)	4
20				none	5
21	OOK	8B10B	15 MHz	RS(64,32)	6
22				RS(160,128)	9.6
23			30 MHz	RS(64,32)	12
24				RS(160,128)	19.2
25			60 MHz	RS(64,32)	24
26				RS(160,128)	38.4
27			120 MHz	RS(64,32)	48
28				RS(160,128)	76.8
29				none	96

TABLE II.4 802.15.7 PHY II operating mode specifications and achievable throughput [90]

5.2-VLC MIMO Techniques:

There are three types of VLC MIMO techniques proposed in literature [94]:

A) **Repetition Coding (RC):** This is the simplest technique where the same signal is transmitted from all the transmitters. The transmitted signal from all LEDs meet constructively at the receivers increasing the overall gain.

B) **Spatial Multiplexing (SMP):** In SMP, different data is transmitted from each transmitter to a receiver photodiode. With multiple transmitters and receivers, this type of MIMO creates multiple parallel SISO streams. The challenge is that receiver photodiodes have to be accurately aligned to the transmitters to avoid any inter-channel interference. SMP MIMO for optical channels has been studied in some of the early works [97]–[92]. In [95], [97], authors proposed optical wireless MIMO communication with subcarrier multiplexing where zero forcing was utilized to cancel the interference from other transmit antennas. It was shown that for the transmitter semi-angle more than 20o , the transmitter-receiver separation should be more than 1.5 meters for lower BER. The impact of optical beat interference on OMIMO scheme of [95] was studied in [96]. Optical beat interference is the signal degradation caused by multiple transmitters transmitting simultaneously on nearby wavelengths.

C) **Spatial Modulation (SM):** This MIMO technique was proposed by [98]–[99] where only one transmitter transmits data at any point of time. The constellation diagram is extended to include the spatial dimension. Each transmitter LED is assigned a specific symbol and when data bits to be transmitted matches the symbol, the LED is activated. The receiver estimates which LED was activated based on the received signal, and uses this to decode the transmitted data. Since the data is encoded in both spatial and signal domain, SM achieves much higher spectral efficiency compared to other techniques.

A comparison of all the three MIMO techniques were provided in [94]. It was shown that RC is less restrictive in terms of its requirement for transmitter-receiver alignment but provides only a limited spectral efficiency. SMP, on the other hand, requires more careful alignment of transmitter-receiver but also provides higher data rates compared to RC. SM achieves the best of both worlds by being robust to correlated channels and providing higher spectral efficiency. Also, it was shown in [100] that imaging receivers can obtain much higher SNR when using SM or SMP technique compared to the non-imaging receivers.

Due to its advantages over other MIMO techniques, SM has been studied further in recent years. It was shown in [101], [102] that power imbalance between the transmitter LEDs can improve the performance of spatial modulation especially when optical paths between the transmitter and receiver are highly correlated. Authors in [103] studied the performance of spatial modulation using an implementation of 4 × 4 MIMO system and showed that the challenge in achieving higher throughput with SM is to maintain symbol separation in the constellation from the receiver's perspective. Researchers investigated the performance of spatial modulation in [101] when only partial channel state information (CSI) is available and

concluded that highly accurate CSI estimation is necessary to realize the full potential of SM. The use of generalized spatial modulation was proposed in [105], [106]. Such modulation extends the original scheme by allowing more than one transmitter to be active during a symbol duration. It was shown that due to additional flexibility of activating multiple LEDs, the generalized scheme can achieve higher spectral efficiency compared to the conventional scheme, however, at the cost of additional complexity in constellation design. Optical MIMO for non-LOS diffuse links has not received much attention. Authors in [107] showed how backward spatial filter can be used for optical wireless MIMO in diffuse channels (no precise alignment of transmitter and receiver). With user movements, such diffuse channel are more likely in practical scenarios and optimizing MIMO performance for such channels should be investigated further.

5.3-Optical Beamforming:

Beamforming allows multiple transmitters to concentrate their signal in a specific direction based on the receiver location. Figure II.21 .This type of transmit beamforming is well studied in RF communication and also utilized by recent WLAN standards such as IEEE 802.11ac. Similar to RF beamforming, emitting light from multiple LEDs can be focused towards the receiver to create optical beamforming. Recently, it was shown in [108] how light emitted from a single LED can be focused in a specific target direction using Spatial Light Modulator (SLM). SLM is an additional device that is required to modulate the phase or amplitude of the visible light signal. It was shown that significant SNR improvements can be achieved by using the optical beamforming with any modulation technique. Authors in [109] derived the transmit beamforming vectors when multiple LEDs are used to perform the optical beamforming. Optical beamforming can improve the performance of a visible light communication link significantly, however, there is only a limited amount of research done towards this. Performing optical beamforming while meeting the illumination constraints is an important direction for research in VLC MIMO systems.

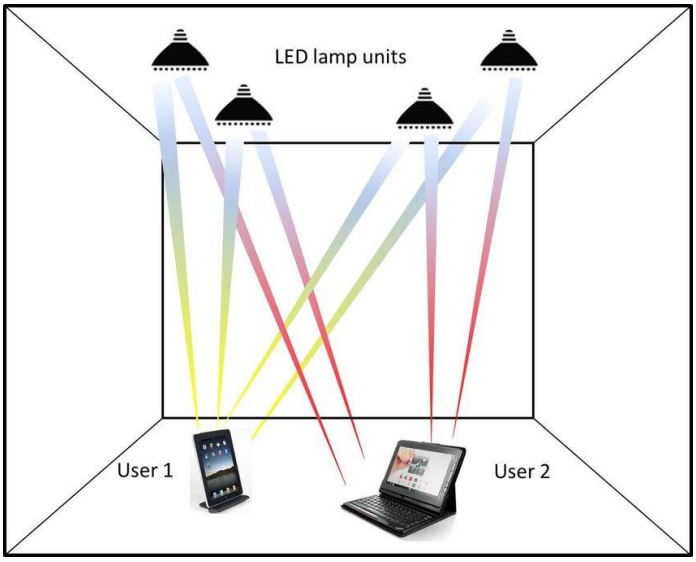

Fig II.21 Optical Beamforming in MIMO illustration [108]

6-Link Layer:

When there exists multiple transmitter LEDs and receiver devices connected to them, it is essential to control the medium access, device association and device mobility. In this section, we provide an overview of different techniques proposed in literature to manage link layer services.

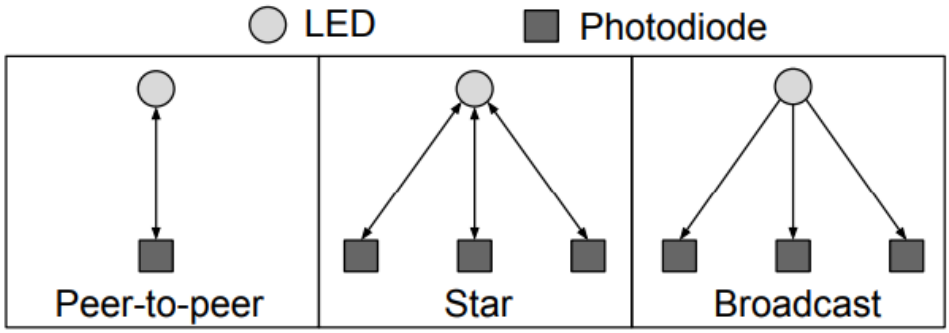

Fig II.22 VLC link layer topologies [108]

6.1 Medium Access Control (MAC):

The application scenarios of VLC can be used to identify the link layer topologies that need to be supported by the MAC protocols. IEEE 802.15.8 [63] proposes three types of link layer topologies for VLC as shown in Fig. II.22 –

1) Peer-to-peer: The peer-to-peer topology involves one device acting as a coordinator (or master) for the link between two devices. Both devices can communicate with each other since the client has an uplink to the master. This topology is typically more suitable for high-speed Near-Field Communication (NFC).

2) Star: In a start topology, there can be many client devices connected to a master device which acts as the coordinator. A typical use case of this topology is VLC wireless access networks. The MAC design is especially challenging in the star topology due to many bi-directional links in the same collision domain.

3) Broadcast: Different from the star topology, the client devices in a broadcast topology can only receive data from the master LED transmitter without forming any uplink. Such topology can be used for broadcasting information via LEDs throughout the network. Since there is no explicit association needed, the broadcast topology simplifies the MAC design

Three types of multiple access control (MAC) schemes are proposed for VLC - Carrier Sense Multiple Access (CSMA), Orthogonal Frequency Division Multiple Access (OFDMA) and Code Division Multiple Access (CDMA).

- **CSMA:** There are two types of random channel access mechanisms proposed by IEEE 802.15.7 standard. In the first type, the beacons from the coordinator are disabled. Such beacon-disabled random access uses an unslotted random channel access with CSMA. Here, if a device wishes to transmit, it first waits for a random back-off period and then senses the channel to be busy or not, before transmitting. If the channel is found to be busy, the device waits for another random period before trying to access the channel again. In the second type where the beacons are enabled, the time is divided into beacon intervals. A superframe within the beacon interval contains Contention Access Periods (CAP) and Contention Free Periods (CFP) as shown in Fig. 18(a). If a device wishes to transmit, it first locates the start of a next backoff slot and then waits for a random number of backoff slots before performing Clear Channel Assessment (CCA). If the channel is found to be idle, the device starts to transmit. If the medium is found to be busy, the device waits for additional random number of backoff slots before performing the CCA again. The beacon-enabled random access also contains contention free period which consists of multiple Guaranteed Time Slots (GTS). This period is used by the coordinator to ensure medium access to devices with delay or bandwidth constrained applications. Depending on the requirement, a coordinator can also assign multiple time slots to one GTS. Figs. 18(b), 18(c) and 18(d) show how different types of slots are used for beacon-disabled access in peer-to-peer topology, beacon-enabled access in star and broadcast topologies respectively.

- **OFDMA:** OFDMA is a multi-carrier multiple access scheme where different users are assigned separate resource blocks (set of subcarriers in time) for communication. Application of OFDMA for multiple access in VLC is a natural extension to utilizing OFDM for modulation in physical layer. Two variations of OFDMA were compared in [106] and it was shown that power efficiency and decoding complexity are two main challenges while applying OFDMA to VLC. Authors in [110] proposed a heuristic solution to subcarrier allocation problem in the case of interfering transmitters. Considering the spectral efficiency of OFMA, further research is necessary to design power-efficient and interference-aware resource allocation schemes for OFDMA. Authors in [111] proposed to use joint transmission from multiple LEDs using OFDMA to improve the SINR of the edge users in a room. It was shown that due to intensity modulation of VLC systems, it is possible to achieve much better coordinated multi-point transmission compared to RF systems.

- **CDMA**: Optical CDMA (OCDMA) relies on optically orthogonal codes to provide access to the same channel by multiple users. The principle of optically orthogonal codes is well-studied for the optical fiber networks [112], [113]. In the OCDMA for VLC, each device is assigned a code (binary sequence) such that the data can be encoded in time domain by turning the LED ON and OFF [114]. These codes are referred as Optical Orthogonal Codes (OOC) [112]. It was shown in [114] synchronous OCDMA can be implemented using the OOC codes and OOK modulation with LED transmitters. A limitation of this technique is that long OOC codes are needed to ensure optimality, which in turn reduces the achievable data rate of devices. Authors in [115] proposed to address this issue using Code Cycle Modulation (CCM) where different cyclic shifts of the sequence assigned to devices are used to transmit an M-ary information. Since any cyclic shift of an OOC code (with length L) is considered a symbol, the spectral efficiency increases by a factor of $\log_2 L$.

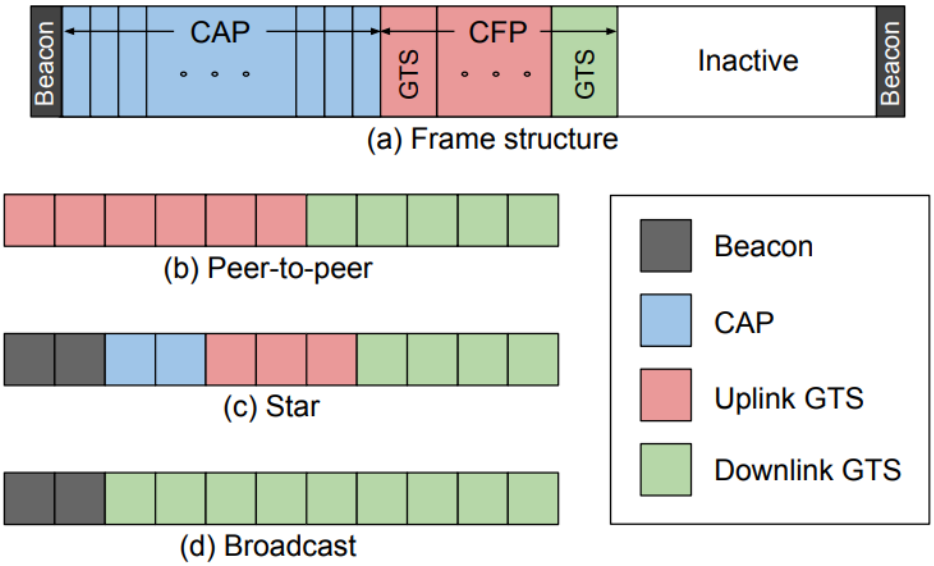

Fig II.23 (a) IEEE 802.15.7 frame structure includes beacon, Contention-based Access Periods (CAP) and Contention Free Periods (CFP), (b-d) Example usage of frame structure in different topologies; reproduced from [63]

Summary & Conclusion:

More than 15 years of research in physical layer techniques for LED-based VLC has provided the fundamental solutions to develop Li-Fi attocell networks that are capable of achieving magnitudes of higher data rates per unit area compared with state-of-the-art RF small cell solutions. Visible light communication has the potential to provide high speed data communication with improved energy efficiency and communication security/privacy. With looming crisis of RF spectrum shortage, VLC can become a practical augmentation technology for the existing RF networks. Increasing interest from research community and industries as well the standardization efforts such as VLCA and IEEE 802.15.7 show that VLC can be successfully commercialized in coming years.

The achievable performances in terms of user data rates, number of users served and increase in total traffic are well aligned with 5G key performance indicators. A key factor enabling this is the radical reduction of cell sizes, and this is possible by using the existing infrastructures through the combination of LED lighting and wireless data networking. The new wireless Li-Fi networking paradigm offers performance enhancements that are not only aimed for by 5G initiatives, but also due to the ubiquitous use of LEDs, that will provide an infrastructure for the emerging IoT.

In this paper we provided an overview of literature covering visible light communication, networking , and discussing various components of a visible light communication. We then provided a comprehensive ideas of VLC communication channel model and its propagation characteristics. This included a discussion of path loss, multi-path, and SNR. With this understanding of channel propagation, This contains a discussion of four major modulation techniques (OOK, PPM, OFDM and CSK). It was shown that due to their higher data rate capacity, OFDM and CSK are likely to be play an important role in future VLC broadband access networks. Additionally, feasibility of VLC MIMO as shown in literature ensures further data rate enhancements. With the link layer protocols for VLC. Also with CSMA, OFDMA, and CDMA protocols.

It was one of the goals of this paper to shed light on the difference between VLC and Li-Fi. Moving on, also showed and discussed the key research areas that are required to realise Li-Fi attocell networks. It summarised the well researched areas such as digital modulation techniques using LEDs, and provided new solutions to those areas which are key to Li-Fi networks such as multiuser access, Li-Fi attocell network analysis under various network deployment scenarios .

III-Section Three

I.Introduction:

This chapter represents a basic simulation of the Li-Fi system of one user with up to 10Gbps , and it contains also a discussion of the results obtained by this simulation.

The simulation of the Li-Fi system is performed using Optisystem software of Optiwave Corporation. Optisystem is a system level simulator for the realistic modelling the optical communication components in order to analyze the performance of the system with minimum cost, effort and time.

OptiSystem is a simulation package for optical communication systems, which can be used to design, test, optimize and produce outputs. OptiSystem is a stand-alone product but other simulation software can also be seamlessly interfaced which help in processing the results. Realistic modelling of optical communication systems is fulfilled by the software

Optisystem enables users to simulate and design

- Access Networks
- Advanced Modulation
- Co-Simulation
- Optical code division multiple access for assive optical networks
- Dispersion Management
- Fiber Analysis and Design
- Multimode Systems
- Optical Amplifiers, receivers, transmitters

The basic operation of the proposed system design can be explained as follows (Figure III.1). The input digital signal is modulated by NRZ-modulator, which is used to modulate the LED signal. To study the influence of ambient noise on the system, an additional light noise is generated. The combined signal is then transmitted through the free space channel. The optical signal received is made to pass through a rectangular optical filter after which is converted into electrical signal by means of PIN photodetector. The signal is amplified by means of transimpedance amplifier. To compensate for the noise, it's again filtered by means of a Bessel filter and the output signal will be obtained.

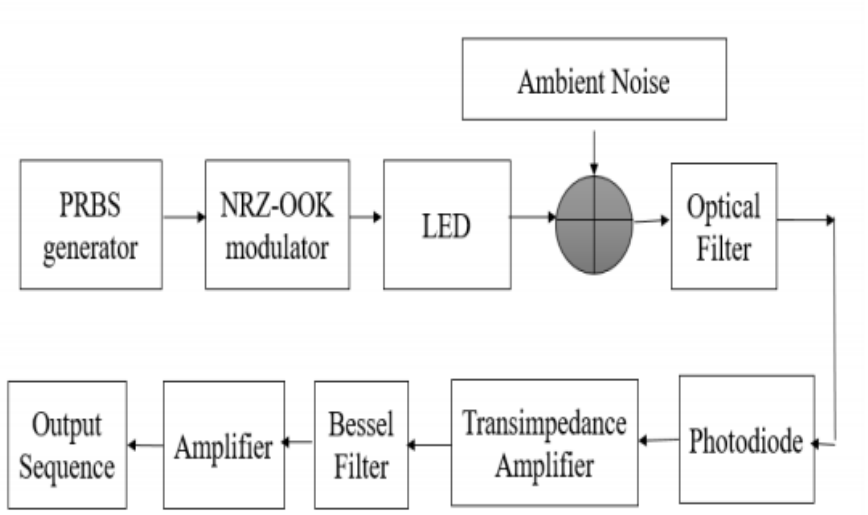

Figure III.1 (Block Diagram of the System)

A. **Transmitter:** The pseudo random bit sequence generator (PRBS) is used to generate the binary inputs which is then modulated using On-Off Keying (OOK) technique. The modulated signal is given as input to the Light Emitting Diode (LED). Thus the binary electrical signal is converted to optical signal and then is transmitted via the free space channel as depicted in figure.
B. **Free Space Channel :**The communication media used in VLC is free space. Here the signal from LED might get distorted due to various ambient light noises due to conventional lightings or other LED light sources. In this project, the influence of ambient
C. **Receiver**: The received optical signal is filtered by means of a rectangular optic filter. The photodiode converts the optical signal back to electrical, which is then amplified by transimpedance amplifier. Bessel filter is used to remove the noise which was added to the system on traversing through the channel [6]. An electrical amplifier is then used and the original input signal is obtained at the output.

2-Simple Experimental setup of Li-Fi :

Figure III.2 shows the designed block diagram for indoor visible light communication system is implemented using OptiSystem v.17 software.

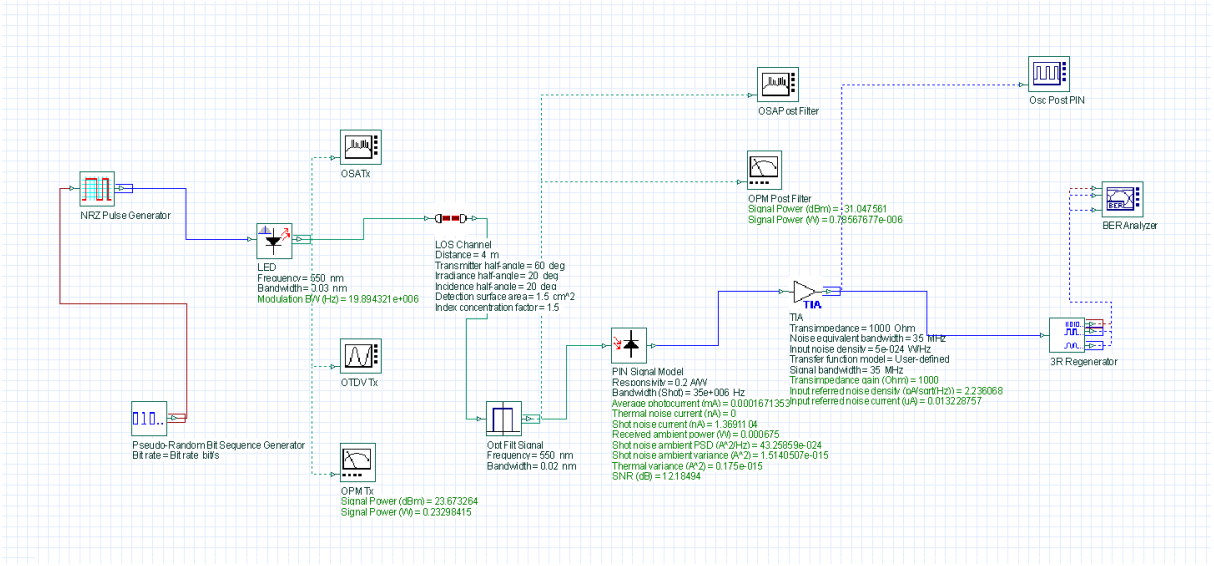

Fig III.2 construction of a simple Li-Fi system

The proposed experimental setup for the Li-Fi system is as in Fig III.2. The input Pseudo random data sequence is converted to NRZ or RZ (in this case we used NRZ) ,electrical pulses and this signal directly derives the white LED. The white LED emits the modulated light as an optical output, this establishes the connection with receiver (silicon photodiode) through (air) at room (from 1m up to 4m) via a LOS Channel, The radiated light power is measured or detected with an optical power meter , and his spectrum is analyzed by an optical spectrum analyzer .

The typical parameter of the white LED and photodiode is as in Table III.1 , A Li-Fi system is designed with help of Optisystem. The LOS Channel (Line of Sigh Channel) component is used for Li-Fi channel and the channel parameters are taken from the practical measurements, without any diffusion from the side wall (LED is illuminated at room center) and the measured LOS Channel parameters are tabulated in Table III.2

LED specifications	
Centre frequency	550nm
Electron carrier life time	1 ns
RC time constant	1 ns
Quantum efficiency	65%
Photodiode specifications	
Responsivity type	Silicon
Dark current	10nA
Shot noise distribution	Gaussian

Table III.1: LED and Photodiode Specification details

LOS Channel specification	
Transmitter half-angle	60°
Beam divergence(FWHM)	63.5
Irradiance half-angle	20°
Incidence half-angle	20°

Table III.2.LOS Channel parameters

Results and discussion:

For the deigned Li-Fi system the white LED having center frequency of 550 nm as in Fig III.3. The designed system is analysed for different bit-rates along with different link distance in meter. Here, we started with range of 3m & speed of 100 Mbit/s.

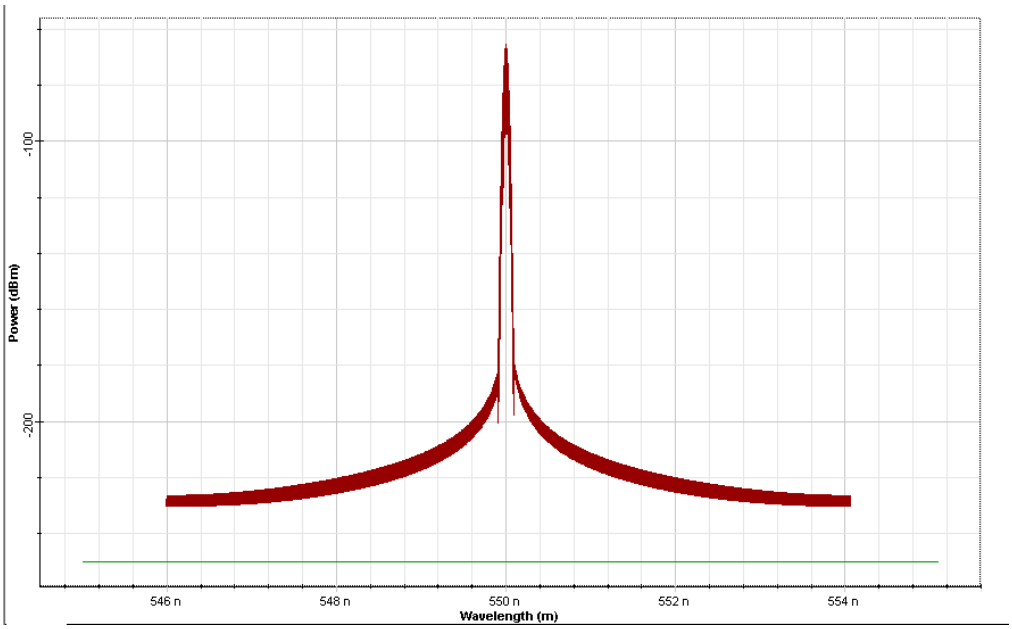

Fig III.3. OSA result

Fig III.4 depicts the Q factor of the detected signals for the bitrate variation from 100 Mbps to 3 Gbps with respect to the link distance up to 3 m. From results, it has been found that our simulated VLC system could support 2 Gbps with an optimum Q factor 5.76 at link range 3m, beyond which the received signals tend to become degraded. At the bit rate of 100 Mbps, our designed system provides the superior performance of about Q factor whose value of 35 for the link range below 1 m. And for the same bit rate, maximum transferable distance is obtained as 4.4 m with Q factor 5.9. Fig III.5 also confirms that our VLC systems could support 2 Gbps up to the link distance of 3 m, and found log of BER -8.399. Fig. 6 and 7 show the eye diagram along with Q factor for the link distance of 2 meter and 4 meter at bitrate of

300Mbps and 2Gbps. It clearly depicts that at lower bitrate the signal can reach upto 4 meter link distance with good eye.

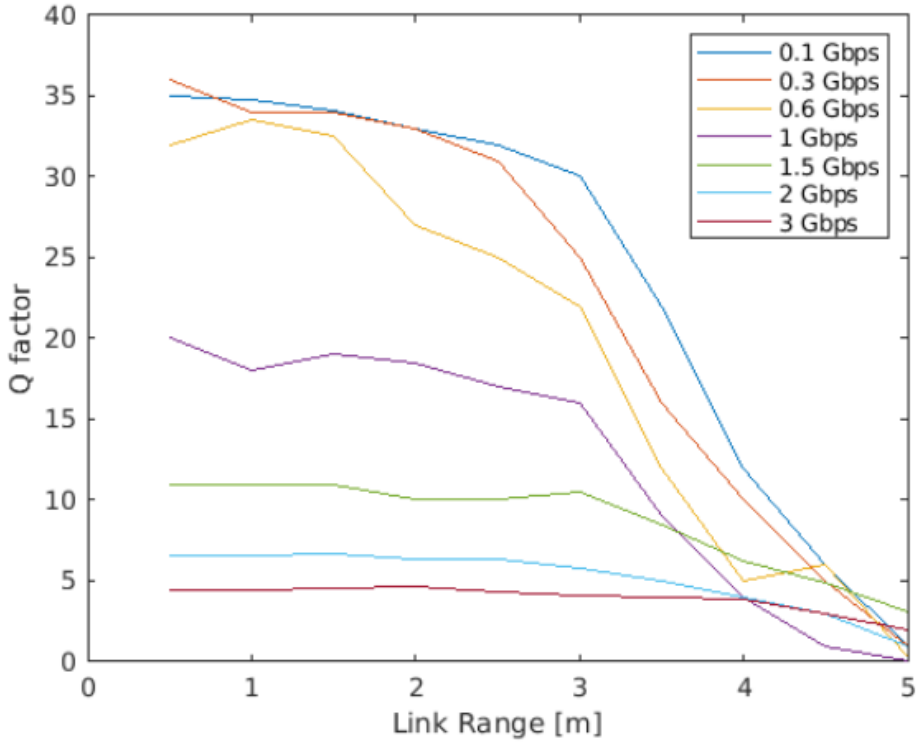

Fig III.4 Q factor value of detected signal for the different bit rate and link range (distance)

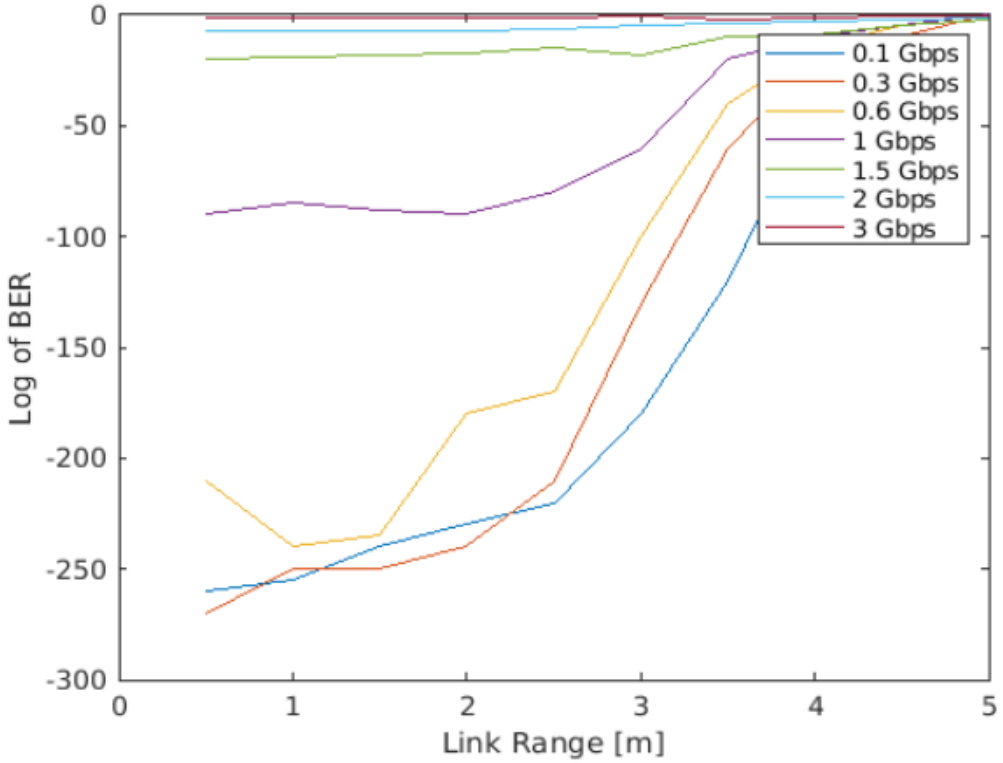

Fig III.5 Log of BER value of detected signal for the different bit rate and link range (distance)

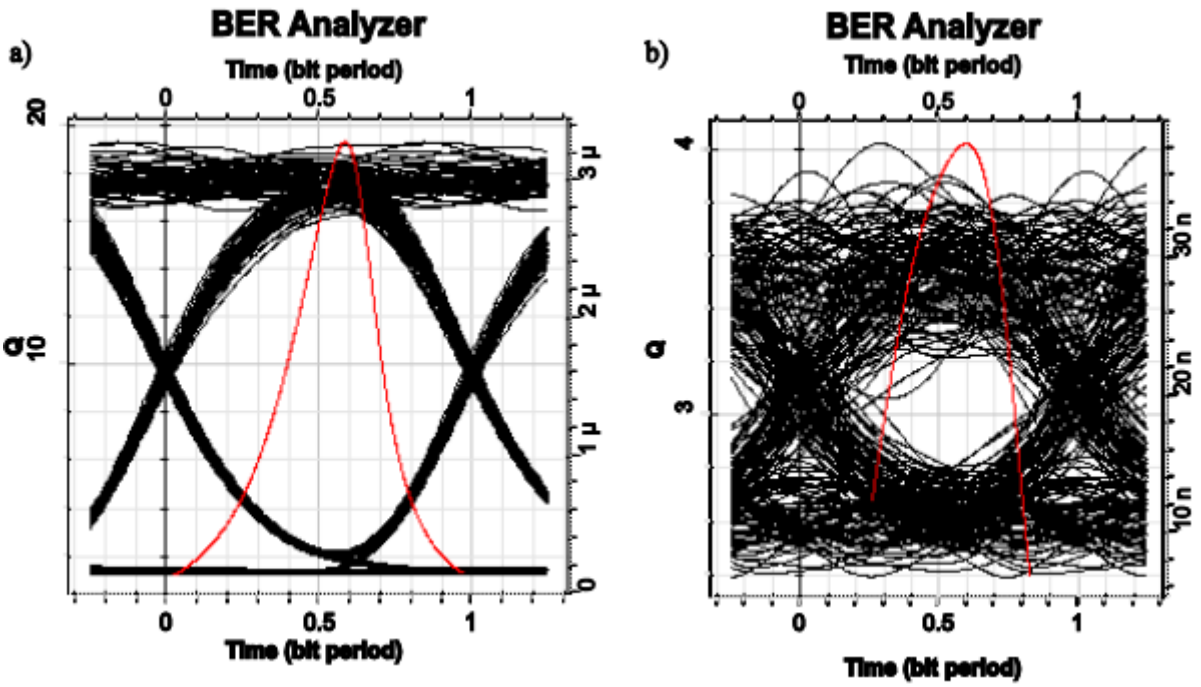

FigIII.6 Eyediagram of the received signal for the bit rate of 300Mbps at (a) 2 meter link distance (b) 4 meter link distance.

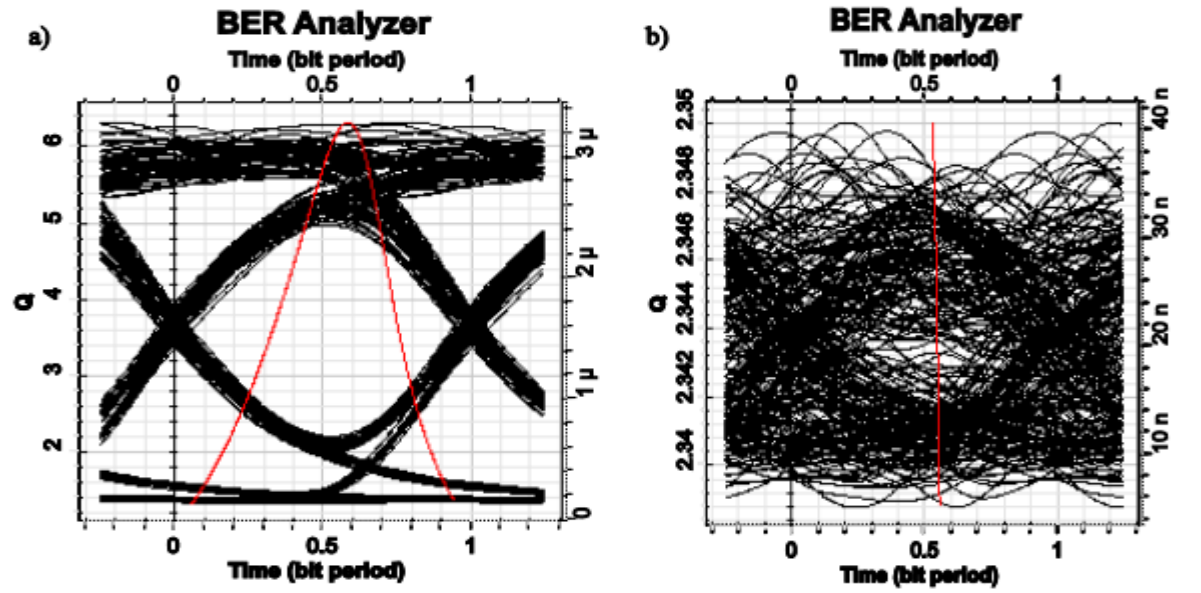

Fig III.7. Eyediagram of the received signal for the bit rate of 2 Gbps at (a) 2 meter link distance (b) 4 meter link distance.

3-Realising the Li-Fi system with an external modulation :

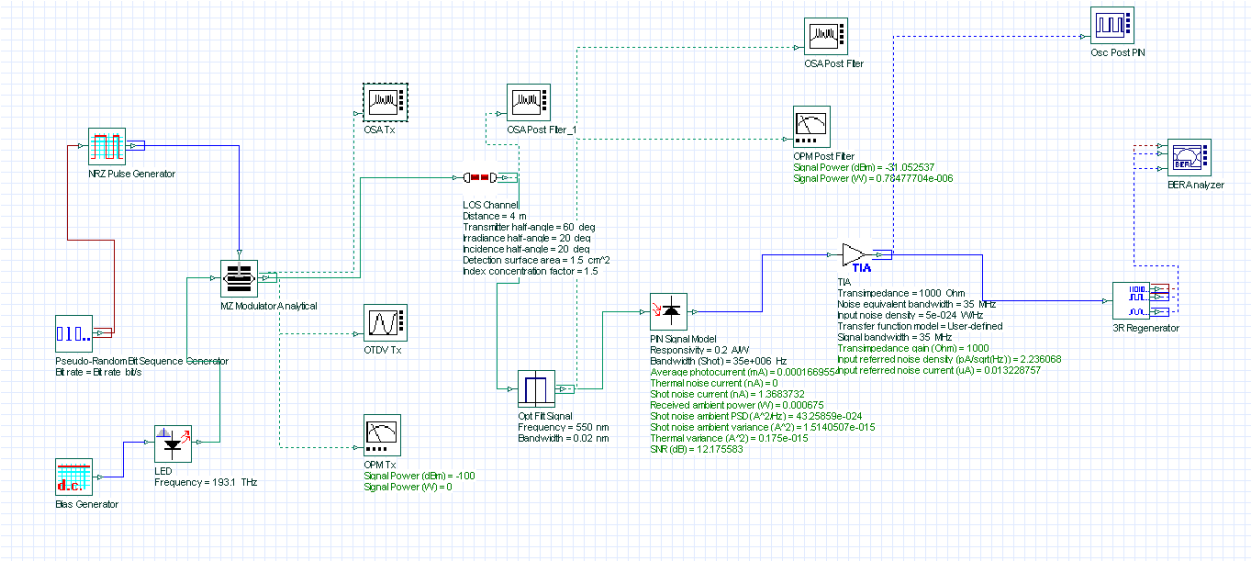

Fig III.8 .construction of li-fi system with an external modulation

Modulation formats also have a significant impact on transmission characteristics of the VLC system. The Fig III.9 shows the comparison of NRZ-OOK and RZ-OOK at bit rate of 2 Gbps. The designed system is analyzed for NRZ-OOK and RZ-OOK at bitrate of 2 Gbps for the different link distance in meter. Due to the nature of distinct transition between the encoded bits of RZ pulses, the reception at the detector enhanced [116] and provides the better Q factor.

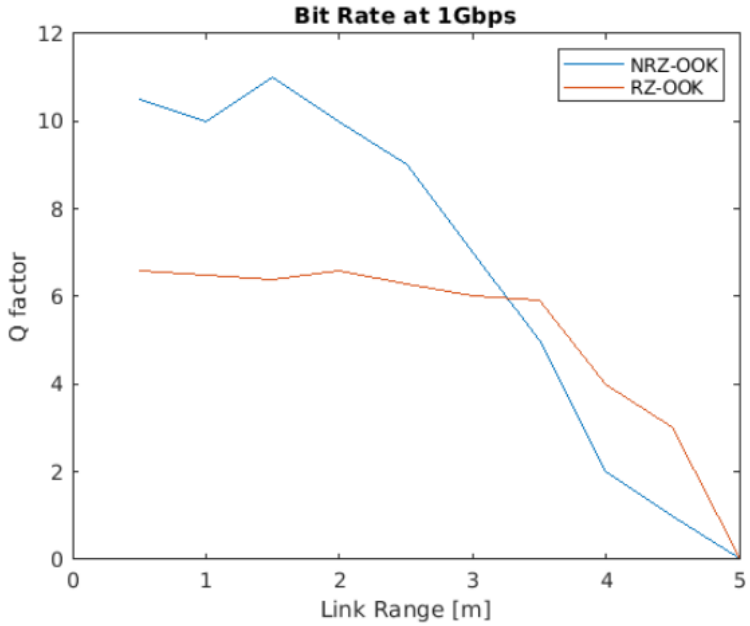

Fig III.9. Q factor of the received signal for the NRZ-OOK and RZ-OOK modulation with respect to the different link range.

The obtained Q factor for the NRZ-OOK is of about 8.73 up to the 3 m of link distance where as RZ is 5.76. Fig III.10 & Fig III.11 depicts the NRZOOK , and the RZOOK signal at transmitter and detector respectively. As well as they shows the detected signal that exactly reproduce the transmitted signal, whereas the blue lines indicate the received signal and green lines indicate the noise.

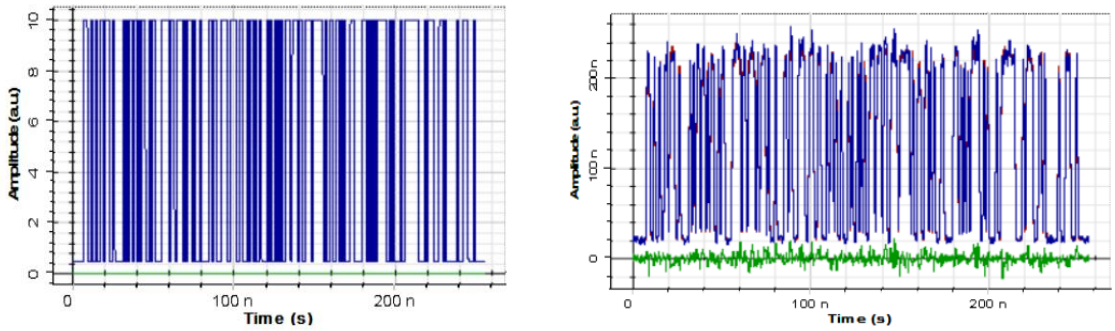

Fig III.10. NRZ electrical drive signal at transmitter & the Received NRZ electrical signal after the low pass Filter

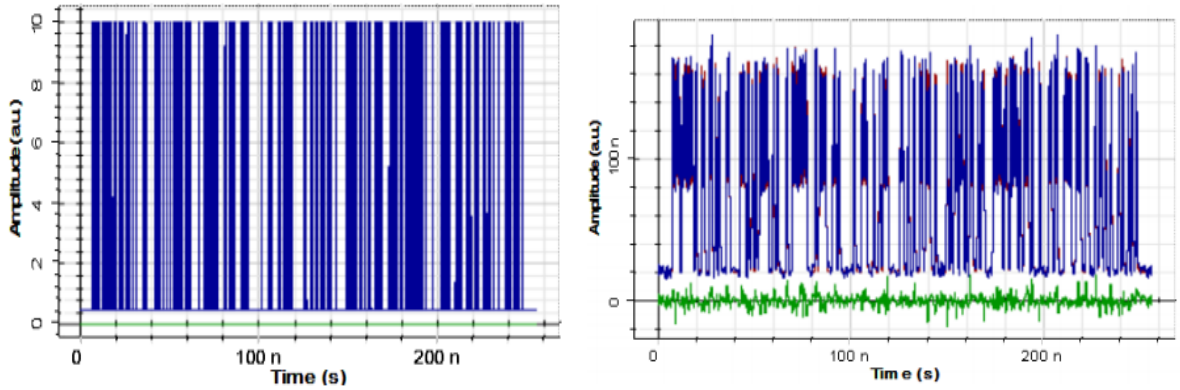

Fig III.11 RZ electrical drive signal at transmitter & the Received RZ electrical signal after the low pass Filter

Authors and year	LED source	Modulation	Data rate	Distance
Joon-Ho Choi et.al [13]	P-LED	NRZ-OOK	1 Mb/s	10 cm
Le-Minh H et.al., [14]	P-LED	OOK	100 Mb/s	10 cm
Fujimoto N et al., [15]	RGB LED (Red LED)	OOK	477 Mb/s	40 cm
Li Honglei et.al., [16]	P-LED	OOK	500 Mb/s	160 cm
Our proposed work	White LED	OOK	2 Gb/s	3 m

Table **III.3**. Comparison of our results with literatures

Table III.3 shows the comparison of results reported by authors in their previous investigations in VLC with our current research work. It clearly indicates that our proposed system could support up to 3 m link distance with the bitrate of 2 Gb/s.

In VLC system, it is essential to analyze the external (atmospheric or artificial) lighting influence on our received signal quality. The external light influence is included in VLC by addition of another one White LED as input without any modulation with different emissive power levels. The external White LED power (noise) level is varied from -130 dBm to -60 dBm and the respective Q factor value of received as in Fig III.12. As the external lighting influence is increased then the received signal getting worsened. Particularly, if the external lighting power increases above -80 dBm then the received signal Q factor is totally disturbed at higher bit rate as in Fig III.12. At bit rate 0.5 Gbps or below, the received signal can be a detectable range even at -70 dBm of external lighting condition. So the received signal tolerance to the higher external lighting condition and the link range can be improved at further lower bit rates.

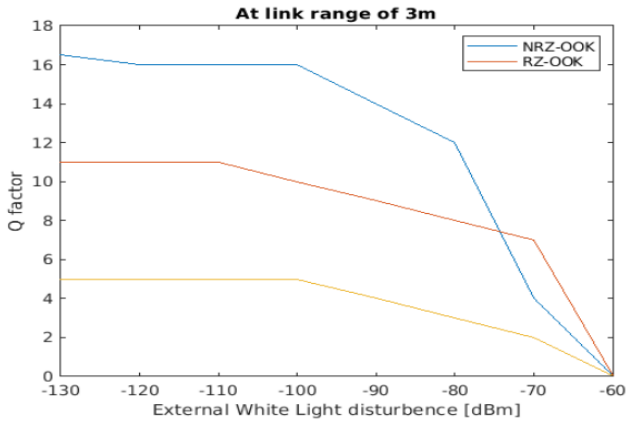

Fig III.12. Q factor of the received signal for the different external white light power in dBm and for the different Bit rate at link range of 3 meter.

4- VLC with OFDM Modulation :

As shown in Fig III.13, VLC communication system using White Light LED setup is realized with the help of Optisystem v17. The Pseudo random data sequence is generated from the BER test set with a reference bit rate. This data sequence is converted into I and Q symbols using QAM sequence generator. The symbols are taken as diferent amplitude levels in both in-phase (I) and quadrature phase (Q) using M-ary sequence generators. The I and Q symbols of QAM are modulated individually with RF subcarriers in OFDM Modulator. Here, the Fast Fourier Transform (FFT) points should be at least double the numbers of subcarrier utilized for the above. FFT points set sub-carrier positions centered at DC or 0 Hz. Modulation from 0 to 2.5 GHz range of frequencies are taken for lower-rate subcarrier tones. The position array in OFDM modulator sets the starting point of the subcarrier from the range of carrier or the position array arranges the position of subcarriers from the central frequency of the OFDM spectra. In order to maintain the bandwidth of the OFDM spectra the position array should be half of the number of subcarriers. Then the OFDM modulated signals are further fltered with low pass raised cosine roll-of flter which will shape the OFDM output pulses and minimise the Inter Symbol Interference (ISI). The generated OFDM signals are further up converted to the RF carrier of 7.5 GHz using Quadrature modulator. The electrical signal at Quadrature modulator is rescaled or dc biased to an optimum level in order to directly drive the White LED source. The White LED establishes the connection with photo detector which is located at few meters away from the transmitter in free space. The free space channel characteristics are measured practically at room temperature environment in a room of size 5×5×3 m by using 2×2 Tekhol® White LED and HTC LUX meter [121].

This White LED was having luminescence of about 120–160 lm, optical output power of 600 mw/LED and view angle of 120°. For the measurement of channel parameters, Line of sight (LOS) model is taken i.e., without any difusion from the side wall is considered. LED is placed and illuminated at the room's centre [121]. The measured parameters are utilized in Free Space Optics (FSO) component in Optisystem in order to realise the channel characteristics on simulation for our Visible light communication using White LED. The electrical drive signal and Quantum efciency are setup to generate 7 W optical power at LED output in order to match the practically measured LED output with average luminescence of 358 lm. The typical parameter values of White LED, Photo diode, and the measured FSO component parameters are tabulated in Tables III.4 and III.5 respectively.

For free space channel, the above measured parameters are utilized in following mathematical equation [121-122]. The link equation is:

$$P_{Received} = P_{Transmitted} \frac{d_R^2}{(d_T + \theta R)^2} 10^{-\alpha R/10} \quad \text{(III.1)}$$

where d_R receiver aperture diameter (m), d_T transmitter aperture diameter (m), θ beam divergence (mrad), R range (km) and α atmospheric attenuation (dB/km). The received signal power for parameter range depends on the propagation distance between transmitter and receiver. The attenuation of the LED's output power depends on two main parameters:

attenuation and geometrical loss. The first parameter describes the attenuation of the light source power in the atmosphere. The second parameter, Geometrical loss, occurs due to spreading of the transmitted beam between the transmitter and the receiver.

Figure III.13 shows the designed block diagram for indoor visible light communication system with OFDM modulation , implemented using OptiSystem v.17 software.

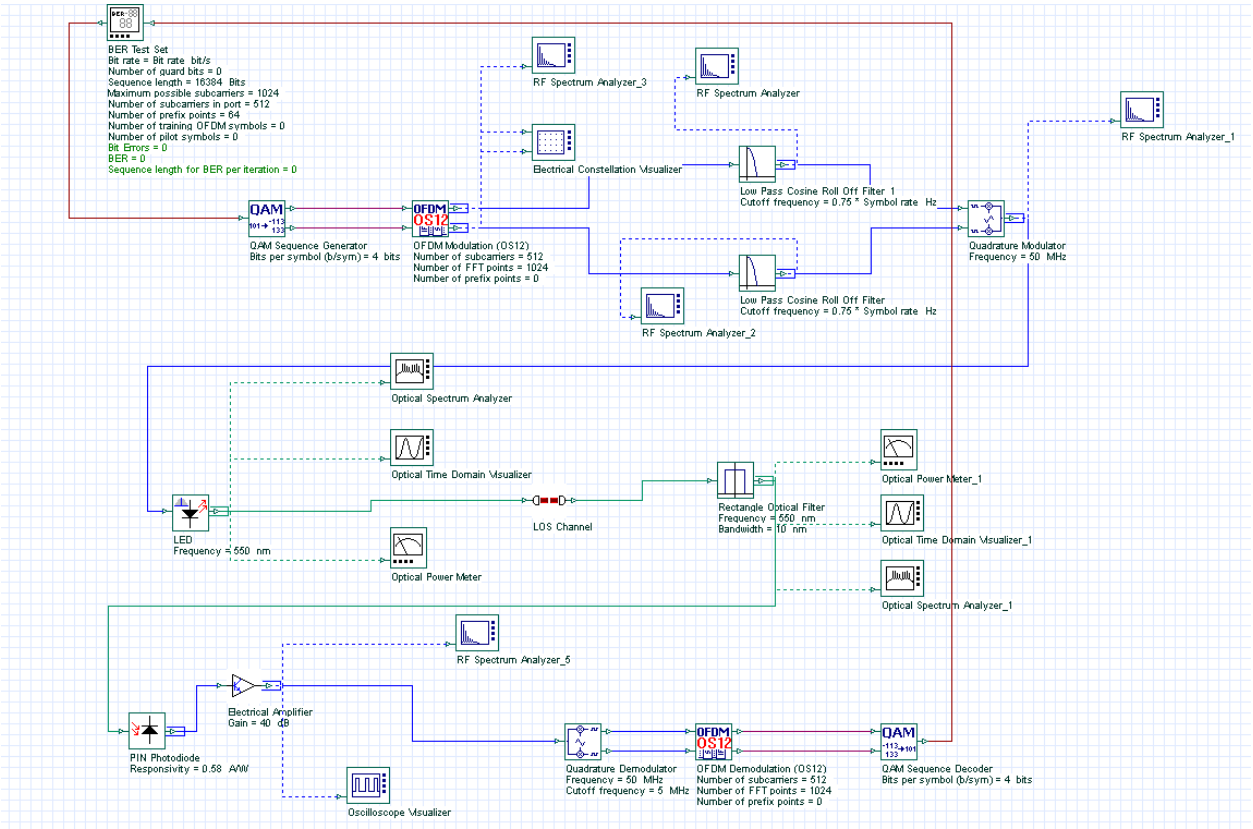

Fig III.13 Experimental setup for the OFDM modulated VLC system using white LED

LED specifications	
Centre frequency	550nm
Electron carrier life time	1 ns
RC time constant	1 ns
Quantum efficiency	65%
Photodiode specifications	
Responsivity type	Silicon
Dark current	10nA
Shot noise distribution	Gaussian

Table III.4: LED and Photodiode Specification details

LOS Channel specification	
Transmitter half-angle	60°
Beam divergence(FWHM)	63.5
Irradiance half-angle	20°
Incidence half-angle	20°

Table III.5. Free space optical components parameters

OFDM Modulator	
Number of subcarriers	512
Position array	256
Number of FFT points	1024
Cyclic prefx	Symbol extension
DAC interpolation	Cubic

Table III.6 OFDM modulator specifcations

Optisystem layout properties	
Bit rate	From 1 to 25 Gbps
Sequence length	16,384
Samples per bit	128
Number of samples	2,097,152

Table III.7 Optisystem layout properties

The received signal power at photo detector is determined by the atmospheric and aperture loss of the channel [121, 122]. And the detected electrical signal at Photo detector output is given to the rectangular flter to flter out the up converted OFDM signal at 7.5 GHz in RF spectrum. The fltered RF signal is then down converted in the Quadrature modulator with the carrier of 7.5 GHz and the intermediate frequency (IF) output of OFDM with its subcarrier signal is recovered between 0 and 2.5 GHz range. OFDM demodulator parameters at receiver should exactly match with transmitter in order to recover the QAM symbols at the output. The OFDM modulator parameter and Optisystem simulation parameters are given in Tables III.6 and Table III.7 respectively. Finally the QAM sequence detector detects the binary sequences and it is compared with transmitted sequence to fnd out the Bit error rate and log of BER.

Result and Discussion:

Our OFDM modulated VLC system in Fig. III.13 is analysed for various bit rates and link ranges using Optisystem simulation. In our simulation, QAM coding is used for symbol generation due to its higher spectral effciency, bandwidth and robustness to noise compared to the other coding techniques such as BPSK, QPSK and M-ary PAK. Performance of this VLC system with component parameters as mentioned in Tables III.3, III.4 ,III.5 and III.6 and for the 4-QAM Coded with OFDM modulation (OFDM parameter: number of subcarriers=512, position array=256, number of FFT points=1024) are evaluated and tabulated in Tables III.8, III.9 and III.10. For various link ranges and bit rates, performance parameters

such as BER versus log of BER, Optical received signal power versus OSNR, and Electrical received signal power versus SNR are tabulated in Tables III.8, III.9, and III.10 respectively.

Bit rate (Gbps)	Link range									
	OFDM parameter: number of subcarriers = 512, position array = 256, number of FFT points = 1024									
	1 m		1.5 m		2 m		2.5 m		3 m	
	BER	log of BER	BER	log of BER	BER	log of BER	BER	log of BER	BER	log of BER
1	0	−1000	0	−1000	0	−1000	0	−1000	4.87E−02	−1.312
2	0	−1000	0	−1000	0	−1000	4.27E−04	−3.369	1.17E−01	−0.093
5	0	−1000	0	−1000	0	−1000	8.17E−03	−2.088	2.22E−01	−0.654
10	0	−1000	0	−1000	0	−1000	3.20E−02	−1.495	2.90E−01	−0.537
20	0	−1000	6.10E−05	−4.214	1.03E−03	−2.984	9.04E−02	−1.044	3.44E−01	−0.464
25	2.40E−04	−3.61	4.27E−04	−3.369	2.07E−03	−2.683	1.16E−01	−0.937	3.61E−01	−0.443

Table III.8 OFDM modulated VLC system performance (BER and Log of BER) for various bit rates and link ranges.

Bit rate (Gbps)	Link range									
	OFDM parameter: number of subcarriers = 512, position array = 256, number of FFT points = 1024									
	1 m		1.5 m		2 m		2.5 m		3 m	
	Received signal power (dBm)	OSNR (dB)	Received signal power (dBm)	OSNR (dB)	Received signal power (dBm)	OSNR (dB)	Received signal power (dBm)	OSNR (dB)	Received signal power (dBm)	OSNR (dB)
1	−19.045	80.954	−26.309	73.690	−38.712	67.287	−38.649	61.350	−44.221	55.778
2	−21.964	78.035	−29.366	70.633	−35.272	64.272	−41.576	58.423	−47.212	52.787
5	−26.016	73.983	−33.188	66.811	−39.827	60.172	−45.693	54.306	−51.027	48.972
10	−28.897	71.102	−36.705	63.294	−42.649	57.350	−48.343	51.656	−54.358	45.641
20	−31.885	68.114	−39.179	60.820	−45.462	54.537	−51.014	48.985	−57.607	42.392
25	−33.130	66.869	−41.664	58.335	−47.005	52.994	−52.477	47.934	−58.281	41.718

Table III.9. OFDM modulated VLC system performance [optical received signal power and optical signal to noise ratio (OSNR)] for various bit rates and link ranges

Bit rate (Gbps)	Link range									
	OFDM parameter: number of subcarriers = 512, position array = 256, number of FFT points = 1024									
	1 m		1.5 m		2 m		2.5 m		3 m	
	Received signal power (dBm)	ESNR (dB)	Received signal power (dBm)	ESNR (dB)	Received signal power (dBm)	ESNR (dB)	Received signal power (dBm)	ESNR (dB)	Received signal power (dBm)	ESNR (dB)
1	−59.043	62.277	−73.162	49.586	−86.339	37.886	−98.173	26.163	−109.329	15.040
2	−59.121	59.524	−73.328	45.932	−86.455	34.828	−98.201	23.153	−109.780	11.625
5	−59.249	55.499	−73.969	43.025	−86.474	30.715	−98.239	19.068	−109.805	7.531
10	−59.658	53.114	−74.859	39.865	−86.720	28.420	−98.802	16.945	−110.071	5.206
20	−62.475	50.301	−76.568	38.073	−90.317	24.851	−100.749	14.313	−111.846	3.447
25	−62.902	49.755	−77.362	37.368	−91.219	24.007	−101.183	14.138	−114.362	2.820

Table III.10. OFDM modulated VLC system performance [electrical received signal power and electrical signal to noise ratio (ESNR)] for various bit rates and link ranges.

Table III.7 shows that the link range is reduced and BER is increased when the data rate is increased. The Proposed VLC system can support a data rate of 10 Gbps up to the link range of 2 m with permissible BER. Beyond which the link distance is drastically reduced to about 1.5 m and below. Tables III.8 and Table III.9 also conform with the above inference in the Table III.8 The optimal FEC (Forward Error correction) BER is obtained at ≈54 dB of OSNR and ≈19 dB of ESNR as per Tables III.9 and III.10 respectively. These OSNR and ESNR values are also better than the minimum acceptable values of ≈50 dB of OSNR and a range of 13.6–15 dB of ESNR as reported by the contemporary literatures. Figure III.14 shows every stage output of our OFDM modulated VLC system for the bit rate of 10 Gbps and the link range of 1 m. Figure III.14a indicates the transmitted bit sequence at 10 Gbps using BER test set and it is converted into QAM format using QAM generator along with M-ary conversion and the resultant constellation of this sequence is shown in Figure III.14b. This QAM modulated I and Q signals are modulated with 512 subcarriers (subcarriers frequency span is 0–2.5 GHz) to generate OFDM signals. Figure III.14c, d show OFDM outputs of I and Q channels respectively after the LP cosine filter. For further transmission of the signal, it is modulated with higher carrier frequency and its center frequency is shifted to 7.5 GHz with either sides of subcarrier bands as depicted in Fig. 13e. As shown in Figure III.14f, electrical pulses at Quadrature modulator output has negative portion of electrical signals which would not allow exactly to reproduce the modulated signal using the LED. Therefore, this electrical pulse is rescaled using DC bias as shown in Figure III.14g. This dc biased electrical pulses are now used to modulate the White LED and the emission spectrum is as shown in Figure III.14h. The emission spectrum produces a Lambertian pattern and it is afected by atmospheric losses before it reaches the Line of sight (LOS) photo diode. This transmitted signal is detected with the help of Photodetector and its output spectrum is noticed as in Figure III.14i in the RF spectrum analyzer. It clearly depicts that the photodiode exactly reproduces the OFDM modulated output with center frequency of 7.5 GHz. This OFDM spectrum is fltered out using Bandpass rectangular flter as depicted in Figure III.14j. This OFDM spectrum is down converted by coherent demodulation with local oscillator frequency of 7.5 GHz and our OFDM subcarriers (I and Q) are extracted as shown in Figure III.14k, III.14l respectively. Finally, OFDM demodulator demodulates the subcarriers and generates the original QAM bit sequence, and it is verifed with constellation diagram as shown in Fig. III.14m. Thereafter, the original bit sequence is decoded with the help of QAM decoder as shown in Figure III.14n and it is fed back to BER test set to compare the received bit sequence with that of the transmitted bit sequence and hence the BER is calculated. From these figures, it is clearly understood that the received sequences exactly match with the transmitted sequences and there is no BER and hence the constellation also very good at receiver point. As shown in Fig. III.15, when the link range is raised to 2.5 m with 10 Gbps bitrate, the received constellation is disturbed so much since the signal is more afected by free space attenuation and signal phase error compared to the link range of 1 m as in Fig. III.14m. Without BER, the maximum link range obtained for the data rate of 1 Gbps was 2.56 m as shown in Tables III.8 III.9, III.10 and Figure III.16. It is possible to extend the link range up to 2.5 m even at 5 Gbps bit rate, in case of receiver with proper equalization arrangement. The large sequence length of 16,384 bits enable us to measure more realistic BER in our OFDM modulated VLC system analysis and it shows drastic variation in log of BER even for 2 or 3-

bit error. The orthogonal nature of subcarrier frequency used in our system along with cosine flter reduce the frequency depended fading and inter symbol interference (ISI) and support higher bit rate of 10 Gbps. Beyond the data rate of 10 Gbps, the signal degradation can be reduced only if the OFDM subcarrier is increased [127]. As shown in Table III.10 and Figure III.17, the BER is good, even for 25 Gbps due to the increase in OFDM modulation subcarrier from 512 to 1024 and the respective increase in orthogonal bit sequences. But the link distance is limited to 1.5 m only. In order to ensure the quality improvement of transmission.

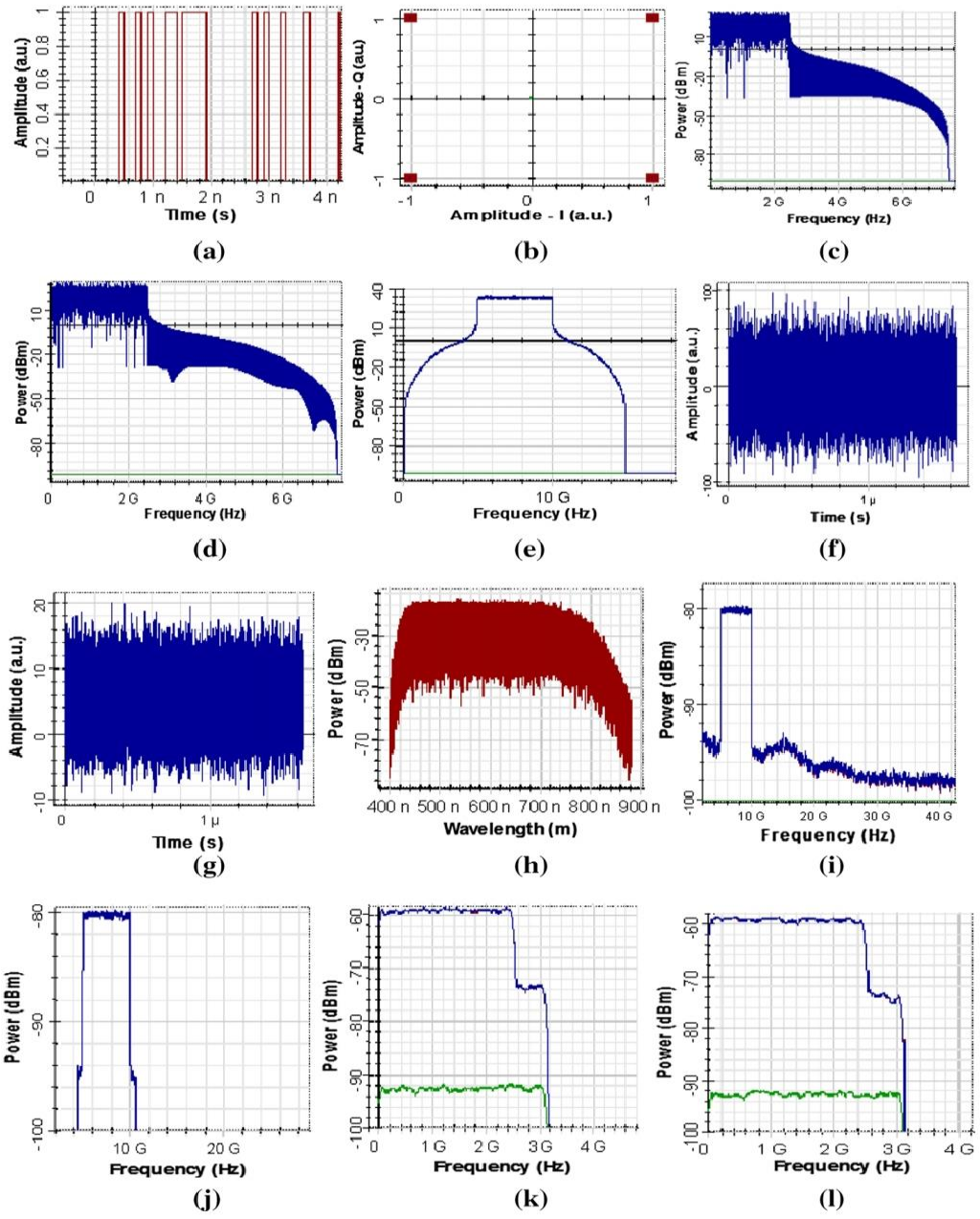

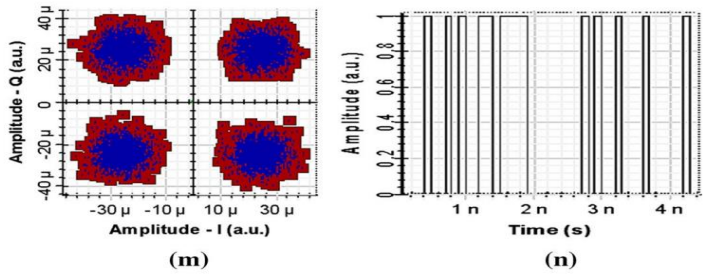

Fig III.14 output of our OFDM modulated VLC system for the bit rate of 10 Gbps and the link range of 1 m

Figure III.14. Shows Our OFDM modulated VLC system outputs at every stage for the bit rate of 10 Gbps and the link range of 1 m. a Transmitted bit sequence, b transmitted QAM constellation, c OFDM output -I channel after the LP cosine filter, d OFDM output -Q channel after the LP cosine filter, e quadrature modulator output at transmitter (7.5 GHz up converted signals), f electrical pulses at quadrature modulator output, g electrical rescale output (DC biasing), h white LED emissive spectrum, i photo detector output RF spectrum, j fltered RF spectrum of OFDM signal, k quadrature demodulator output (down converted) I channel, l quadrature demodulator output (down converted) Q channel, m after OFDM demodulation-received QAM constellation diagram, n received bit sequences.

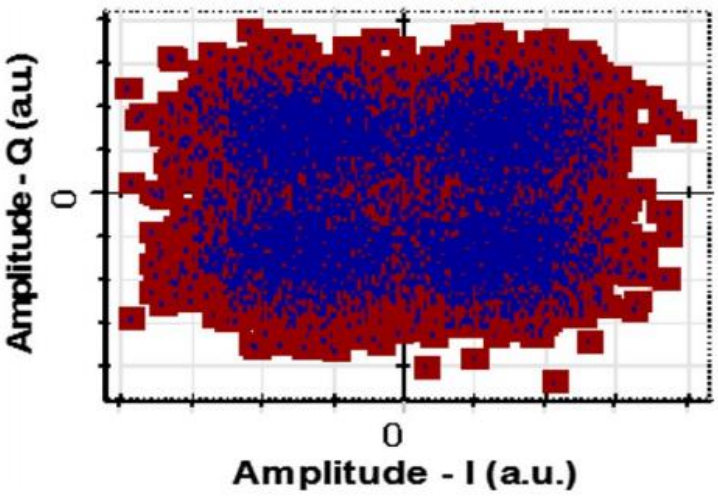

Fig III.15 .Received signal constellation diagram for the bit rate of 10 Gbps and link range of 2.5 m

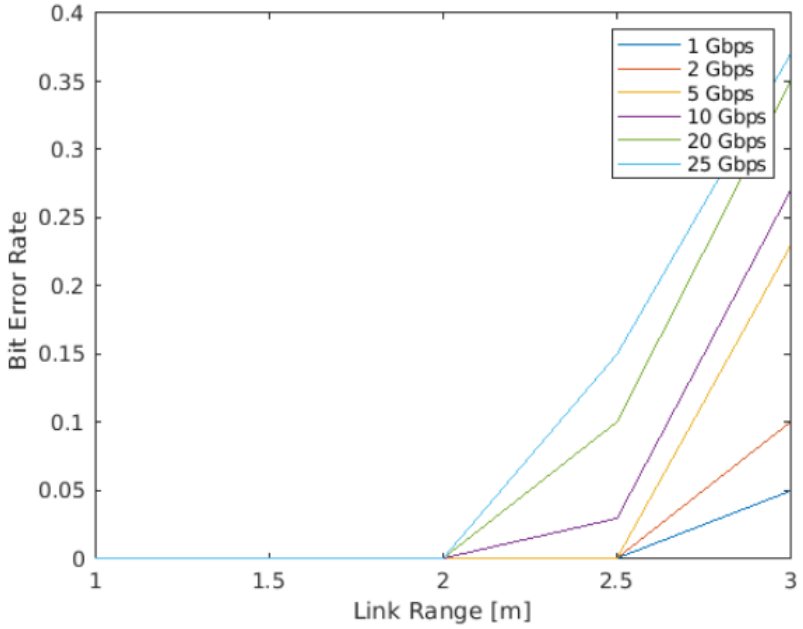

Fig III.16 Bit error rate of the received signal for various bit rates and link ranges

Bit rate (Gbps)	Link range									
	OFDM parameter: number of subcarriers = 1024, position array = 512, number of FFT points = 2048									
	1 m		1.5 m		2 m		2.5 m		3 m	
	BER	log of BER	BER	log of BER	BER	log of BER	BER	log of BER	BER	log of BER
20	0	−1000	0	−1000	5.49E−04	−3.26	7.61E−02	−1.119	3.30E−01	−0.482
25	0	−1000	0	−1000	4.88E−04	−3.311	9.73E−02	−1.012	3.52E−01	−0.455

Table III.11 OFDM modulated VLC system performance (BER and log of BER) for higher bit rates and link ranges at large number of subcarriers

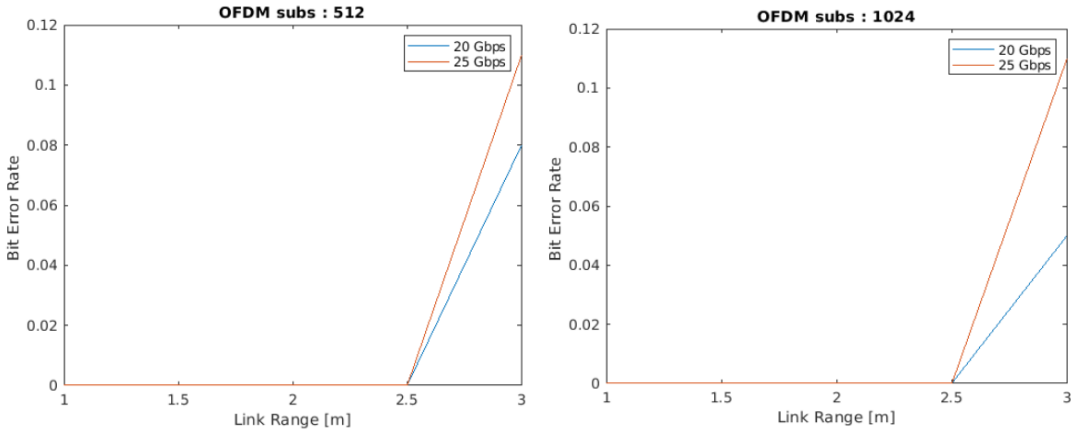

Fig III.17. Bit error rate of the received signal for large number of subcarriers and for diferent link ranges at higher bit rates

by increasing the number of subcarriers, in addition to the Table III.11, the received signal power versus SNR also measured and given in Table III.12 and Table III.13. They clearly indicate the signifcant improvement in the observed SNR when the subcarriers increase from 512 to 1024. For the number of OFDM subcarrier variation, the received QAM signal constellation diagram is observed. Constellation diagrams for 20 Gbps bit rate and link range of 1.5 m are shown in Figs. 6 and 7 respectively for 512 and 1024 subcarriers. They clearly depict if OFDM subcarrier is increased from 512 to 1024, then the signal gets less distorted and constellation phase error is reduced notably. Moreover, the signal BER is also improved.

Bit rate (Gbps)	Link range									
	OFDM parameter: number of subcarriers = 1024, position array = 512, number of FFT points = 2048									
	1 m		1.5 m		2 m		2.5 m		3 m	
	Received signal power (dBm)	OSNR (dB)	Received signal power (dBm)	OSNR (dB)	Received signal power (dBm)	OSNR (dB)	Received signal power (dBm)	OSNR (dB)	Received signal power (dBm)	OSNR (dB)
20	− 31.346	68.653	− 38.843	61.156	− 45.492	54.507	− 51.038	48.961	− 57.307	42.693
25	− 32.626	67.373	− 39.809	60.191	− 46.672	53.327	− 51.137	48.862	− 58.222	41.778

Table III.12 OFDM modulated VLC system performance [optical received signal power and optical signal to noise ratio (OSNR)] for higher bit rates and link ranges at large number of subscribers

Bit rate (Gbps)	Link range									
	OFDM parameter: number of subcarriers = 1024, position array = 512, number of FFT points = 2048									
	1 m		1.5 m		2 m		2.5 m		3 m	
	Received signal power (dBm)	ESNR (dB)	Received signal power (dBm)	ESNR (dB)	Received signal power (dBm)	ESNR (dB)	Received signal power (dBm)	ESNR (dB)	Received signal power (dBm)	ESNR (dB)
20	− 61.788	50.918	− 76.036	38.591	− 88.785	26.326	− 100.409	14.841	− 111.754	3.537
25	− 62.328	50.238	− 77.241	37.476	− 90.289	24.927	− 101.027	14.346	− 113.918	2.839

Table III.13 OFDM modulated VLC system performance [electrical received signal power and electrical signal to noise ratio (ESNR)] for higher bit rates and link ranges at large number of subcarriers

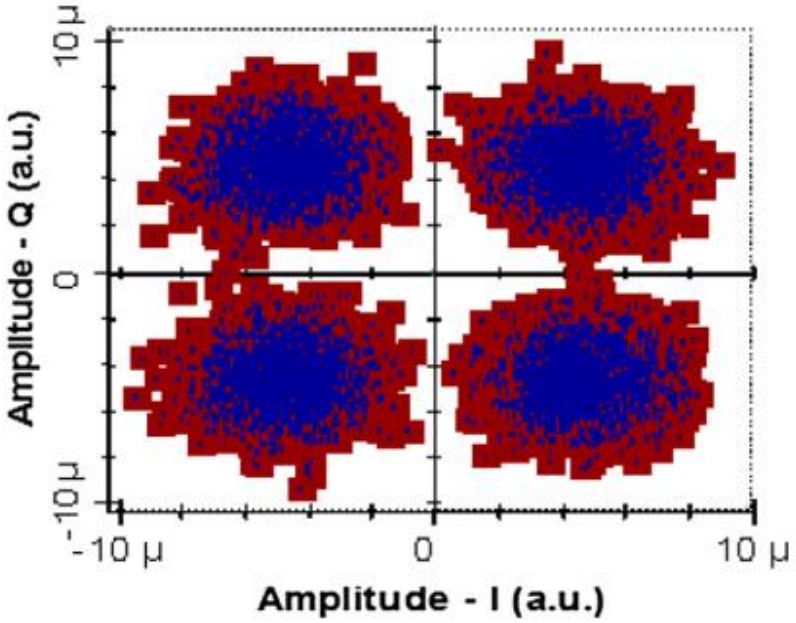

Fig III.18. Received signal constellation diagram for 512 OFDM subcarrier and bit rate of 20 Gbps at the link range of 1.5 m

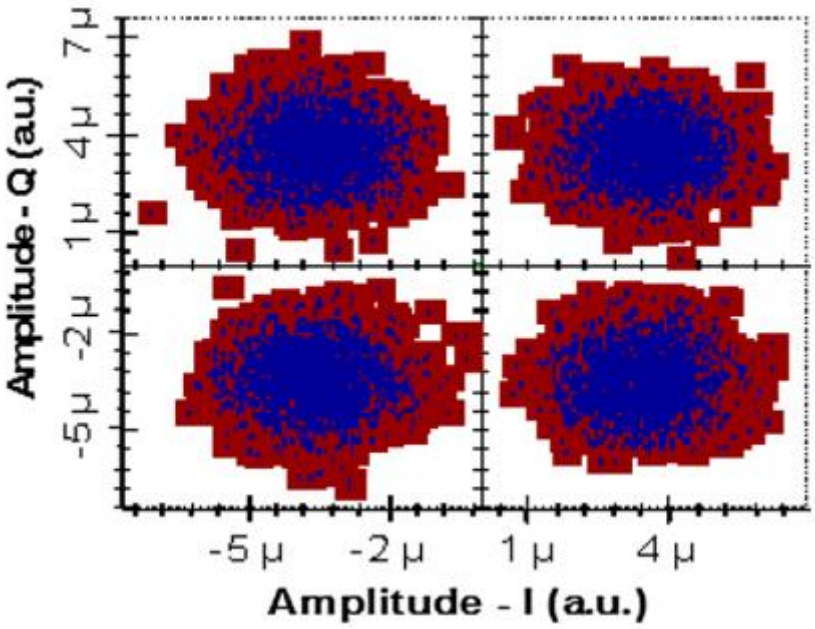

Fig III.19. Received signal constellation diagram for 1024 OFDM subcarrier and bit rate of 20 Gbps at the link range of 1.5 m

IV.Conclusion:

We have simulated a White LED visible light communication with a simple & basic diagram with internal & external modulation ,and also with OFDM modulation for a practically measured free space channel parameters. For the analysis of different bit rates and link ranges using Optisystem tool, our designed system can support up to 2 m of link range with a bit rate of 10 Gbps. The link range can be extended up to 3.5 m for a lower bit rate of 1 Gbps. In addition, we have discussed the influence of OFDM subcarrier numbers on the system performance. The signal distortion at higher bit rate is overcome significantly by increasing the number of OFDM subcarriers. By increasing the OFDM subcarriers, signal can be detected with improved BER up to 25 Gbps data rate. But the distance is limited to 1.5 m only. The designed system can open up the option for higher bit rate communication in future VLC systems. However, this work has a limitation of Line of Sight communication from White LED. But, multiple reflections from the walls and corners are also received by the receiver in practical scenario which would drastically vary the power and phase of the received signal in this Non-Line of sight (NLOS) case. Hence there is lot of scope for furthering this research for NLOS along with MIMO cases in future to ascertain the reality of the signal transmission in VLC.

REFERENCES:

[1] https://www.actiontec.com/wifihelp/evolution-wi-fi-standards-look-802-11abgnac/

[2] https://purelifi.com/lifi-technology/

[3] H. Haas and S. McLaughlin, eds., Next Generation Mobile Access Technologies: Implementing TDD. Cambridge University Press, Jan. 2008.

[4] . http://andy96877.blogspot.com/p/visible-light-communication-vlc-isdata.html. Visible light communication- VLC & Pure VLCTM. [Weblink: http://andy96877.blogspot.com/p/visiblelight-communication-vlc-is-data.html]

[5] https://www.researchgate.net/publication/260672666_Comparison_of_Orthogonal_Frequency-Division_Multiplexing_and_Pulse-Amplitude_Modulation_in_Indoor_Optical_Wireless_Links

[6] S. Rajagopal, R. Roberts, and S.-K. Lim, "IEEE 802.15.7 Visible Light communication: Modulation schemes and Dimming Support," IEEE Communications Magazine, vol. 50, no. 3, pp. 72–82, March 2012.

[7] E. Sarbazi, M. Uysal, M. Abdallah, and K. Qaraqe, "Ray Tracing Based Channel Modeling for Visible Light Communications," in 2014 22nd Signal Processing and Communications Applications Conference (SIU), April 2014, pp. 702–705

[8] A. Farid and S. Hranilovic, "Capacity Bounds for Wireless Optical Intensity Channels With Gaussian Noise," IEEE Transactions on Information Theory, vol. 56, no. 12, pp. 6066–6077, Dec 2010.

[9] B. Rofoee, K. Katsalis, Y. Yan, Y. Shu, T. Korakis, L. Tassiulas, A. Tzanakaki, G. Zervas, and D. Simeonidou, "First Demonstration of Service-Differentiated Converged Optical Sub-Wavelength and LTE/WiFiNetworks over GEAN," in Optical Fiber Communications Conference and Exhibition (OFC), 2015, March 2015, pp. 1–3.

[10] K. Lee, H. Park, and J. Barry, "Indoor Channel Characteristics for Visible Light Communications," Communications Letters, IEEE, vol. 15, no. 2, pp. 217–219, February 2011.

[11] Z. Chen and H. Haas, "Space Division Multiple Access in Visible Light Communications," in Proc. IEEE International Conference on Communications (ICC), London, UK, June 2015, pp. 5115–5119.

[12] Y. Saito, Y. Kishiyama, A. Benjebbour, T. Nakamura, A. Li, and K. Higuchi, "Non-Orthogonal Multiple Access (NOMA) for Cellular Future Radio Access," in Proc. IEEE Vehicular Technology Conference (VTC Spring), Dresden, Germany, Jun. 2013, pp. 1–5.

[13] L. Yin, X. Wu, and H. Haas, "On the Performance of Non-Orthogonal Multiple Access in Visible Light Communication," in Proc. IEEE 26th Annual Symposium on Personal, Indoor and Mobile Radio Communications (PIMRC), Hong Kong, China, Sept. 2015, pp. 1376–1381.

[14] L. Dai, B. Wang, Y. Yuan, S. Han, C. L. I, and Z. Wang, "NonOrthogonal Multiple Access for 5G: Solutions, Challenges, Opportunities, and Future Research Trends," IEEE Commun. Mag., vol. 53, no. 9, pp. 74–81, Sept. 2015.

[15] BS EN 62471:2008, Photobiological Safety of Lamps and Lamp Systems, BSI British Standards Std., Sept. 2008.

[16] S. Dimitrov, S. Sinanovic, and H. Haas, "Signal Shaping and Modulation for Optical Wireless Communication," IEEE/OSA Journal on Lightwave Technology (IEEE/OSA JLT), vol. 30, no. 9, pp. 1319–1328, May 2012.

[17] S. Dimitrov, S. Sinanovic, and H. Haas, "Clipping Noise in OFDM-based Optical Wireless Communication Systems," IEEE Transactions on Communications (IEEE TCOM), vol. 60, no. 4, pp. 1072–1081, April 2012.

[18] S. Dimitrov and H. Haas, "Information Rate of OFDM-Based Optical Wireless Communication Systems With Nonlinear Distortion," Journal Lightweight Technology, vol. 31, no. 6, pp. 918 – 929, March 15, 2013.

[19] S. Dimitrov, "Analysis of OFDM-based Intensity Modulation Techniques for Optical Wireless Communications," Ph.D. dissertation, The University of Edinburgh, Edinburgh, Aug. 2012.

[20] M. S. Rea, The IESNA Lighting Handbook: Reference & Application.

[21] New York, NY, USA: Illuminating Eng. Soc. North America, 2000.

[22] S. M. Berman, D. S. Greehouse, I. L. Bailey, R. D. Clear, and T. W. Raasch, "Human electroretinogram responses to video displays, fluorescent lighting, and other high-frequency sources," Optom. Vis. Sci.,

[23] IEEE Standard for Local and Metropolitan Area NetworksPart 15.7: Short-Range Wireless Optical Communication Using Visible Light, IEEE Std. 802.15.7, Sep. 2011.

[24] J. Grubor, S. C. J. Lee, K.-D. Langer, T. Koonen, and J. W. Walewski, "Wireless high-speed data transmission with phosphorescent white-light LEDs," in Proc. 33rd Eur. Conf. Exhib. Opt. Commun.—Post-Deadline Papers (published 2008), Sep. 2007, pp. 1–2.

[25] S. Park et al., "Information broadcasting system based on visible light signboard," Proc. Wireless Opt. Commun., 2007, pp. 311–313.

[26] H. L. Minh et al., "High-speed visible light communications using multiple-resonant equalization," IEEE Photon. Technol. Lett., vol. 20, no. 14, pp. 1243–1245, Jul. 2008.

[27] J. Fakidis, D. Tsonev, and H. Haas, "A Comparison between DCO-OFDMA and Synchronous One-dimensional OCDMA for Optical Wireless Communications," in 2013 IEEE 24th International Symposium on Personal Indoor and Mobile Radio Communications (PIMRC), London, Sept. 8–11, 2013, pp. 3605–3609.

[28] M. B. Rahaim, A. M. Vegni, and T. D. C. Little, "A Hybrid Radio Frequency and Broadcast Visible Light Communication System," in IEEE Global Communications Conference (GLOBECOM 2011) Workshops, Dec. 5-9, 2011, pp. 792–796.

[29] pureVLC. pureVLC Li-1st. video. http://purevlc.co.uk/li-fire/purevlc-li-1st/

[30] A. M. Khalid, G. Cossu, R. Corsini, P. Choudhury, and E. Ciaramella, "1-Gb/s Transmission Over a Phosphorescent White LED by Using Rate-Adaptive Discrete Multitone Modulation," IEEE Photonics Journal, vol. 4, no. 5, pp. 1465–1473, Oct. 2012.

[31] A. Azhar, T. Tran, and D. O'Brien, "A Gigabit/s Indoor Wireless Transmission Using MIMO-OFDM Visible-Light Communications," IEEE Photonics Technology Letters, vol. 25, no. 2, pp. 171–174, Jan. 15, 2013.

[32] J. M. Kahn and J. R. Barry, "Wireless Infrared Communications," Proceedings of the IEEE, vol. 85, no. 2, pp. 265–298, Feb. 1997.

[33] S. Dimitrov, R. Mesleh, H. Haas, M. Cappitelli, M. Olbert, and E. Bassow, "On the SIR of a Cellular Infrared Optical Wireless System for an Aircraft," IEEE Journal on Selected Areas in Communications (IEEE JSAC), vol. 27, no. 9, pp. 1623–1638, Dec. 2009.

[34] G. W. Marsh and J. M. Kahn, "Channel Reuse Strategies for Indoor Infrared Wireless Communications," IEEE Transactions on Communications, vol. 45, no. 10, pp. 1280–1290, Oct. 1997.

[35] F. R. Gfeller, P. Bernasconi, W. Hirt, C. Elisii, and B. Weiss, "Dynamic Cell Planning for Wireless Infrared In-House Data Transmission," Mobile Communications Advanced Systems and Components, ser. Lecture Notes in Computer Science. Springer Berlin/Heidelberg, 1994, vol. 783, pp. 261–272.

[36] S. B. Alexander, Optical Communication Receiver Design, 1st edn. SPIE Press Book, Jan. 1997.

[37] D. C. O'Brien, G. E. Faulkner, S. Zikic, and N. P. Schmitt, "High Data-Rate Optical Wireless Communications in Passenger Aircraft: Measurements and Simulations," in 6th International Symposium on Communication Systems, Networks and Digital Signal Processing (CSNDSP'08), Graz, Austria, July 23–25, 2008, pp. 68–71

[38] S. Ortiz, "The Wireless Industry Begins to Embrace Femtocells," Computer, vol. 41, no. 7, pp. 14–17, July 2008.

[39] V. Chandrasekhar, J. Andrews, and A. Gatherer, "Femtocell Networks: A Survey," IEEE Communications Magazine, vol. 46, no. 9, pp. 59–67, 2008.

[40] H. Haas, "High-Speed Wireless Networking Using Visible Light," retrieved from https://spie.org/x93593.xml, 2013.

[41] I. Stefan, H. Burchardt, and H. Haas, "Area Spectral Efficiency Performance Comparison between VLC and RF Femtocell Networks," in Proceedings of the International Conference on Communications (ICC), Budapest, Hungary, Jun. 2013, pp. 1–5.

[42] J. Vucic et al., "125 Mbit/s over 5 m wireless distance by use of OOK-Modulated phosphorescent white LEDs," in Proc. 35th ECOC, Sep. 2009, pp. 1–2.

[43] J. Vucic et al., "230 Mbit/s via a wireless visible-light link based on OOK modulation of phosphorescent white LEDs," in Proc. Conf. OFC/NFOEC, Mar. 2010, pp. 1–3.

[44] N. Fujimoto and H. Mochizuki, "477 Mbit/s visible light transmission based on OOK-NRZ modulation using a single commercially available visible LED and a practical LED driver with a pre-emphasis circuit," presented at the Optical Fiber Communication Conf./Nat. Fiber Optic Engineers Conf., Anaheim, CA, USA, Mar. 17–21, 2013, Paper JTh2A.73.

[45] S. Muthu and J. Gaines, "Red, green and blue LED-based white light source: Implementation challenges and control design," in Conf. Rec. IEEE 38th IAS Annu. Meeting, Oct 2003, vol. 1, pp. 515–522.

[46] S. Kaur, W. Liu, and D. Castor, VLC dimming support IEEE 802.15-09- 0641-00-0007. [Online]. Available: https://mentor.ieee.org/802.15/dcn/09/15-09-0641-00-0007- vlc-dimming-proposal.pdf

[47] J. K. Kwon, "Inverse source coding for dimming in visible light communications using NRZ-OOK on reliable links," IEEE Photon. Technol. Lett., vol. 22, no. 19, pp. 1455–1457, Oct. 2010.

[48] G. Ntogari, T. Kamalakis, J. Walewski, and T. Sphicopoulos, "Combining illumination dimming based on pulse-width modulation with visible light communications based on discrete multitone," IEEE/OSA J. Opt.Commun. Netw., vol. 3, no. 1, pp. 56–65, Jan. 2011.

[49] H. Sugiyama, S. Haruyama, and M. Nakagawa, "Brightness control methods for illumination and visible-light communication systems," in Proc. 3rd ICWMC, Mar. 2007, p. 78.

[50] C. Georghiades, "Modulation and coding for throughputefficient optical systems," IEEE Trans. Inf. Theory, vol. 40, no. 5, pp. 1313–1326, Sep. 1994.

[51] D. shan Shiu and J. Kahn, "Differential pulse-position modulation for power-efficient optical communication," IEEE Trans. Commun., vol. 47, no. 8, pp. 1201–1210, Aug. 1999.

[52] F. Gfeller, W. Hirt, M. de Lange, and B. Weiss, "Wireless infrared transmission: How to reach all office space," in Proc. IEEE 46th Veh. Technol Conf., Mobile Technol. Hum. Race, Apr 1996, vol. 3, pp. 1535–1539.

[53] T. Ohtsuki, "Rate-adaptive transmission scheme using punctured convolutional codes in a fixed channel reuse strategy with PPM CDMA," in Proc. GLOBECOM, Bridge Global Integr., 1998, vol. 1, pp. 207–212.

[54] T. Ohtsuki, "Rate-adaptive indoor infrared wireless communication systems using repeated and punctured convolutional codes," vol. 4, no. 2, pp. 56–58, Feb. 2000.

[55] B. Bai, Z. Xu, and Y. Fan, "Joint LED dimming and high capacity visible light communication by overlapping PPM," in Proc. 19th Annu. WOCC, May 2010, pp. 1–5.

[56] H. Sugiyama and K. Nosu, "MPPM: A method for improving the band-utilization efficiency in optical PPM," J. Lightw. Technol., vol. 7, no. 3, pp. 465–472, Mar. 1989.

[57] T. Ohtsuki, I. Sasase, and S. Mori, "Overlapping multi-pulse pulse position modulation in optical direct detection channel," in Techn. Program, Conf. Rec. IEEE ICC, May 1993, vol. 2, pp. 1123–1127.

[58] T. Ohtsuki, I. Sasase, and S. Mori, "Performance analysis of overlapping multi-pulse pulse position modulation (OMPPM) in noisy photon counting channel," in Proc. IEEE Int. Symp. Inf. Theory, Jun. 1994, p. 80.

[59] T. Ohtsuki and I. Sasase, "Capacity and cutoff rate of overlapping multi-pulse pulse position modulation (OMPPM) in optical direct-detection channel: Quantumlimited case," IEICE Trans. Fundam Electron., Commun. Comput. Sci., vol. 77, no. 8, pp. 1298–1308, 1994.

[60] T. Ohtsuki, I. Sasase, and S. Mori, "Trellis-coded overlapping multipulse pulse position modulation in optical direct detection channel," in Proc. IEEE SUPERCOMM/ICC, Conf. Rec., May 1994, vol. 2, pp. 675–679.

[61] T. Ohtsuki and I. Sasase, "Error performance of overlapping multipulse

[62] pulse position modulation (OMPPM) and trellis coded OMPPM in the optical direct-detection channel," IEICE Trans. Commun., vol. 77, no. 9, pp. 1133–1143, 1994.

[63] Institute of Electrical and Electronics Engineers (IEEE), "802.15.7 IEEE Standard for Local and Metropolitan Area Networks–Part 15.7: Short-Range Wireless Optical Communication Using Visible Light," 2011.

[64] H. Elgala, R. Mesleh, H. Haas, and B. Pricope, "OFDM Visible Light Wireless Communication Based on White LEDs," in Vehicular Technology Conference, 2007. VTC2007-Spring. IEEE 65th, April 2007, pp. 2185–2189.

[65] A. Yokoi, J. Son, and T. Bae, CSK constellation in all color band combinations, http://mentor.ieee.org/ 802.15/dcn/11/15-11- 0247-00-0007-csk-constellati on-in-all-color-bandcombinations. pdf.

[66] CIE, "Commission Internationale de lEclairage Proc." Cambridge University Press, 1931.

[67] CIE 1931 Chromaticity diagram. [Online]. Available: http://commons.wikimedia.org/wiki/File:Cie chromaticity diagram wavelength.png

[68] R. Drost and B. Sadler, "Constellation design for color-shift keying using billiards algorithms," in GLOBECOM Workshops (GC Wkshps), 2010 IEEE, Dec 2010, pp. 980–984.

[69] R. Singh, T. O'Farrell, and J. David, "An Enhanced Color Shift Keying Modulation Scheme for High-Speed Wireless Visible Light Communications," Lightwave Technology, Journal of, vol. 32, no. 14, pp. 2582–2592, July 2014.

[70] E. Monteiro and S. Hranilovic, "Constellation design for colorshift keying using interior point methods," in Globecom Workshops (GC Wkshps), 2012 IEEE, Dec 2012, pp. 1224–1228.

[71] ——, “Design and implementation of color-shift keying for visible light communications,” Lightwave Technology, Journal of, vol. 32, no. 10, pp. 2053–2060, May 2014.

[72] J. Vucic, C. Kottke, K. Habel, and K.-D. Langer, “803 Mbit/s visible light WDM link based on DMT modulation of a single RGB LED luminary,” in Optical Fiber Communication Conference and Exposition (OFC/NFOEC), 2011 and the National Fiber Optic Engineers Conference, March 2011, pp. 1–3.

[73] F.-M. Wu, C.-T. Lin, C.-C. Wei, C.-W. Chen, Z.-Y. Chen, and K. Huang, “3.22-Gb/s WDM Visible Light Communication of a Single RGB LED Employing Carrier-Less Amplitude and Phase Modulation,” in Optical Fiber Communication Conference/National Fiber Optic Engineers Conference 2013. Optical Society of America, 2013, p. OTh1G.4. [Online]. Available: http://www. osapublishing.org/abstract.cfm?URI=OFC-2013-OTh1G.4

[74] Y. Tanaka, T. Komine, S. Haruyama and M. Nakagawa, Indoor visible communication utilizing plural white LEDs as lighting, 12th IEEE International Symposium on Personal, Indoor and Mobile Radio Communications, vol. 2, pp. 81–85, San Diego, CA, 30 September–03 October 2001

[75] N. LaSorte, W. Justin Barnes and H. H. Refai, The history of orthogonal frequency division multiplexing, Proceedings of the IEEE Global Telecommunications Conference (GLOBECOM), New Orleans, LA, 30 November–4 December 2008.

[76] H. Elgala, R. Mesleh and H. Haas, Indoor broadcasting via white LEDs and OFDM, IEEE Trans. Consum. Electron., vol. 55, no. 3. pp. 1127–1134, 2009.

[77] R. Prasad, OFDM for Wireless Communication Systems, Artech House, Boston, MA, 2004.

[78] K. Asadzadeh, Efficient OFDM signaling schemes for visible light communication systems, Open Access Dissertations and Theses, Paper 6079, 2011.

[79] X. Li, R. Mardling and J. Armstrong, Channel capacity of IM/DD optical communication systems and of ACO-OFDM, IEEE International Conference on Communications 2007, ICC’07, Glasgow, pp. 2128–2133, 24–28 June 2007.

[80] J. Armstrong, B. J. C. Schmidt, D. Kalra, H. A. Suraweera, A. J. Lowery, Performance of asymmetrically clipped optical OFDM in AWGN for an intensity modulated direct detection system, IEEE Global Telecommunications Conference, (GLOBECOM '06), San Francisco, CA, pp. 1–5, 27 November–01 December 2006.

[81] N. Kumar, Visible Light Communication Systems for Road Safety Applications, PhD Thesis, Universidade de Aviero, chapter 3, pp. 31–71, 2011.

[82] J. Armstrong, “OFDM for optical communications,” J. Lightw. Technol., vol. 27, no. 3, pp. 189–204, Feb. 2009.

[83] R. Gitlin and E. Ho, “The performance of staggered quadrature amplitude modulation in the presence of phase jitter,” IEEE Trans. Commun., vol. 23, no. 3, pp. 348–352, Mar. 1975.

[84] J. M. Kahn and J. R. Barry, “Wireless infrared communications,” Proc. IEEE, vol. 85, no. 2, pp. 265–298, Feb. 1997.

[85] R.Mesleh,H. Elgala andH. Haas, An overview ofindoor OFDM/DMT optical wireless communication systems, 7th International Symposium on Communication Systems Networks and Digital Dignal Processing (CSNDSP), July 2010, Newcastle upon Tyne.

[86] D. Tsonev, S. Sinanovic and H. Haas, Novel unipolar orthogonal frequency division multiplexing (U-OFDM) for optical wireless, IEEE 75th Vehicular Technology Conference (VTC Spring), 6–9 May, Yokohama, 2012.

[87] V. Vijayarangan and R. Sukanesh, An overview of techniques for reducing peak to average power ratio and its selection criteria for orthogonal frequency division multiplexing, J. Theor. Appl. Inform. Technol., vol. 5, no. 9, pp. 25–36, 2009.

[88] J. Armstrong and B. J. C. Schmidt, Comparison of asymmetrically clipped optical OFDM and DC-biased optical OFDM in AWGN, IEEE Commun. Lett., vol. 12, no. 5, pp. 343–345, 2008.

[89] A. R. S. Bahai and B. R. Saltzberg, Multicarrier Digital Communications, Theory and Applications of OFDM, Kulwer Academic, New York, NY, 2002.

[90] L. Zeng, D. O'brien, H. Minh, G. Faulkner, K. Lee, D. Jung, Y. Oh, and E. T. Won, "High data rate multiple input multiple output (MIMO) optical wireless communications using white led lighting," Selected Areas in Communications, IEEE Journal on, vol. 27, no. 9, pp. 1654–1662, December 2009.

[91] D. O'Brien, "Multi-input multi-output (MIMO) indoor optical wireless communications," in Signals, Systems and Computers, 2009 Conference Record of the Forty-Third Asilomar Conference on, Nov 2009, pp. 1636–1639.

[92] D. Tsonev, S. Sinanovic, and H. Haas, "Practical MIMO Capacity for Indoor Optical Wireless Communication with White LEDs," in Vehicular Technology Conference (VTC Spring), 2013 IEEE 77th, June 2013, pp. 1–5.

[93] J. C. Chau and T. D. Little, "Scalable imaging VLC receivers with token-based pixel selection for spatial multiplexing," in Proceedings of the 1st ACM MobiCom workshop on Visible light communication systems. ACM, 2014, pp. 21–26.

[94] T. Fath and H. Haas, "Performance Comparison of MIMO Techniques for Optical Wireless Communications in Indoor Environments," Communications, IEEE Transactions on, vol. 61, no. 2, pp. 733–742, February 2013

[95] D. Takase and T. Ohtsuki, "Optical wireless MIMO communications (OMIMO)," in Global Telecommunications Conference, 2004. GLOBECOM '04. IEEE, vol. 2, Nov 2004, pp. 928–932 Vol.2.

[96] ——, "Performance analysis of optical wireless MIMO with optical beat interference," in Communications, 2005. ICC 2005. 2005 IEEE International Conference on, vol. 2, May 2005, pp. 954– 958 Vol. 2.

[97] ——, "Spatial multiplexing in optical wireless MIMO communications over indoor environment," IEICE transactions on communications, vol. 89, no. 4, pp. 1364–1371, 2006.

[98] Y. Chau and S.-H. Yu, "Space modulation on wireless fading channels," in Vehicular Technology Conference, 2001. VTC 2001 Fall. IEEE VTS 54th, vol. 3, 2001, pp. 1668–1671 vol.3.

[99] T. Fath, H. Haas, M. Di Renzo, and R. Mesleh, "Spatial Modulation Applied to Optical Wireless Communications in Indoor LOS Environments," in Global Telecommunications Conference (GLOBECOM 2011), 2011 IEEE, Dec 2011, pp. 1–5.

[100] P. Butala, H. Elgala, and T. Little, "Performance of optical spatial modulation and spatial multiplexing with imaging receiver," in Wireless Communications and Networking Conference (WCNC), 2014 IEEE, April 2014, pp. 394–399.

[101] T. Fath, M. Di Renzo, and H. Haas, "On the performance of Space Shift Keying for optical wireless communications," in GLOBECOM Workshops (GC Wkshps), 2010 IEEE, Dec 2010, pp. 990–994.

[102] M. Di Renzo and H. Haas, "On the performance of Space Shift Keying MIMO systems over correlated Rician fading channels, in Smart Antennas (WSA), 2010 International ITG Workshop on, Feb 2010, pp. 72–79.

[103] S. Videv and H. Haas, "Practical space shift keying VLC system," in Wireless Communications and Networking Conference (WCNC), 2014 IEEE, April 2014, pp. 405–409

[104] M. Di Renzo and H. Haas, "Space Shift Keying (SSK) Modulation with Partial Channel State Information: Optimal Detector and Performance Analysis over Fading Channels," Communications, IEEE Transactions on, vol. 58, no. 11, pp. 3196–3210, November 2010.

[105] W. Popoola, E. Poves, and H. Haas, "Generalised space shift keying for visible light communications," in Communication Systems, Networks Digital Signal Processing (CSNDSP), 2012 8th International Symposium on, July 2012, pp. 1–4.

[106] T. Fath, M. Di Renzo, and H. Haas, "On the performance of Space Shift Keying for optical wireless communications," in GLOBECOM Workshops (GC Wkshps), 2010 IEEE, Dec 2010, pp. 990–994. 104[107] D. Takase and T. Ohtsuki, "Optical Wireless MIMO (OMIMO) with Backward Spatial Filter (BSF) in Diffuse Channels," in Communications, 2007. ICC '07. IEEE International Conference on, June 2007, pp. 2462–2467.

[108] S.-M. Kim and S.-M. Kim, "Performance improvement of visible light communications using optical beamforming," in Ubiquitous and Future Networks (ICUFN), 2013 Fifth International Conference on, July 2013, pp. 362–365.

[109] L. Wu, Z. Zhang, and H. Liu, "Transmit Beamforming for MIMO Optical Wireless Communication Systems," Wireless Personal Communications, vol. 78, no. 1, pp. 615–628, 2014. [Online]. Available: http://dx.doi.org/10.1007/s11277-014-1774-3

[110] D. Bykhovsky and S. Arnon, "Multiple Access Resource Allocation in Visible Light Communication Systems," Lightwave Technology, Journal of, vol. 32, no. 8, pp. 1594–1600, April 2014. 111[111] C. Chen, D. Tsonev, and H. Haas, "Joint transmission in indoor visible light communication downlink cellular networks," in Globecom Workshops (GC Wkshps), 2013 IEEE, Dec 2013, pp. 1127– 1132

[112] J. Salehi, "Code division multiple-access techniques in optical fiber networks. I. Fundamental principles," Communications, IEEE Transactions on, vol. 37, no. 8, pp. 824–833, Aug 1989.

[113] J. Salehi and C. Brackett, "Code division multiple-access techniques in optical fiber networks. II. Systems performance analysis," Communications, IEEE Transactions on, vol. 37, no. 8, pp. 834–842, Aug 1989.

[114] M. Guerra-Medina, O. Gonzalez, B. Rojas-Guillama, J. MartinGonzalez, F. Delgado, and J. Rabadan, "Ethernet-OCDMA system for multi-user visible light communications," Electronics Letters, vol. 48, no. 4, pp. 227–228, February 2012.

[115] P. Kumar, R. Omrani, J. Touch, A. Willner, and P. Saghari, "A Novel Optical CDMA Modulation Scheme: Code Cycle Modulation," in Global Telecommunications Conference, 2006. GLOBECOM '06. IEEE, Nov 2006, pp. 1–5.

[116] Harsimranjit Kaur, Gaurav Sonil, "Performance Analysis of Free Space Optical Communication Link Using Different Modulation and Wavelength" Journal of Scientific Research & Reports, Vol. 6(3), Article no.JSRR.2015.145 ISSN: 2320-0227, pp. 201-209, February 2015.

[117] Joon-Ho Choi, Eun-Byeol Cho, Z. Ghassemlooy, Chung Ghiu Lee, "1 Mb/s Data Transmission Employing NRZ-OOK in a Visible Light Communication System" IQEC/CLEO Pacific Rim, Sydney, Australia, pp. 1659-1660, Aug. – Sep. 2011.

[118] Le-Minh H, O'Brien D C, Faulkner G, et al., "100-Mb/s NRZ visible light communications using a postequalized white LED", IEEE Photonics Technol Lett, Vol. 21(15), pp. 1063, August 2009.

[119] Fujimoto N, Mochizuki H., "477 Mbit/s visible light transmission based on OOK-NRZ modulation using a single commercially available visible LED and a practical LED driver with a preemphasis circuit", Optical Fiber Communication Conference and Exposition (OFC/NFOEC), March 2013.

[120] Li Honglei, Chen Xiongbin, Guo Junqing, et al., "A 550 Mbit/s real-time visible light communication system based on phosphorescent white light LED for practical high-speed low complexity application", Opt Express, Vol. 22(22), pp. 27203, November 2014.

[121]. Manivannan, K., Sivanantha Raja, A., & Selvendran, S. (2015). Channel characterization for visible light communication with the help of MATLAB. International Journal of Advanced Research in Computer Science and Software Engineering, 5(12), ISSN: 2277 128X.

[122]. Kaur, H., & Sonil, G. (2015). Performance analysis of free space optical communication link using diferent modulation and wavelength. Journal of Scientifc Research and Reports, 6(3), 201–209. Article no. JSRR.2015.145 ISSN: 2320-0227.

[123]. Mase, S., Arai, S., Yamazato, T., Yendo, T., Fujii, T., Tanimoto, M., & Kimura, Y. (2008). Error correcting scheme for road-to-vehicle visible light communication using LED

array. In Proceedings of the 11th international IEEE, conference on intelligent transportation systems. Beijing.

[124]. Kim, S., & Jung, S.-Y. (2011). Novel FEC coding scheme for dimmable visible light communication based on the modifed Reed–Muller codes. IEEE Photonics Technology Letters, 23(20), 11–13.

[125] . Wang, L., Wang, C., Chi, X., Zhao, L., & Dong, X. (2017). Optimizing SNR for indoor visible light communication via selecting communicating LEDs. Optics Communications, 387, 174–181.

[126]. Ab-Rahman, M. S., Shuhaimi, N. I., Al-Hakim Azizan, L., & Hassan, M. R. (2012). Analytical study of signal-to-noise ratio for visible light communication by using single source. Journal of Computer Science, 8(1), 141–144.

[127]. Afgani, M. Z, Haas, H., Elgala, H., & Knipp, D. (2006). Visible light communication using OFDM. In Testbeds and research infrastructures for the development of networks and communities (pp. 6–134). New